

APPENDIX N: Water Quality Modeling Report

BLACK BUTTE COPPER PROJECT, MONTANA

FINAL WATER QUALITY MODEL REPORT Revised Mine Operating Permit Application

Prepared for

**Tintina Montana, Inc.
White Sulphur Springs, MT**

Prepared by



524 Professional Drive
PO Box 1685 (59771)
Bozeman, Montana 59718

24 April 2017

Executive Summary

Tintina Montana, Inc. is in the process of submitting a Mine Operating Permit Application for its Black Butte Copper Project, located approximately 17 miles north of the town of White Sulphur Springs, Montana. Using hydrogeochemical monitoring, hydrogeological modeling and geochemical testing data, Tintina has designed its underground (UG) workings, temporary waste rock storage pad (WRS), cemented tailings facility (CTF), process water pond (PWP), contact water pond (CWP), and water treatment plant (WTP) to minimize impacts to water quality. Here, Enviromin presents water quality predictions for Tintina's proposed facilities, during operations and at closure.

Objectives

Enviromin has predicted water quality for the proposed i) UG workings (i.e., access, declines, and stopes), ii) WRS, iii) CTF, and iv) PWP. In the UG, we estimate water quality at year 6 of mining operations and at post-closure conditions, when the top of the water table has recovered to near premining conditions. For the WRS facility, we estimate water quality only at the end of year 2, when it will begin to be dismantled to provide material for the tailing impoundment interior liner, ramp, and rock drain. For the CTF, we estimate water quality at year 6 of production and at the start of closure, prior to placement of the synthetic cover which is expected to eliminate all subsequent seepage. Apart from groundwater in the underground workings at closure, water from all of the modeled facilities during construction and operations will ultimately report to the water treatment facility, where it will be treated to meet non-degradation standards and discharged to groundwater.

Methods and Assumptions

- The UG model estimates contributions from fractured walls based on a calculated reactive mass (R_m) within an equivalent porous media (EPM) model. The measured R_m and flow rate in humidity cell tests (HCT) are scaled to estimated field conditions to calculate mass loads (e.g., metals and acidity) from each unit.
- For the paste backfill and the cemented tailings, the model uses the surface area and flow rate to scale mass loads using diffusion test results (in the underground workings) or HCT tests (in the CTF runoff).
- The model estimates mass loads from waste rock in the CTF and WRS by scaling HCT test data to surface areas and flow rates. Because the predicted water flow is low relative to the surface area, the reactive mass is estimated by calculating the maximum amount of waste rock that could be saturated with the estimated flow over the relevant time frame, i.e. six months for the WRS and one week for the CTF.
- Only the final, mixed solutions are allowed to precipitate minerals (**Table 3-1**) and exchange metals with mineral surfaces through sorption to precipitated ferrihydrite and available sulfide. We use the *minteq.dat* thermodynamic database option in the USGS equilibrium model, PHREEQC and published sulfide sorption isotherm data to predict mineral precipitation, metal sorption, and resulting water quality.

Results

Our predictions indicate that water in the backfilled UG will have circumneutral pH, abundant alkalinity, and moderate sulfate, with metal concentrations that meet Montana groundwater standards and non-degradation criteria post-closure. During operations, increases in NO_3^- , SO_4^{2-} , F, Mn, Ni, Sb, Se, Tl, and U relative to background water quality are predicted in UG sump water that will be collected for storage in the PWP prior to treatment to meet Montana water quality standards. Predicted concentrations of NO_3^- , As, Sb, Sr, Tl, and U exceed

groundwater quality standards in one or more model scenarios. Of these elements, the background concentrations of both As and Sr in groundwater exceed Montana water quality guidelines. Water collected on the temporary, lined WRS and the doubly lined CTF will be more acidic than the UG, with elevated metal concentrations. This water will also be routed to the PWP prior to treatment to meet water quality standards. At closure, the CTF will be covered with a final lift of 4% cemented paste, resulting in increased pH and reduced metal concentrations, followed by placement of a geosynthetic membrane to cut off infiltration and eliminate water discharge. Specific results are summarized by facility below.

- **UG:** For the UG model, we predict water quality in year 6 of operations to be neutral, with a pH of 6.67, abundant alkalinity (183 mg/L) and a moderate increase over background concentrations in sulfate (304 mg/L) (**Table 4-4**). We predict potential precipitation of alunite, $Ba_3(AsO_4)_2$, Cr_2O_3 , ferrihydrite, and quartz, based on PHREEQC predictions of supersaturation in the mixed influent water in the sump. The formation of these minerals, followed by metal sorption, removes solutes from the water and allows calculation of a final of water quality. The metals As, Ba, Be, Cu, Pb, Ni, and Zn are predicted to sorb to ferrihydrite in the base case and most sensitivity scenarios, apart from the 'All HCT' scenario which does not predict ferrihydrite precipitation.

The model includes several sensitivity analyses of the predicted underground water quality, addressing uncertainty in model inputs for i) HCT data (i.e., all data vs. weeks 1-4), ii) fracture density, iii) fracture zone thickness, iv) reactive zone thickness, v) estimated surface area, and vi) sulfide oxidation rate. In general, the assumptions about fracture density and reactive-zone thickness have the greatest effect on predicted metal release, and the inclusion of all week HCT data has the greatest effect on the pH. Alkalinity is abundant in all sensitivity scenarios, including the analysis of several upper bound estimates of rim thickness, sulfide oxidation rate, and fracture density which together create a conservative evaluation of the reactive mass. Predicted pH ranges from 4.87 to 6.68 and sulfate ranges from 262 to 672 mg/L across the various sensitivity analyses (**Table 4-4**). Nitrate, Sr, and U are predicted to exceed the Montana DEQ groundwater quality standards in the operational base case as well as in several sensitivity scenarios (**Table 4-4**). Antimony, As, Sr and TI are predicted to exceed the groundwater standard only in select sensitivity analyses which include conservative (upper bound) estimates of input parameters. However, because all water will be collected for treatment to meet water quality standards, these operational exceedances will not affect downgradient water.

At closure, following completion of mining, stopes will be backfilled. Treated groundwater will be pumped to flood the workings and rinse stored oxidation products from exposed rock surfaces, after which the groundwater table will be allowed to recover its original elevation (as discussed in Section 7.3.3.6 of the MOP). The pH (6.81) of water under these steady state conditions is predicted to be higher, with lower sulfate (115 mg/L), alkalinity (144 mg/L) and metal concentrations than predicted during operations, as sulfide oxidation will be inhibited in the flooded workings (**Table 4-5**). The predictive model is most sensitive to the estimate of reactive surface area for cemented backfill. The lower mine workings are separated from the surface by the Volcano Valley Fault (VVF) and the base rock permeability is so low there is little to no flow through these units. In addition, the lower workings will be separated from the upper groundwater system by construction of two

hydraulic plugs where the access ramps penetrate through the VVF. Since the lower mine workings transmit little to no water, and will be separated from the upper workings and shallower hydro-stratigraphic units, they were not included in the closure model. Enviromin predicts potential precipitation of $Ba_3(AsO_4)_2$, barite, Cr_2O_3 , ferrihydrite, gibbsite, and quartz, based on PHREEQC predictions of supersaturation in the mixed water at closure. Metals sorb to both ferrihydrite and sulfide under closure conditions.

Mine water will be collected during dewatering operations for treatment, so the predicted chemistry at closure is the most important from an environmental perspective. The predicted changes at closure represent minor changes in water quality, relative to the background water quality (pH of 6.97, with alkalinity of 193 mg/L and sulfate 111 mg/L). The limited variation between the base case and sensitivity scenarios reflects the robust design and plan for management of the UG, which limits open stope area through concurrent backfilling with a low transmissivity material; provides for water treatment in operations and early closure; floods the lower workings with RO treated water at closure, and isolates the upper and lower workings using hydraulic plugs. No exceedances of groundwater quality standards or non-degradation criteria are predicted.

- **WRS:** Water quality predicted for the WRS base case at year 2 of mining is moderately acidic (pH 5.80) and high in sulfate (2,212 mg/L), with elevated NO_3^- , Sr, and Tl. (**Table 5-1**). However, the volume of WRS seepage is small (0.9 gpm average in year two) and water will be collected on a lined pad for treatment. This prediction is conservative, as a result of the very small amount of water into which the mass of solutes released from the aggressively weathered HCT is scaled. We predict potential precipitation of alunite, barite, celestite, and jarosite, with no sorption due to lack of ferrihydrite precipitation. Sensitivity analyses show that the predicted concentrations of Ni, Sr and Tl are sensitive to the rock:water ratio and surface area (reactive mass) assumptions. Because the WRS will be removed before year 3, no closure evaluation was needed.
- **CTF:** For the CTF, water quality predicted at year 6 of mining is acidic (pH 4.13) with 765 mg/L sulfate and elevated metal concentrations (**Table 6-1**). More acidity and metals are contributed by the surface of cemented tailings than the co-deposited waste rock or access ramp/rock drain, while most sulfate comes from the wet paste and the waste rock contribution. The minerals predicted by PHREEQC to form during operations include alunite, barite, jarosite, and quartz. At closure, following placement of a 4% cement paste lift immediately prior to cover placement, a more neutral solution (pH 4.95) is predicted, with no exceedances of groundwater standards for metals predicted for the base case following precipitation of barite, and jarosite (**Table 6-2**). Limited exceedances of groundwater standards for As and Tl were predicted for the high surface area sensitivity scenario in closure. The planned reclamation procedures (e.g., welded HDPE cover, revegetation, etc.) are not accounted for in the model, which predicts water quality prior to use of the cover to eliminate infiltration.

Results for the CTF show that the finely ground, sulfide-rich tailings will generate higher acidity and metals, but proportionally lower sulfate due to precipitation of sulfate-rich minerals, e.g., alunite, barite and jarosite. Water quality predictions for the CTF are sensitive to the calculated surface area, implying that the surface area

- should be managed to limit weathering through frequent placement of fresh lifts of pasted tailings. Higher concentrations of cement (e.g., 4%) could be used to reduce disaggregation of the surface if a delay in operations will prevent frequent placement of fresh lifts.
- **PWP:** All water from the CTF sump and some water from the WTP will report to the PWP. These inflows mix with thickener overflow from the mill and direct precipitation. The model predicts that the overall chemistry of the PWP is dominated by the thickener overflow, which provides 93% of the flow. The predicted solution has a pH of 5.81, moderate sulfate (903 mg/L), and elevated concentrations of NO_3^- and metals, including As, Cu, NO_3^- , Ni, Pb, Sb, Sr, and Tl (**Table 7-1**). PHREEQC predicts that alunite, $\text{Ba}_3(\text{AsO}_4)_2$, barite, and jarosite could form, based on supersaturation.

TABLE OF CONTENTS

Executive Summary	i
1 Introduction	1
1.1 Purpose and Scope	1
2 Model Source Data	7
2.1 Black Butte Copper Mine Plan	7
2.2 Black Butte Copper Project Geology.....	8
2.3 Groundwater Chemistry Data.....	11
2.4 Groundwater Flow Data	16
2.5 Environmental Geochemistry Data.....	16
3 Modeling Approach	20
3.1 Mass Load Assumptions.....	20
3.2 Geochemical Modeling of Mineral Precipitation and Metal Sorption.....	21
3.3 Sensitivity Analyses	22
4 Underground Workings Water Quality Model	23
4.1 Conceptual Model.....	23
4.2 Data Sources.....	24
4.2.1 Groundwater Quality Data	24
4.2.2 HCT Data.....	26
4.3 Mass Load Model Calculations	27
4.3.1 Surface Area Calculations	27
4.3.2 Calculation of Reactive Mass.....	30
4.3.3 Scaling of HCT Data to Reactive Mass	32
4.4 Geochemical Modeling of Underground Water.....	33
4.5 Water Quality Prediction for Year 6 Operations.....	33
4.6 Water Quality at Closure.....	35
5 Waste Rock Storage Facility Water Quality Model	38
5.1 Conceptual Model.....	38
5.2 Data Sources.....	38
5.2.1 Waste Rock HCT Data.....	38
5.2.2 Water Balance	39
5.3 Mass Load Model Calculations	39
5.3.1 Calculation of Reactive Mass and Surface Area	39
5.3.2 Scaling of HCT Data to Reactive Surface Area.....	40
5.4 Predicted Water Quality at Year 2 of Mining	41
6 Cement Tailings Facility Water Quality Model	42
6.1 Conceptual Model.....	42
6.2 Data Sources.....	44
6.2.1 Cemented Paste HCT Data	44
6.3 Mass Load Calculations.....	44
6.3.1 Estimation of Paste Material Surface Area.....	44
6.3.2 Estimations of Waste Rock Reactive Surface	45
6.3.3 Water Balance	46
6.4 Predicted Water Quality at Year 6.....	46
6.5 Predicted Water Quality at Closure.....	48
7 Process Water Pond Water Quality Model	49
7.1 Process Water Pond Water Balance.....	50

7.2	Predicted Water Quality in PWP	50
8	Conclusions and Recommendations	52
9	References	55

LIST OF TABLES

Table 2-1.	Summary of Hydrostratigraphic Units and Associated Well Completions (from Hydrometrics, 2015)	12
Table 2-2.	Summary of Monitoring Wells from Groundwater Baseline Study, after Hydrometrics (2015)	14
Table 2-3.	Simulated Maximum Annual Inflow to Mine Workings.....	16
Table 3-1.	Mineral Phases Allowed to Precipitate in PHREEQC Modeling	22
Table 4-1.	Wells Used for Groundwater Input Data	25
Table 4-2.	Three Sigma Evaluation Results Groundwater Input Data.....	26
Table 4-3.	Surface Area Values for Year 6 and Closure.....	29
Table 4-4.	Model Predictions for Underground Water Quality at Year 6 of Operations	36
Table 4-5.	Model Predictions for Underground Water Quality after closure	37
Table 5-1.	Year 2 Results for Waste Rock Storage Facility	42
Table 6-1.	Predicted Water Quality in the CTF Sump at Year 6, Including Sensitivity Analyses.....	47
Table 6-2.	Predicted Water Quality in the CTF Sump at Closure, Including Sensitivity Analyses.....	49
Table 7-1.	Predicted Water Quality in PWP at Year 6	51

LIST OF FIGURES

Figure 1-1.	Project Location Map	2
Figure 1-2.	Black Butte Copper Project Site Facilities	3
Figure 1-3.	Cross-section of proposed BBC mine workings showing stratigraphic units (Ynl A, USZ, Ynl B, and LZ FW).....	6
Figure 2-1.	Black Butte Copper Site Geologic Map	9
Figure 2-2.	Black Butte Copper Stratigraphic Section.....	10
Figure 2-3.	Location of Black Butte Copper Groundwater Monitoring Wells.....	13
Figure 4-1.	Conceptual model of the seven hydrostratigraphic units, each providing input to the sump.....	23
Figure 4-2.	Conceptual Model of Surface Area Within Backfilled Stopes at Year 6 (above) and at Closure (below).....	28
Figure 4-3.	Schematic Cross-Section of Mine Workings with an Oxidized Zone That Grows Outward.....	31
Figure 4-4.	Schematic Showing Scaling of HCT Data to Predict Chemistry.....	32
Figure 5-1.	Conceptual Model of Waste Rock Storage Facility (from Knight Piesold).....	38
Figure 5-2.	Waste Rock Gradation from Ashanti Mine (Hyle, 2016)	40
Figure 6-1.	Conceptual Model of CTF Showing Waste Rock Ramp and Local Placement of Waste Rock Mined from UG, Year 6 of Tailings Production.....	43
Figure 6-2.	Polynomial Fit for Sulfate Data, Used to Estimate Surface Area.....	45
Figure 7-1.	Water Balance for Process Water Pond.....	50

LIST OF APPENDICES

- APPENDIX A: Average HCT data for weeks 1-4 (from Enviromin, 2015)
- APPENDIX B: Average HCT Data for All Weeks (from Enviromin, 2015)
- APPENDIX C: PHREEQC Input for Underground Operations at Year 6
- APPENDIX D: Base Case and Sensitivity Scenarios for UG, WRS, CTF, and PWP Models
- APPENDIX E: Groundwater Chemistry Model Inputs, from Hydrometrics Inc. (2015)
- APPENDIX F: Prediction of Metal Attenuation by Sulfide in Bedrock Post-Closure
- APPENDIX G: Mass-Load Inputs from the Base Case Underground Model at Year 6
- APPENDIX H: Mass-Load Inputs from the Base Case Underground Model at Closure
- APPENDIX I: Mass-Load Inputs from the Base Case Model for the WRS at Year 2
- APPENDIX J: Data Used for Wet Paste Seepage and 2% Paste in the Cement Tailings Facility
- APPENDIX K: Mass-Load Inputs from the Base Case CTF at Year 6 of Mining
- APPENDIX L: Mass-Load Inputs from the Base Case CTF at Closure
- APPENDIX M: Mass-Load Inputs from Water Process Plant
- APPENDIX N: Prediction of Rinsing Required at Closure of Underground Mine Workings

1 Introduction

Tintina Resources has submitted a Mine Operating Permit (MOP) application for its Black Butte Copper Project, located approximately 17 miles north of the town of White Sulphur Springs, Montana (**Figure 1-1**). Copper in the shaley dolomite of the lower Newland Formation is associated with sulfide mineralization that is locally massive, but hosted in carbonaceous and carbonate-rich sediments with fracture-controlled transmissivity in the vicinity of the proposed underground workings. Using hydrogeochemical monitoring, hydrogeological modeling and geochemical testing data, Tintina has designed its facilities to address the potential for sulfide mineralization to impact water quality. Facilities where water may be influenced by geochemistry include the underground workings (UG), temporary waste rock storage pad (WRS), cemented tailings facility (CTF), process water pond (PWP), contact water pond (CWP), and the water treatment plant (WTP) (Figure 1-2).

In this report, we present water quality predictions developed for key facilities during operations and at closure. These models integrate Tintina's proposed designs with hydrological, geochemical, and water balance data. Models predict future water quality and related uncertainty based on sensitivity analyses at four locations:

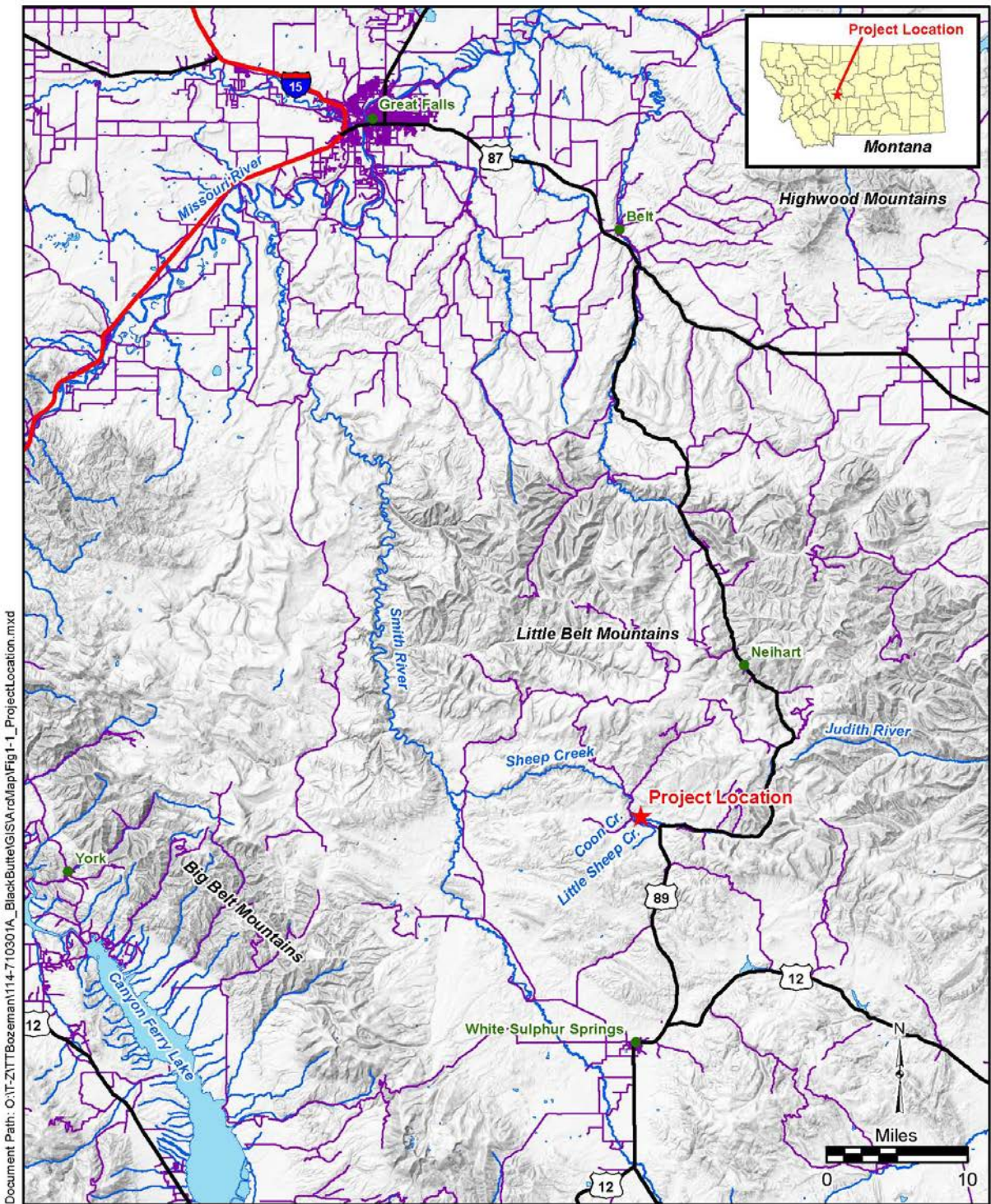
- Groundwater quality in the UG at year 6 of mining operations and at closure;
- Seepage from temporary waste rock storage, which will be collected and transported to the CWP, in year 2 of mining;
- CTF seepage/runoff quality, which will ultimately return to the PWP and WTP for release following treatment and discharge to an underground infiltration gallery, in year 6 of tailing production and at closure; and
- Updated water quality data predictions for PWP water reporting to the WTP based on RO brine and CTF predictions, for year 6 of production.

The underground model applies groundwater quality, geochemistry, flow predictions, and water treatment design model results to facility-specific conceptual models describing conditions during operations and at closure. The analytical approach recognizes changes in the operational water balance and extent of oxidation throughout mine life, as well as solubility and sorption constraints on the quality of water in each setting. Uncertainty has been addressed through sensitivity analyses. Results have been compared with Montana groundwater standards and non-degradation criteria, where appropriate.

1.1 Purpose and Scope

The purpose of Enviromin's development of the models is to predict water quality in the UG workings, the (WRS) and the CTF, as well as the overall quality of water in the PWP, which will report to the WTP. We use the operational plans provided by Tintina, together with the groundwater quality data (Hydrometrics 2015 and 2017, MOP, Appendix B); geochemical test results (Enviromin, 2017, MOP, Appendix D); the hydrogeological modeling (Hydrometrics, 2017, MOP, Appendix M); and the water treatment design predictions (Appendix V of the MOP application, AMEC 2017) to develop a mass-load calculation of water quality for each facility under base case and sensitivity scenarios. Each mass load solution is then evaluated for solubility and sorption controls using the USGS PHREEQC equilibrium model to calculate mineral saturation indices and metal sorption to precipitated ferrihydrite (Parkhurst and Appelo, 1999). Sorption of metals to sulfide in saturated bedrock at closure is calculated using published isotherm data (Appendix F).

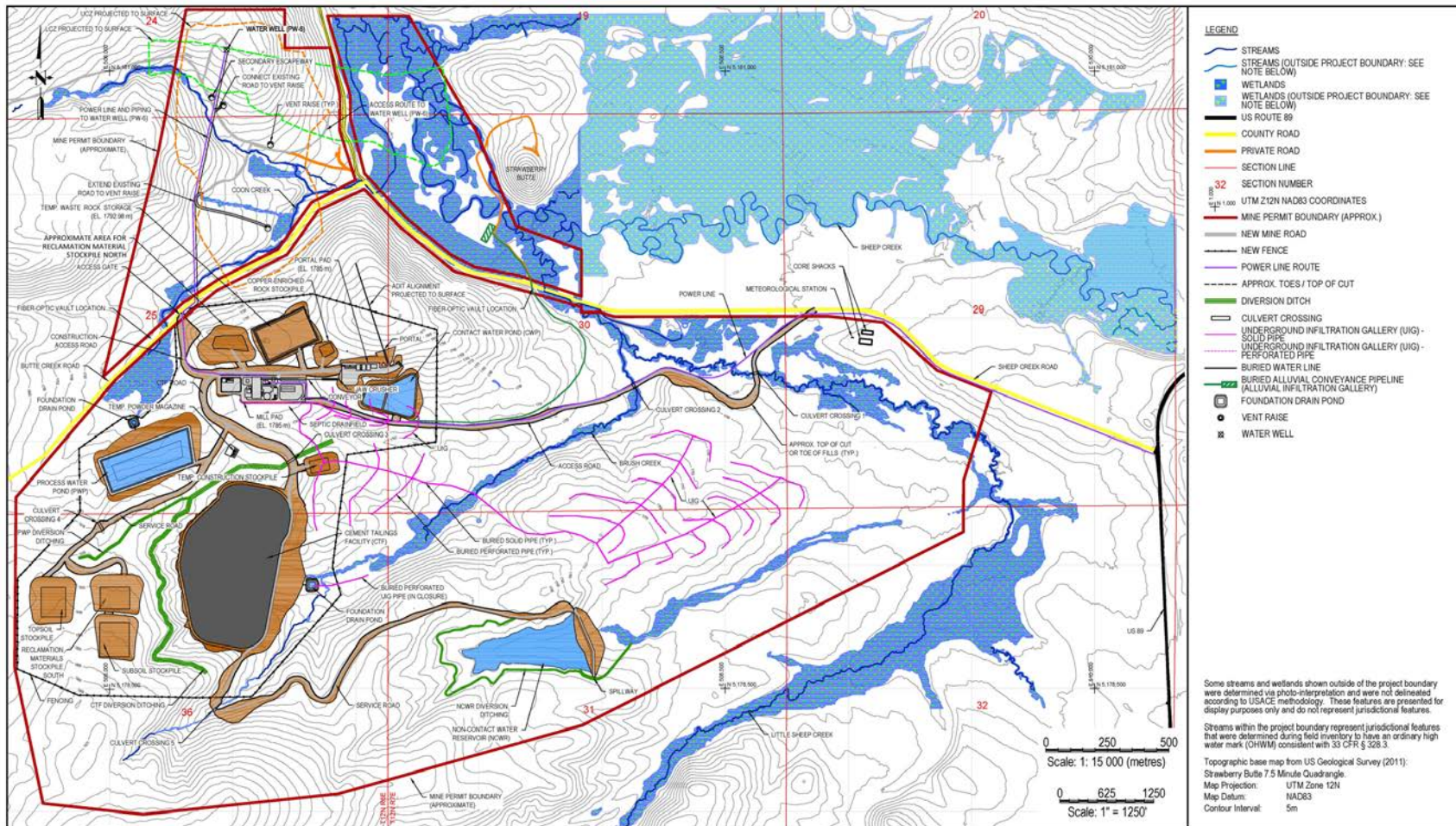
Figure 1-1. Project Location Map



Legend

- ★ Project Location
- City
- Interstate
- U.S. Route
- Local Road
- ~ Stream
- ☪ Lake

Figure 1-2. Black Butte Copper Project Site Facilities



Underground Workings (UG) – Tintina plans to advance underground operations through the proposed decline into the Upper Sulfide Zone (USZ) and deeper into the Lower Copper Zone (LCZ) (**Figure 1-3**). Copper-enriched rock will be mined within stopes that will be open for less than 90 days at any time. An average of 0.7% of the deposit will be open at any given time during concurrent development, extraction, and backfilling within the stopes. Tintina proposes to produce tailings via flotation and to blend them with cement to create 4% cemented paste tailings. Using a drift and fill mining method, 45% of produced tailings will be placed as backfill into mined out underground stopes and access headings during operations. The workings will be flooded at closure. In addition to the Upper and Lower Copper Zones (UCZ and LCZ), the exposed lithotypes include, from largest to smallest surface area contribution; Ynl B, LZ FW, and Ynl A. Most groundwater influx comes from the USZ/UCZ unit (50%), the Ynl B (lower decline) unit (22%) and the Ynl A (upper decline) unit (19%) (Hydrometrics, 2016). Exposed access headings will be flooded with water collected for treatment during early closure; bulkheads will be placed to isolate rinsed and flooded zones, allowing long-term steady state equilibrium with groundwater in closure.

Waste Rock Storage (WRS) – Rock will be stored on the WRS pad (shown in **Figure 1-2**) for 2 years, and then placed in the CTF. Waste rock will be mined primarily from (in stratigraphic order) the upper portion of the lower Newland Formation (Ynl A, 4%), the Upper Sulfide Zone (USZ, 28%), the lower portion of the lower Newland Formation (Ynl B, 32%), and the Lower Zone Foot Wall (LZ FW, 35%) as the decline is driven to access the copper-enriched rock. This waste will be placed in lifts on the lined WRS waste rock storage pile. Little if any LZ FW will be placed on the WRS, as this formation is not anticipated to be mined before CTF construction is scheduled to be complete and the WRS pad is reclaimed.

The seepage rate through the WRS was estimated using the HELP model at an average rate of 0.9 gallon per minute (gpm) (Hydrometrics, 2016). This water will report directly to the CWP until year 2 to 3, when waste rock will be removed from the stockpile altogether for placement in the CTF.

Cement Tailing Facility (CTF) – Tintina has proposed an innovative, cemented tailings storage design. Tailings that are not backfilled (approximately 55%) will be placed as 0.5 to 2% cement-amended paste into a double lined surface tailing impoundment (the CTF, shown in **Figure 1-2**). Most waste rock produced during construction of the decline and other UG workings will be placed into the lowermost CTF and used to construct the ramp, where it will subsequently be covered by cemented paste tailings. Run of mine (ROM) waste rock will also be placed around the sump to develop a positive drain within the CTF, and ROM waste rock produced later will be co-disposed with (and encapsulated by) paste tailings.

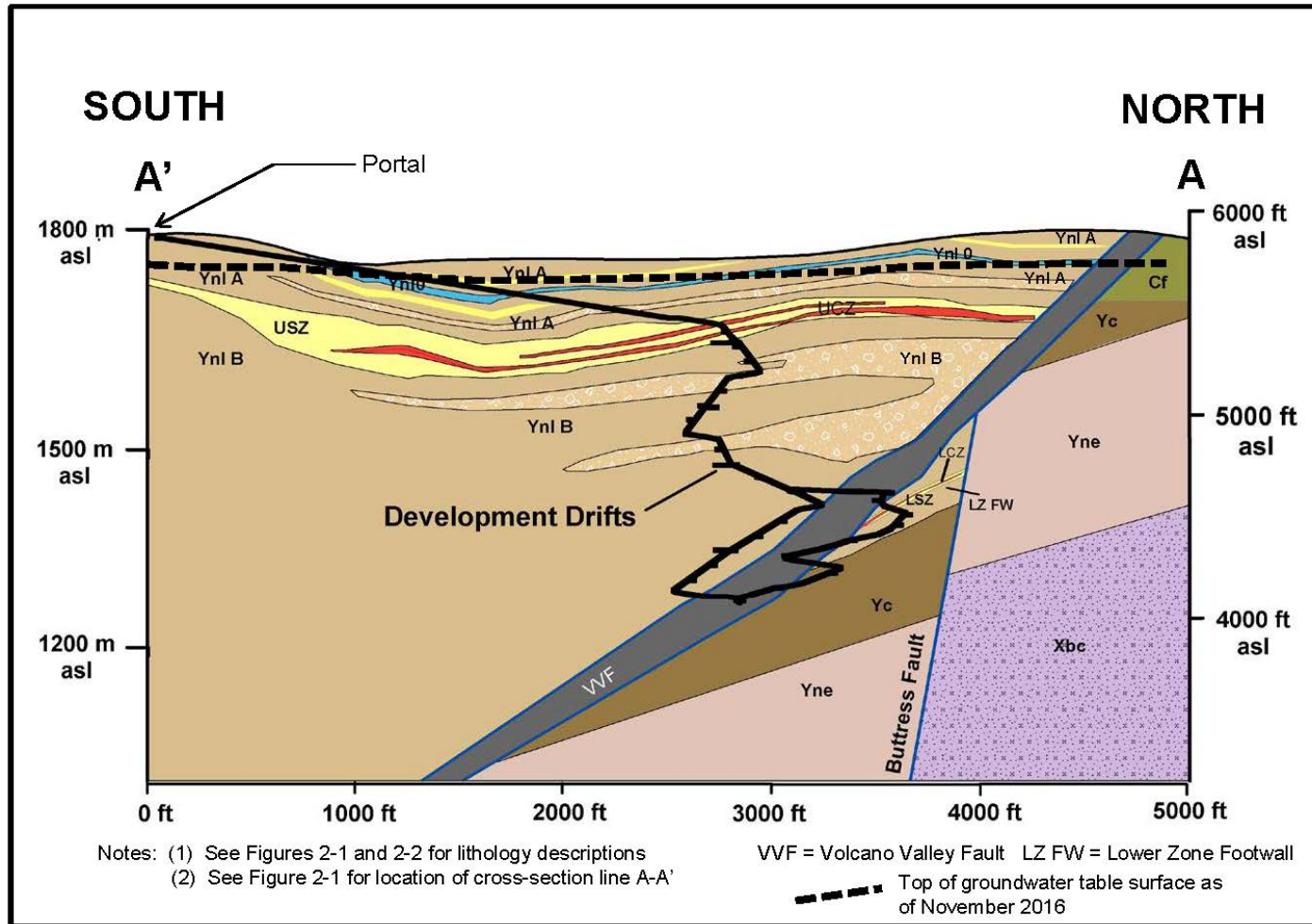
By incorporating cement with binders (i.e., fly ash and/or slag) into the tailings as they are placed in the lined CTF, Tintina will encapsulate sulfide minerals in a non-flowable mass of tailings and limit their exposure to oxygen and water, thereby limiting acid and metal release potential from the waste rock. The majority of waste rock will be produced from the decline early in operations, and will therefore be placed into the lowermost part of the lined CTF. Waste rock produced subsequently will be dumped from the ramp and encapsulated within the cemented paste backfill. Water seeping from tailings as they consolidate and solidify will mix with runoff from direct precipitation onto the CTF; this water will be collected in a waste rock-lined sump prior to being pumped back to the PWP. The CTF is designed to have little or no water stored in the facility.

Process Water Pond (PWP) – Water from the UG and RO brine (**Figure 1-2**) will mix with process water and direct precipitation in the PWP. Excess volume accumulating on the

PWP will report to the water treatment plant (WTP). Using the calculated predictions for the CTF and predicted RO brine chemistry from AMEC (2017), we have predicted water quality for the PWP. This model is provided for comparison with previous predictions of water quality requiring treatment that were based solely on mixed metallurgical process water and groundwater for design purposes.

At closure, the water balance will change. The WRS facility will no longer exist. Mining will cease and all UG stopes will be backfilled. Dewatering will cease and groundwater will return to its original elevation, filling the decline and any gaps in backfilled stopes. Water from the UG will no longer report to the PWP or the WTP. Contributions from the WRS will have been eliminated, reducing the solute load both to and from the CWP. Following the placement of final tailings lifts, a geomembrane will be used to cap the CTF and a fill and soil cap will be placed over the HDPE cover, eliminating incident precipitation and greatly reducing the availability of oxygen. Progressively less water will report to the CTF sump during closure, and solute load is expected to decline, so that the volume and chemistry of water requiring treatment will change, and ultimately be eliminated. Water from the PWP will be treated to meet water quality standards.

Figure 1-3. Cross-section of proposed BBC mine workings showing stratigraphic units (Ynl A, USZ, Ynl B, and LZ FW) to be mined as waste rock and exposed in the underground workings. Volcano Valley Fault (VVF) and Buttress Fault are shown bounding the Lower Copper Zone (LCZ).



2 Model Source Data

The models account for data that characterize facility design, operation, closure, site geology, groundwater quality, groundwater flow, and geochemistry. Data sources are described generally here and later examined in detail for each of the models.

2.1 Black Butte Copper Mine Plan

Tintina Montana's Black Butte Copper Project will produce and ship copper concentrate mined from both the upper and lower Johnny Lee deposit zones. The proposed operation will mine approximately 15.3 million tons (13.9 million tonnes (Mt)) of rock. This total includes 14.5 million tons (13.2 Mt) of copper-enriched rock with an average grade of 3.1% copper, and 0.8 million tons (0.7 Mt) of waste. Mining will occur at a rate of approximately 1.3 million tons/year (1.2 Mt/year) or 3,640 tons (3,300 tonnes) per day, over a mine life of approximately 19 years (including construction and reclamation) (Tintina MOP, 2016).

Mining will use a drift and fill method. Approximately 45% of the mill tailings will be mixed with cement and binder to form a paste, and used to backfill all production workings during the mining of sequential drifts in the UG. Although much of the waste rock that will be trucked to surface will be non-acid generating, as a safeguard, all waste rock will be assumed to contain sulfide minerals and will be treated as potentially acidic or metal generating. A geomembrane lined, temporary WRS facility will be constructed between the portal and the mill. It will receive all of the pre-production waste rock generated until construction of the CTF is completed (**Figure 1-2**). The pre-production waste rock will be placed over a protective sub-grade bedding layer that will be placed and compacted over a double high-density polyethylene (HDPE) lining system. All future waste rock generated during production mining will be placed into the CTF along with the mill tailings. The temporary WRS facility will be completely reclaimed in year's two to three. No waste rock will be left on the surface after closure. The CTF will be dewatered (if any water is present), sealed with a cover of HDPE, and reclaimed in closure. A separate stockpile on a smaller lined pad will be constructed off of the northwest corner of the portal pad (Figure 1-2) near the end of the construction period to contain the copper-enriched rock for mill feed.

Dewatering of UG mine workings will provide all water required for mining and milling (approximately 210 gallons per minute [gpm] or 795 Lpm). Excess water pumped from the mine will be treated to meet non-degradation standards and released through an underground infiltration gallery to shallow bedrock.

A double HDPE-lined PWP with an underlying foundation drain and pond will store water needed for milling. Water will be recycled between the PWP and the mill during operations. A paste plant in the mill complex will mix fine-grained tailings from the milling process with cement for placement both UG and in the CTF. The plant will mix approximately 45% of the tailings with approximately 4% cement and other binders to be used as paste backfill in the UG mine workings.

The remaining 55% of the tailings will be mixed with 0.5 to 2% cement and other binders to form a paste which will be pumped to the CTF. The small amount of free water that collects in the CTF from cemented tailings seepage, precipitation and snowmelt will be pumped to the PWP. Water not needed in the mill will be pumped directly to the reverse osmosis water treatment facility for treatment and then released to the underground infiltration galleries.

Both the CTF and the PWP will use liner systems comprised of a high-flow geonet-layer sandwiched between two layers of 100 mil HDPE geomembrane liner. Both facilities will

also incorporate foundation drains beneath the liners. The CTF will also have an internal basin underdrain system.

The closure and reclamation plan will maintain physical and chemical stability of all facilities, to protect water quality and quantity. No waste rock will be left on surface in closure. Water will be removed from the tailings facility (if any is present), and from the PWP and CWP, and treated to meet standards prior to discharge. The CTF will be covered with a welded HDPE cover, followed by fill, subsoil and topsoil (at a slope or shape designed to preclude standing water), re-grading and re-vegetation. This plan will eliminate long-term exposure of the final lifts to oxygen and water. The double lined CTF with drainage collection is designed to prevent discharge to surface water and groundwater. Any water produced from the CTF sump in closure (if any) will go directly to the water treatment plant. This will continue into closure while water quality and inflow are monitored, with gradually decreased monitoring until sufficient data is available to evidence that final closure objectives have been met (i.e., at some point in closure the water treatment plant will no longer be required).

2.2 Black Butte Copper Project Geology

The geology and subsurface stratigraphy within the project area has been reported by Tintina, based on geologic mapping and extensive exploratory drilling, and is summarized here. Further hydrogeological detail is described by Hydrometrics in Appendices B and M of the MOP (Tintina, 2015).

A geologic map of the project area is shown in **Figure 2-1** and a stratigraphic section for the project area is shown in **Figure 2-2**. The mine will be developed within dolomitic and silicic shales of the Proterozoic Newland Formation that dip gently to the southeast and are bounded to the north by a prominent northeast trending thrust fault known as the Volcano Valley Fault (VVF). **Figure 1-3** shows the principal stratigraphic units that will be encountered during development of the Johnny Lee deposits. There are the Upper (UCZ) and Lower Copper Zones (LCZ) hosted within the Upper and Lower Sulfide Zones (USZ, LSZ, respectively) of the lower Newland Formation. The UCZ lies approximately 250 to 600 feet below ground surface and is overlain by shale and dolostone (Ynl A), and dolomite (Ynl O) interbeds. The UCZ is underlain by the lower Newland shale and conglomerate (Ynl B). These units are cut by the southward-dipping VVF to the north, shown as a heavy purple line in **Figure 1-3**. A thin slice of the lower Newland Formation lies below the VVF and contains the LCZ at a depth of approximately 1,100 to 1,500 feet below surface. The LCZ and Lower Newland shales lie just above the contact with the Chamberlain Formation and are cut to the north by the Buttress Fault, shown as a thin purple line in **Figure 1-3**. Lower Newland rock lying stratigraphically below the VVF are generally referred to as LZ FW (Lower Zone Footwall) rocks.

Figure 2-1. Black Butte Copper Site Geologic Map

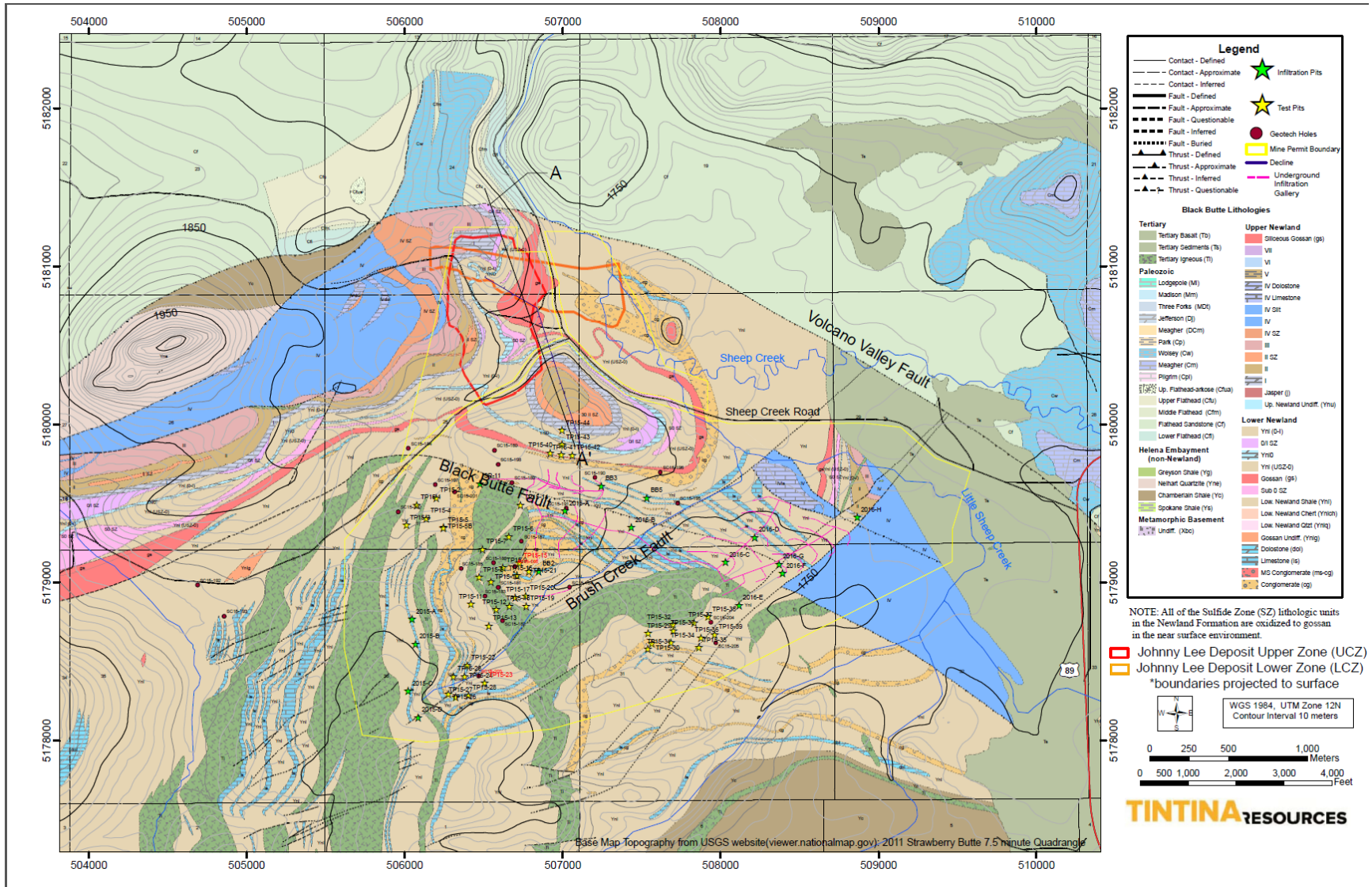
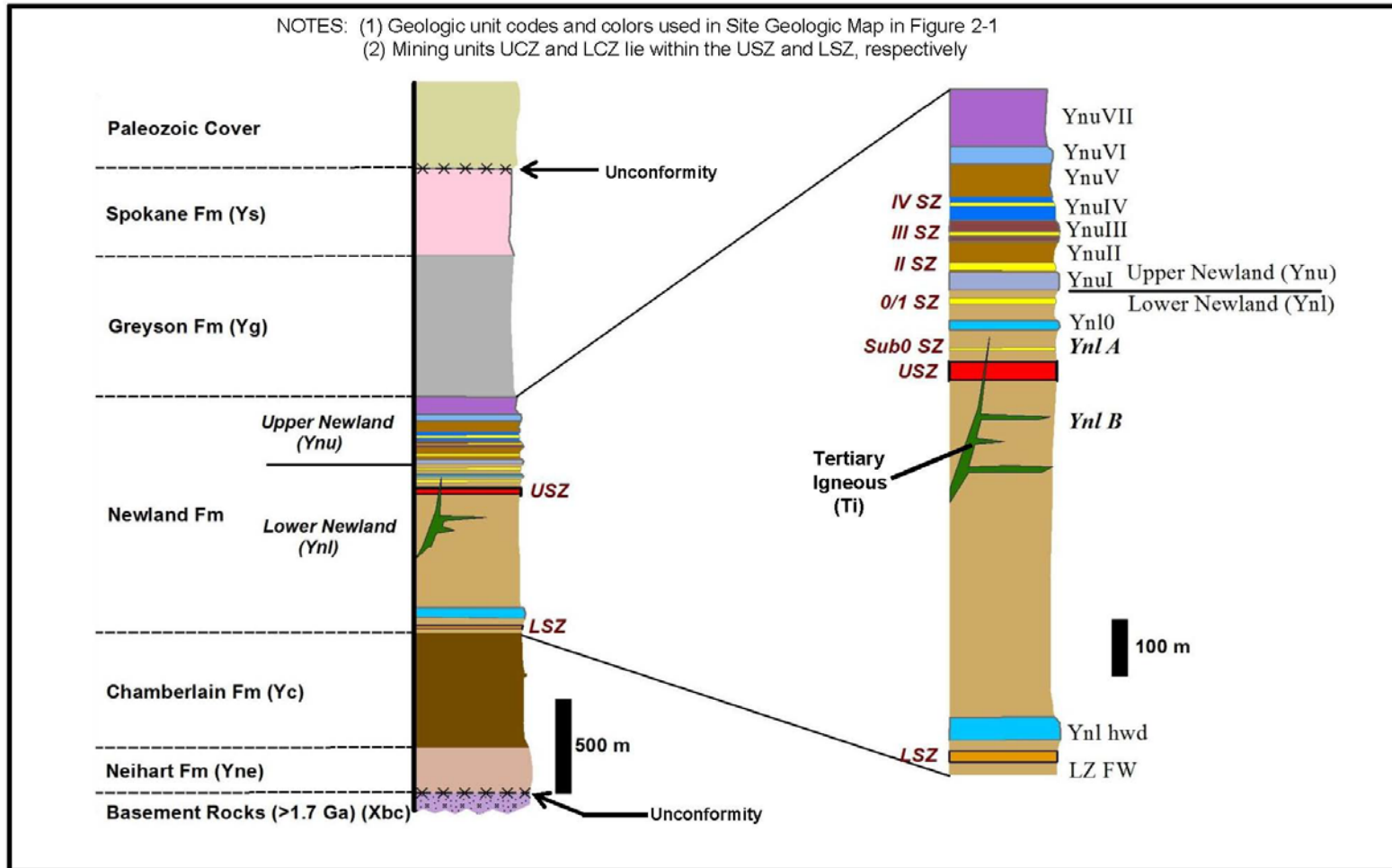


Figure 2-2. Black Butte Copper Stratigraphic Section



Prepared by: Tintina Resources (2016)

Abbreviations: Fm = Formation; FW = footwall; hwd = hanging wall dolomite SZ = Sulfide Zone; LZ FW = Lower Zone Footwall

Other geologic units not listed on this stratigraphic section but that are included in Figure 2-1 site geologic map include: Ts (Tertiary sediments) and Paleozoic cover units (Cw = Wolsey Formation; Cf = Flathead sandstone; cg = conglomerate interbeds in Ynu and Ynl; and ls = limestone interbeds in the Ynu and Ynl. The Ynl unit is divided into the Ynl A and the Ynl B subunits relative to the location above or below the USZ, respectively.

2.3 Groundwater Chemistry Data

The quality of groundwater flowing from exposed bedrock units is an essential component of the UG water quality model. Groundwater monitoring for the Black Butte Copper project was initiated by Hydrometrics, Inc. in May of 2011 as part of a larger baseline study of flow, water levels, and water quality in the project area. The groundwater baseline data can be reviewed in detail in Appendix B of the MOP.

Monitoring wells and test wells have been completed within the shallow and deep stratigraphic units described above to define baseline water levels, groundwater flow directions and groundwater quality within the project area (**Table 2-1**). A series of paired monitoring wells (MW-1A, -1B; MW-2A, -2B; MW-4A, -4B; and MW-6A, -6B) were installed between 2011 and 2013 to document baseline conditions within the unconsolidated Quaternary/Tertiary clay-rich gravel deposits and in the underlying shallow bedrock groundwater system (**Figure 2-3**). Monitoring well MW-3 was also completed in November 2011 near the proposed terminus of the exploration decline within the UCZ. In 2014, an additional monitoring well, MW-9, was installed in the Ynl A zone above the sulfide and copper-enriched zones as a monitoring point to assess the effects of mine dewatering on overlying units during development.

An additional 10 test wells (PW-1 through PW-10) were installed for aquifer testing to provide hydrologic characteristics and water quality data for representative stratigraphic units. Of these wells, problems were experienced while drilling through the VVF in well PW-7, requiring the use of drilling muds which could not be fully purged from the well during development due to very low flow conditions. This has affected water quality data collected from this well, preventing their inclusion in the modeling work. As a conservative replacement, the water chemistry from PW-9 is used, which has the highest dissolved concentrations of all monitored wells.

Groundwater monitoring is conducted quarterly at 12 monitoring well sites and static water levels are measured quarterly at 22 additional test wells and piezometer sites. Water quality data have also been collected at ten test wells during site investigations; however, these wells are not routinely monitored during baseline monitoring events. In addition to baseline monitoring, a number of groundwater investigations have been conducted to characterize hydrostratigraphic units in the project area (Hydrometrics, 2012, 2013, and 2015). **Table 2-2** summarizes the groundwater quality data collected by Hydrometrics and the period of record available for each of the monitoring wells.

Table 2-1. Summary of Hydrostratigraphic Units and Associated Well Completions (from Hydrometrics, 2015)

Hydrostratigraphic Unit/ Structure	Monitoring Well	Test Well
Qa/Overburden	MW-1A MW-4A MW-6A	NA
Ynl (Dolostone)	MW-6B MW-7 MW-8	NA
Ynl-A	MW-1B MW-2A MW-2B MW-9	PW-1 PW-3 PW-8
USZ	MW-3	PW-2 PW-4
UCZ	NA	PW-9
Ynl-B	MW-4B	PW-10
LCZ	NA	PW-7
Yne	NA	PW-6N
Volcano Valley Fault	NA	PW-5
Buttress Fault	NA	PW-6

Figure 2-3. Location of Black Butte Copper Groundwater Monitoring Wells (from Hydrometrics, 2015)

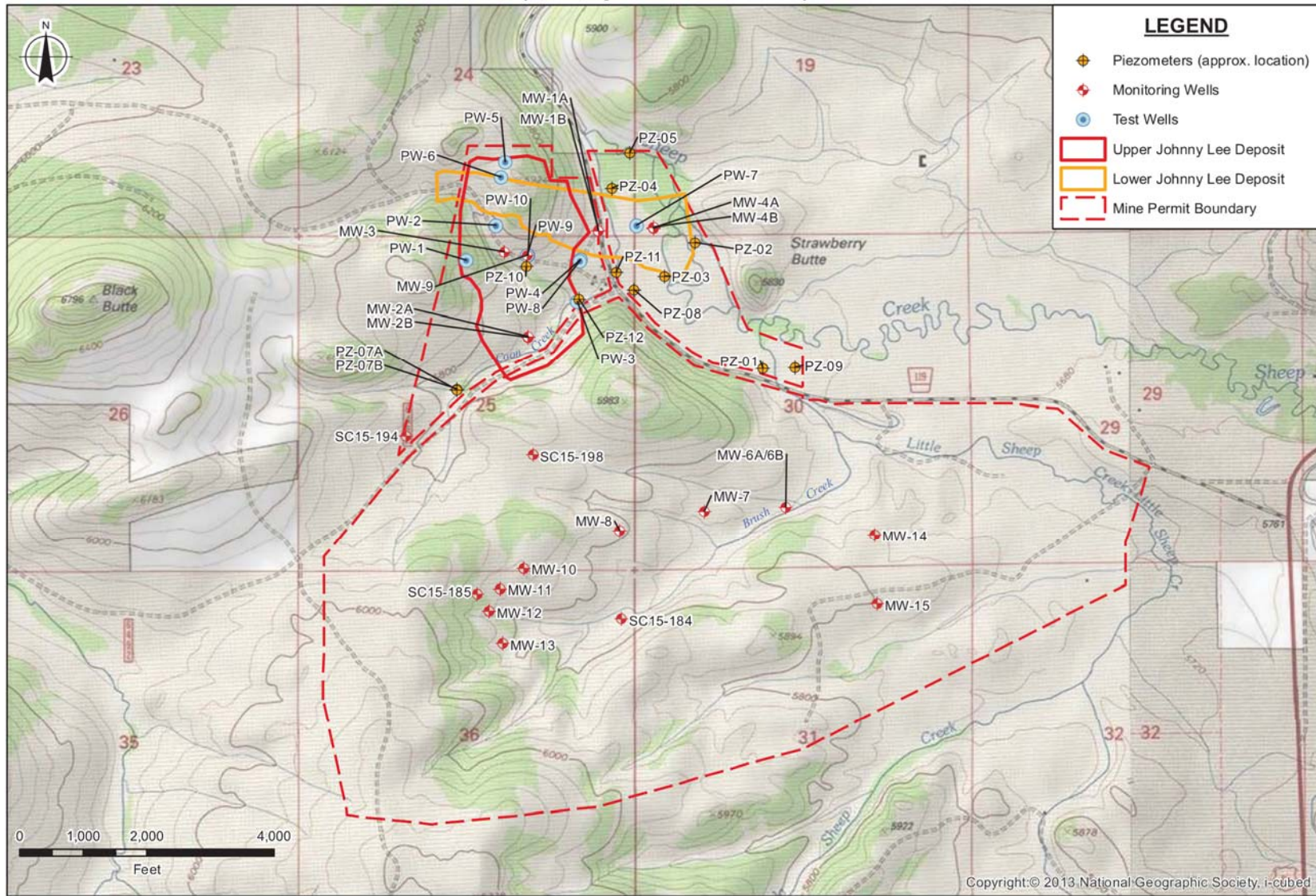


Table 2-2. Summary of Monitoring Wells from Groundwater Baseline Study, after Hydrometrics (2015)

Monitoring Site	Easting (meters)	Northing (meters)	Monitoring Frequency	Period of record	Flow or Water Level	Field Parameters	Lab Parameters	Comments
	UTM-WGS 1984 Zone 12							
Monitoring Wells								
MW-1A	506935.22	5180841.5	Quarterly	2011-2015	X	X	X	
MW-1B	506934.19	5180845.5	Quarterly	2011-2015	X	X	X	
MW-2A	506598.18	5180331.93	Quarterly	2011-2015	X	X	X	
MW-2B	506596.96	5180328.73	Quarterly	2011-2015	X	X	X	
MW-3	506484.1	5180740.2	Quarterly	2011-2015	X	X	X	
MW-4A	507201.5	5180855.4	Quarterly	2012-2015	X	X	X	
MW-4B	507200.1	5180858.5	Quarterly	2012-2015	X	X	X	
MW-6A	507809.2	5179492.9	Quarterly	2013-2015	X	X	X	
MW-6B	507792.8	5179490.7	Quarterly	2013-2015	X	X	X	
MW-7	507451.7	5179500.7	Quarterly	2013-2015	X	X	X	
MW-8	507036.0	5179398.3	Quarterly	2013-2015	X	X	X	
MW-9	506593.0	5180725.5	Quarterly	2014-2015	X	X	X	
SC15-184	507047.3	5178972.5	Quarterly	2015-2016	X	X	X	first monitoring July 2015
SC15-185	506355.5	5179094.2	Quarterly	2015-2016	X	X	X	first monitoring July 2015
SC15-194	506014.1	5179854.9	Quarterly	2015-2016	X	X	X	first monitoring July 2015
SC15-198	506621.4	5179854.9	Quarterly	2015-2016	X	X	X	first monitoring July 2015

Table 2-2. Sampling Summary for Baseline Monitoring Sites (continued)

Monitoring Site	Easting (meters)	Northing (meters)	Monitoring Frequency	Period of record	Flow or Water Level	Field Parameters	Lab Parameters	Comments
	UTM-WGS 1984 Zone 12							
Test Wells								
PW-1	506301.4	5180698.4	Quarterly	2011-2015	X	One Time	One Time	Lab Data from Pumping Test
PW-2	506443.2	5180865.0	Quarterly	2011-2015	X	One Time	One Time	Lab Data from Pumping Test
PW-3	506846.4	5180479.4	Quarterly	2012-2015	X	twice	twice	Lab Data from Pumping Test
PW-4	506901.8	5180688.3	Quarterly	2012-2015	X	One Time	One Time	Lab Data from Pumping Test
PW-5	506490.7	5181172.8	Quarterly	2013-2015	X	--	--	
PW-6	506468.1	5181097.9	Quarterly	2012-2015	X	--	--	Lab Data from Pumping Test
PW-6N	506468.1	5181097.9	Quarterly	2015	X	--	--	
PW-7	506846.2	5180695.5	Quarterly	2013-2015	X	twice	twice	Lab Data from Pumping Test
PW-8	506598.4	5180721.9	Quarterly	2014-2015	X	twice	twice	Lab Data from Pumping Test
PW-10	506593.6	5180721.9	Quarterly	2014-2015	X	twice	twice	Lab Data from Pumping Test
Piezometers								
PZ-01	507650.0	5180255.6	Quarterly	2012-2014	X	--	--	
PZ-02	507400.7	5180778.8	Quarterly	2012-2014	X	--	--	
PZ-03	507249.2	5180618.9	Quarterly	2012-2015	X	--	--	
PZ-04	506991.7	5181110.8	Quarterly	2012-2015	X	--	--	
PZ-05	507080.0	5181214.7	Quarterly	2012-2015	X	--	--	
PZ-07A	506258.4	5180074.7	Quarterly	Nov-14	X	--	--	
PZ-07B	506258.5	5180075.0	Quarterly	Nov-14	X	--	--	
PZ-08	507090.3	5180573.8	Quarterly	2014-2015	X	--	--	
PZ-09	507883.8	5180178.6	Quarterly	2014-2015	X	--	--	
PZ-10	ND	ND	One-Time	Nov-14	X	--	--	PW-8 Aq Test temporary piezometers
PZ-11	ND	ND	Twice	Nov-14, Mar-15	X	--	--	PW-8 Aq Test temporary piezometers
PZ-12	ND	ND	One-Time	Nov-14	X	--	--	PW-8 Aq Test temporary piezometers

2.4 Groundwater Flow Data

Hydrometrics, Inc. has developed a three-dimensional numerical groundwater model of the proposed Black Butte Copper Mine (Appendix M of the MOP). This model evaluates the effects of mine dewatering on groundwater and surface water in the vicinity of the project and estimates groundwater inflow to the mine working from different hydro-stratigraphic units that are encountered by the UG workings (**Table 2-3**). The maximum extent of drawdown at the top of the water table calculated by the model was in year 4, followed by gradual recession of the drawdown cone as stopes are backfilled with cement paste causing mine inflows to decrease. The water quality model herein uses estimated mine inflow rates at year 6 from the high storage sensitivity analysis to predict water quality during operations. These were selected as a conservative approach as the greatest inflow rates were simulated in the high storage sensitivity analysis. Groundwater flux through different hydro-stratigraphic units was provided by Hydrometrics for year 10 of post-closure. **Table 2-3** summarizes the mine inflow rates at year 6 and the post closure groundwater flux through different HSUs.

Table 2-3. Simulated Maximum Annual Inflow to Mine Workings (Hydrometrics, 2016b)

Mine Structure	Mine Inflow at Yr 6 (gpm)	Post Closure Groundwater Flux (gpm)
Surface Decline Total	111	99
Surface Decline (Ynl A)	102	91
Surface Decline (UCZ)	9	8
Upper Access and Stopes Total	287	8
UZ Access/Stopes (USZ/UCZ)	274	5
UZ Access (Ynl B)	13	3
Lower Decline Total	119	3
Lower Decline (Ynl B)	119	3
Lower Access and Stopes Total	27	1.3 (assume 0 in model)
LZ Access/Stopes (LCZ)	10	0.3
LZ Access (Ynl B)	17	1
Total Mine Inflow	544	111

2.5 Environmental Geochemistry Data

The acid generation and metal release potential of rock and tailings have been characterized using static multi-element analysis, acid-base accounting, net acid generation potential, and kinetic methods. Results are reported in the final report of environmental geochemical characterization in Appendix D of Tintina's Mine Operating Permit.

Waste rock from the Lower-Zone Footwall (*LZ FW*, 35% of waste rock tonnage), the Lower Newland shale below the *USZ* zone (*Ynl B*, 32%), the Upper Sulfide Zone (*USZ*, 28%), and the Lower Newland shale above the *USZ* (*Ynl A*, 4%) will be produced by the project. This rock will be exposed in underground access workings. It will also be stockpiled for up to 2 years on a lined surface pad prior to being co-disposed with cemented tailings early in mine

life. Tailings will also be produced and mixed into cemented paste, for use as backfill (4%) and placement in the surface cement tailing facility (up to 2%).

Waste Rock Geochemistry

A total of 5,642 whole rock samples of the four dominant waste rock lithotypes were analyzed to characterize overall geochemical variability within multiple rock units. Results of ABA and NAG tests indicate that the majority of *Ynl A* and *Ynl B* samples (90%) are unlikely to form acid, while many *USZ* and *LZ FW* samples have an uncertain potential or are likely to generate acid. Metal mobility predictions have been based on kinetic test results Appendix D, MOP).

Kinetic tests of *LZ FW* (2015), *Ynl B* (2012 and 2015), *USZ* (2012 and 2015), and *Ynl A* (2012) waste rock were completed following ASTM protocol D5744. The averaged humidity cell test (HCT) effluent data (weeks 1 to 4, as well as all weeks, which varied for each HCT) used as model inputs are presented for each of the relevant hydrostratigraphic units in Appendices A and B.

The four dominant waste rock units to be mined showed evidence of sulfide oxidation in the HCT tests. However, consistent with static test results and the presence of abundant carbonate mineralization, oxidation in the *Ynl B*, *Ynl A*, and *LZ FW* tests did not produce sufficient acidity to deplete alkalinity nor did these tests produce acidic pH values. Despite a duration of only 24 weeks, the 2012 *USZ* HCT of samples collected from the vicinity of the Johnny Lee Decline demonstrated notably lower sulfide oxidation than was observed even in the early weeks of the 2015 *USZ* test, which included samples collected site-wide. Furthermore, the 2012 test exhibited high alkalinity, almost no acidity, and pH was consistently above 7, which is demonstrably less acidity than was observed in the first 24 weeks, and thereafter, in the 2015 test. The pH in the 2012 test remained neutral throughout its 24 week duration, while the 2015 test maintained a neutral pH from week 3 through 45, after which pH became unstable and finally dropped in week 60, as was predicted by static tests. This reflects the variation in sulfide mineralization within the *USZ*. The 2012 test focused on samples collected from the *USZ* in the immediate vicinity of the Johnny Lee Decline, while the 2015 composite includes samples collected site-wide and includes copper-enriched rock access zones.

The concentrations of regulated metals were measured in HCT effluent from weeks 0, 1, 2, 4, and every 4 weeks thereafter. Despite maintaining neutral pH in the test cells, the *Ynl B*, *Ynl A*, and *LZ FW* units have shown potential to exceed surface water quality standards for some metals in early weeks of kinetic testing, but do not exceed groundwater standards after week 2. The 2012 *USZ* HCT exceeded Pb, Ni, and Tl groundwater standards in leachate from week 0, which is considered a product of sample preparation and was only included in the "all weeks" sensitivity analysis. Only Tl in week 1 exceeded groundwater standards after week 0, and is included in the base-case model. In contrast to low metal release in the 2012 *USZ* HCT, the 2015 sample exceeded groundwater standards for As, Be, Cd, Cu, Pb, and Ni in week 0 and some later weeks (included in "all weeks" sensitivity analysis). Groundwater exceedances were also observed in 2015 *USZ* effluent for Hg (weeks 1 and 2) and Sr and Tl (all weeks).

Tailings Geochemistry

Splits of homogenized tailings reject produced in bench-scale metallurgical testing were used in static and kinetic tests. Cement was added to provide structural strength in support of drift and fill mining methods underground, and to change the physical properties of the

material to a stable, non-flowable material with low hydraulic conductivity on the order of 10^{-8} cm/sec in both surface and underground settings. Static ABA and NAG tests indicate that the tailings will have a strong potential to generate acid, with or without paste amendment. The following tests have been used for the purpose of modeling, as described below.

Five conventional or modified HCTs (ASTM D5744) were conducted on cemented paste tailing cylinders and non-amended tailings, and diffusion tests (C1308) were performed on two cemented paste tailing cylinders, all of which are described in the Final Baseline Geochemistry Report of Waste Rock and Tailings (Enviromin, 2017). For modeling, the 4% paste cylinder diffusion test was used for predicting the underground conditions at closure, the 4% paste cylinder HCT was used for underground conditions during operations, and the 2% paste cylinder HCT was used for predictions in the CTF at operations and the 4% paste HCT was used for the CTF at closure.

Cemented paste tailing cylinders were tested (without crushing) using the conventional ASTM method D5744 (HCT) to simulate sub-aerial weathering in the underground (during operations) and the CTF, and in ASTM C1308 diffusion tests to simulate diffusion through backfill in saturated underground workings.

Despite the low ABA and NAG results, the 4% paste cylinder yielded largely neutral pH values, and low sulfate and metal release. This is a result of reduced surface area and limited oxidation reactions under saturated test conditions. The diffusion test data for the 4% cylinder (average of all data points) that were used as model inputs for the backfilled stopes are presented in Appendices A and B.

Rates of metal release were substantially lower in diffusion tests of saturated cement paste tailings than in unsaturated humidity cell tests of cemented paste tailings, because oxidation rates are greatly reduced under saturated conditions. Under unsaturated weathering conditions, all of the cemented paste tailings treatments have potential to oxidize after a lag time, with some release of sulfate, acidity, and metals if left exposed to air and water.

Acid and sulfate production in the HCTs varied between the cemented paste treatments, with the 2% test exhibiting greater release than the 4% test, which is reasonably attributable to rapid disaggregation. All tests began at a pH above 6. While the 2% cemented paste began to trend downward in pH between weeks 2 and 4, the 4% paste amended material held pH for several weeks, until sulfide oxidation began to increase in week 8. This suggests that the massive character and lateral support of cemented paste tailings is important in controlling sulfide exposure for oxidation.

Metal concentrations in effluent from the 4% paste cement backfill were lower, and in weeks 1-4 (used for modeling) only exceeded the groundwater quality standard for TI in week 4. Subsequently, exceedances of As, Be, Cr, Cu, Ni, and TI groundwater standards were observed. In the early weeks of testing, metal concentrations in effluent from the 2% cemented paste only exceeded groundwater standards for As, Ni, and TI. Concentrations of Sb, Be, Cu, U, and Zn, were observed to exceed groundwater standards in later weeks. Subsequent to week 4, frequent groundwater exceedances were observed, which is likely the result of disaggregation of the highly weathered, poorly confined cylinder geometry.

Tintina proposes to place 0.5 to 2% cemented paste tailings in its surface CTF, and to continuously collect and remove water from that impoundment. Importantly, the observed disaggregation in the 2% HCT did not occur immediately, and the rate of weathering in a

HCT is recognized to be greater than in the field, particularly for the small, unconfined cylinder of paste cement with a high surface area to mass ratio as was used in the HCTs. Therefore, in the CTF, each newly added lift of cemented paste tailings will behave as a massive block of material with low transmissivity, with a thin upper surface that will be exposed to some degree of oxidation before being covered by fresh paste tails within 60 days of placement. If material is covered in the manner described in the mine operation plan (generally within a week but never more than 60 days), oxidation, acidity, and leaching of metals would be limited to the immediate surface of the cemented paste tailings. Any water interacting with oxidized tailings will subsequently travel through the ramp and rock drain, where it will react with waste rock as it is collected for treatment to meet water quality standards prior to discharge in the infiltration galleries.

3 Modeling Approach

To predict impacts to water quality, Enviromin developed a mass-load model for i) the UG, ii) the temporary WRS pad, iii) the CTF, and iv) the combined input to the PWP. We predict a mass load for each facility under a base case scenario and various sensitivity scenarios. The model evaluates UG, CTF, WRS and PWP facilities under operational scenarios, and the UG and CTF at closure. For each facility and time, the mass-load solution is evaluated for equilibrium solubility and sorption constraints using the USGS PHREEQC geochemical model, as discussed below.

3.1 Mass Load Assumptions

The predicted water chemistries for each facility are divided by rock or material type and described using estimated water flows (Hydrometrics, 2015) and kinetic (or diffusion) test results, described in Section 2. The models scale the mass load (i.e., release of ions, metals, and protons) from each rock unit according to the reactive mass (or surface area, for diffusion test data) and the water flow. Scaling is appropriate because the surface area (or reactive mass) of bench scale test reactors (e.g., HCTs) differ from those anticipated under field conditions. To provide a final mass prediction in the collection sump for each facility, the mass contributed by each rock unit is added to the groundwater chemistry at each location, and then mixed together in the sump. This mass-load approach is conservative because it neglects phase removal at isolated, high-concentration sources. We assume an exposure time of one week for flow calculations and release rates, and because the available test data are generally based on one week of exposure. The models estimate water quality for each facility at future times that represent conditions during full operations and closure (if applicable).

- For the UG, we predict the water quality in the sump at year 6 of operation and at closure (i.e., >13 years). We divide the underground workings into seven rock units with estimated surface areas (Tintina operational plans), groundwater flow rates and chemistries (Hydrometrics), and kinetic test data (Enviromin). By design, the 4% cemented paste used underground for roof support will consume added water during the curing process; less than 1% water (by weight) will be released during the consolidation within the stopes so this is not included in the mass load model (AMEC, 2016, Appendix K7 of Tintina's MOP). In the sump, the flow rates and chemical inputs from all seven units are mixed and allowed to precipitate and sorb according to PHREEQC.
- For the WRS, we estimate a reactive mass based on the volume of waste rock that could be saturated in six months of flow. After one year, the average flow, based on HELP model predictions is 0.9 gpm (Hydrometrics, 2016a). The saturated reactive mass was then converted to a surface area based on an assumed distribution of blast fragments (Hyle, 2016). The HCT data were then scaled to the appropriate rock type using surface area data.
- For the CTF, we estimate the water quality at year 6 of mining, and at closure (i.e., >13 years). We assume that the entire surface of the cemented tailings facility is exposed to an estimated precipitation rate of 84,000 m³/yr (Knight Piesold, 2015). The surface includes 2% paste tailings during operations with an average of 4,000 tonnes of co-deposited waste rock that is assumed to be exposed to weathering at any given time. A portion of the runoff (10%) is also exposed to the waste rock used to construct the ramp/basin drain. During operations, we include water that releases from the wet paste, which has higher water content to ensure pumpability and due to

atmospheric precipitation onto the CTF (see AMEC, 2016b, Appendix K-7 of Tintina's MOP). Water comprising 5% of the paste deposited each week by weight (i.e., 29,029 m³/yr) was represented using water chemistry measured in process water during metallurgy tests. At closure, we assume the surface to be 4% cemented paste tailings.

- For the PWP, we use the predicted chemistry for the CTF at year 6 of tailings production. We add direct precipitation and runoff, RO brine, and water from the mill. We equilibrate the mixed solution with PHREEQC to estimate the chemistry of water reporting to the WTP.

3.2 Geochemical Modeling of Mineral Precipitation and Metal Sorption

Enviromin estimates equilibrium conditions of the mixed solutions using the USGS code PHREEQC (Parkhurst and Appelo, 1999), which has been rigorously tested and is the industry standard for aqueous geochemistry. We used the *minteq.dat* thermodynamic database supplied with version 3.1.1-8288 version of PHREEQC. Redox conditions were determined based on the recognized pe/pH conditions in natural water, as reported by Baas Becking in his time honored study of water worldwide (1960). For the UG during operations, and CTF at closure, we set $pe + pH = 13$, to represent moderately oxidizing conditions within the open workings. During UG closure, we set $pe + pH = 7$, to represent a more suboxic environment in the flooded and backfilled mine workings. In the surface facilities, i.e. WRS, PWP and CTF during operations, we set $pe + pH = 15$ to represent the fully oxidizing surface environment modeled for these settings. Charge is initially balanced on magnesium, and charge is maintained by balancing on pH after reactions occur. Appendix C shows an example input model, for the UG model at year 6.

At the sump of each facility, we predict the mineral phases that will precipitate and the metals that will sorb to precipitated iron oxide (specifically, ferrihydrite). In the event of supersaturation, the following phases were allowed to precipitate: alunite, celestite, gypsum, K-jarosite, barite, Ba₃(AO₄)₂, gibbsite, ferrihydrite, fluorite, quartz, MnHPO₄, SbO₂, and Cr₂O₃. These minerals were chosen based on initial supersaturation in some solutions, and general likelihood to occur in mine-affected water associated with the Black Butte Copper deposit. Understanding the saturation states of these minerals is not only important to predict water quality, but also to assess potential mineral scaling in the system.

Table 3-1. Mineral Phases Allowed to Precipitate in PHREEQC Modeling

Equilibrium Phase	Ideal Formula	Rationale for Inclusion in PHREEQC Model
Alunite	$K_2Al_6(SO_4)_4(OH)_{12}$	Primary control on aluminum in mine affected water (Eary, 1999).
Celestite	$SrSO_4$	Oversaturated in sump water.
$Ba_3(AsO_4)_2$	$Ba_3(AsO_4)_2$	Close to saturation in sump water
Barite	$BaSO_4$	Primary control on barium (Eary, 1999).
K-jarosite	$KFe_3(SO_4)_2(OH)_6$	Common secondary product of sulfide oxidation
Cr_2O_3	Cr_2O_3	Oversaturated in sump water.
Ferrihydrite	$5Fe_2O_3 \cdot 9H_2O$	Major control on iron. Thermodynamic properties well defined (Dzombak and Morel, 1990). Sorption substrate for various metals and oxyanions.
Quartz	SiO_2	Close to or saturated in sump water
Fluorite	CaF_2	Primary control on fluoride (Eary, 1999).
Gibbsite	$Al(OH)_3$	Primary control on aluminum at pH >4.5 (Eary, 1999). Oversaturated in sump water.
Gypsum	$CaSO_4 \cdot 2H_2O$	Primary control on sulfate in mine pit lakes (Eary, 1999). Close to saturation in sump water
$MnHPO_4$	$MnHPO_4$	Primary control on manganese at circum-neutral pH (Eary, 1999). Oversaturated in sump water
SbO_2	SbO_2	Close to saturation in sump water

Metals are allowed to sorb to ferrihydrite precipitated from modeled solutions under oxidizing conditions using the default PHREEQC parameters for sorption site surface area and density of strong/weak sites in diffuse layer calculations (Parkhurst and Appelo, 2013). All metals with ferrihydrite sorption isotherm data provided in the *minteq.dat* database were allowed to potentially sorb. Sorption to sulfide minerals stable under reducing conditions (based on isotherms which are not incorporated in the PHREEQC database) were calculated using published isotherm data.

3.3 Sensitivity Analyses

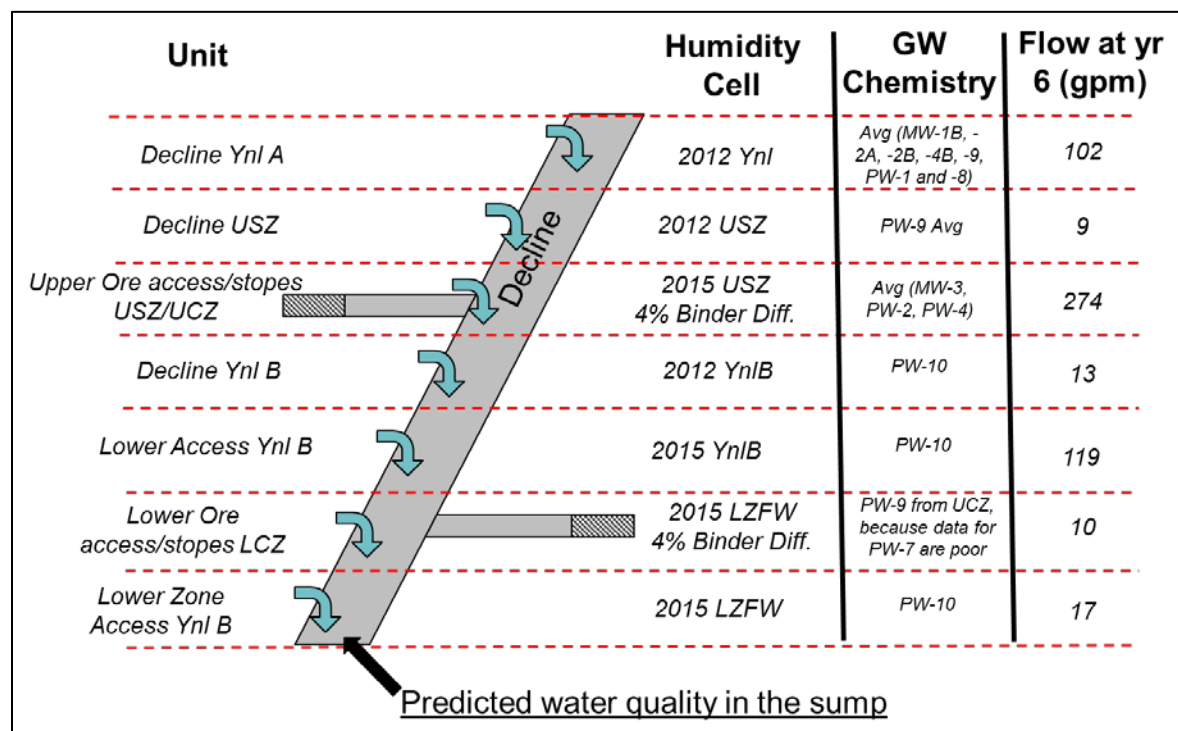
To evaluate uncertainty in model predictions, we assessed the sensitivity of the models to key assumptions and input parameters. These sensitivity scenarios, which vary between the UG, WRS, CTF, and PWP models, are summarized here and as Appendix D to this report, and presented in detail for each model in Sections 4, 5, 6, and 7 below.

4 Underground Workings Water Quality Model

4.1 Conceptual Model

The access tunnels, decline, access workings and stopes, will transect various rock types in the subsurface, as shown in **Figure 4-1**. To be consistent with groundwater flow data (from Hydrometrics, 2016b), we divided the underground model into seven hydrostratigraphic units, each providing input to the sump.

Figure 4-1. Conceptual model of the seven hydrostratigraphic units, each providing input to the sump



Each of the units was assigned a total flow input, a surface area (based on operational plans), and a rock type that correlates with kinetic test data. For the model, each unit can be conceptually viewed as a large kinetic test, scaled based on surface area and flow rate. The scaling approach is described in detail in Section 4.3.3. The mixed solution incorporating inflow from all seven units is allowed to reach geochemical equilibrium, using PHREEQC, and then the water reports to the water treatment facility.

The quality of water in the UG was predicted during operations at year 6 and post-closure, following rebound of the groundwater to original elevation. The assumptions and inputs used in these base cases are compared with changes made in sensitivity analyses in Appendix D. For the UG at year 6 of operations, the sensitivity of modeled predictions was tested by halving and doubling the base case fracture density; using an average of HCT data from all weeks instead of weeks 1-4; increasing the base case oxidation rate from 6 to 40 kg/m²/yr; increasing the fracture zone thickness from 1 to 2 m; increasing the reactive

zone thickness to 15 m; doubling the area of paste backfill; and testing the combined influence of oxidation rate, fracture zone thickness, fracture density, and backfill surface area assumptions on the reactive mass calculations. The reactive mass scenario compounds conservatism by using upper bound values for all of the assumptions together in a highly conservative prediction of water quality. In the post-closure model for the UG, factors affecting modeled sulfide oxidation (oxidation rate, fracture density, rim thickness, etc.) are no longer relevant under suboxic conditions. The sensitivity analyses for the UG closure model therefore evaluate the influence of doubling backfill surface area and tests the effect of propagating detection limits through the mass load calculations. Supporting evidence for these assumptions and inputs is provided below.

4.2 Data Sources

The model incorporates groundwater flow and chemistry data and geochemistry data from kinetic tests to predict future underground water quality. These data are describe below.

4.2.1 Groundwater Quality Data

To represent groundwater chemistries, the model uses data collected from wells, listed under GW Chemistry in **Figure 4-1**. Appendix E summarizes the groundwater chemistry provided by Hydrometrics and used to develop averages for wells and hydrostratigraphic units. These data varied in the number of samples collected per well (over time) and the number of wells completed in each lithotype. Additionally, the parameters analyzed for individual samples varied. In some cases, data were reported both above and below method detection limits, and in other instances, all results were reported below method detection limits. The reported method detection limits were used as values when analyzing the data. For all of these reasons, the data were thoroughly evaluated from a quality control standpoint. Statistical methods were used to test for the presence of outliers in the data prior to their inclusion in the water quality model. Also, well PW-7, which was contaminated by drill fluids, was excluded from use in the modeling calculations.

Enviromin evaluated the full groundwater data set to identify and possibly reject any results that failed due to statistical or quality assurance/quality control (QA/QC) criteria. The data were provided to Enviromin in a spreadsheet format by Hydrometrics, Inc. As discussed below, out of a total of 2,490 data points, only six were rejected as statistical outliers and none were rejected due to QA/QC issues.

4.2.1.1 Representative Data

Some rock types have larger data sets and thus narrower confidence intervals than others. This is the result of more wells used to characterize the rock type as well as more sampling events. Limited data for certain rock types relative to others does not imply the data misrepresents groundwater in those rock types, but there is greater uncertainty in the model input parameters derived from the smaller data sets.

4.2.1.2 Average Calculations

We evaluated seven different groundwater-bearing rock types and used data from 13 monitoring wells within those rock types, listed in **Figure 4-1**. The 13 monitoring wells are not evenly distributed among the seven rock types. Further, the single well (PW-7) completed in the LZ FW produced so little water that it could not be properly developed; resulting water quality issues have led to its exclusion from this analysis. Water quality data from PW-9, conservatively representing the poorest quality groundwater from the UCZ, was used to represent the LZ FW.

The number of monitoring events ranged from sixteen events for MW-1B to a single event for wells PW-1, PW-2, PW-4 and PW-10. The number of monitoring events per well is indicated in parentheses for each well in

Table 4-1, which total 91 individual well-specific monitoring events.

Table 4-1. Wells Used for Groundwater Input Data

(number of monitoring events per well); UA, underground access; LD, lower decline

Ynl A	USZ/UCZ	UCZ	Ynl B-UA	Ynl B-LD	LCZ	Ynl B-LA
MW-1B (16)	MW-3 (13)	PW-9 (5)	PW-10 (1)	PW-10 (1)	PW-9 (5)	PW-10 (1)
MW-2A (14)	PW-2 (1)					
MW-2B (14)	PW-4 (1)					
MW-4B (13)						
MW-9 (3)						
PW-1 (1)						
PW-8 (5)						

Some 29 to 31 groundwater parameters were used as model input parameters, depending on the sampling event. This is because phosphorus and silicon were included in only a small number of laboratory analyses from certain wells, so in many cases the number of parameters totaled only 29. Laboratory results were below detection for a large number of many analytes, and for all censored values, the detection limit was used.

With a total of 91 well-specific monitoring events, the maximum number of data points in the evaluation is 2,821 based on 31 groundwater parameters per well per event. However, as discussed above, because phosphorus and silicon were included in only small number of laboratory analyses, the actual number of total data points in the full data set used for groundwater input is 2,490.

For each rock type, the average value of each of the 29 to 31 input parameters was calculated using all of the statistically valid data (see below) provided by Hydrometrics. The number of significant figures in the average calculations was determined by the value for each analyte with the fewest number of decimal places. For most of the laboratory results, the number of significant figures remained constant for a given analyte throughout all monitoring events in a set, although there were some instances where results had a different reporting limit.

4.2.1.3 Three Sigma Evaluation

Enviromin performed a statistical evaluation of the data set to ensure the groundwater data set represented each of the seven hydrostratigraphic units. Groundwater input parameters consist of various parameters and analytes reported by Energy Laboratory of Billings, Montana for groundwater samples collected from multiple wells at the site by Hydrometrics. The data were provided to Enviromin by Hydrometrics as tabulated spreadsheet entries.

Enviromin used the "empirical rule" of statistics to identify outliers, which were excluded from the averages used as individual model input values. For a normal distribution of random data points, the "three sigma test," states that 68 percent of the data in the set fall within one

standard deviation (σ) of the mean (μ) of the full set, 95 percent fall within two standard deviations (2σ), and 99.7 percent fall within three standard deviations (3σ). Therefore, any result larger than the mean plus three standard deviations was rejected, i.e.,

$$\text{If Value} > \mu + 3\sigma, \text{ then reject.}$$

For laboratory results that were below reporting limits, the value of the reporting limit was used in the calculations. Furthermore, in events where both a natural and duplicate sample were collected, only the natural sample was used in the calculations.

Additionally, Enviromin also looked at Energy Laboratory's internal data quality assurance/quality control evaluation and the subsequent data QA/QC evaluation conducted by Hydrometrics conducted on all laboratory groundwater data and concluded that the data used to establish model input parameters are valid.

The results of the three sigma evaluation of the groundwater data are summarized below in **Table 4-2**. As shown in the table, only 6 out of 2,490 data points were rejected as outliers from the three-sigma evaluation. Furthermore, all of those rejected data points came from the two largest data sets, i.e., Ynl A and USZ/UCZ which had 1,769 and 429 data points, respectively.

Table 4-2. Three Sigma Evaluation Results Groundwater Input Data

	Ynl A	USZ/UCZ	UCZ	LCZ	Ynl B Upper Access	Ynl B Lower Decline	Ynl B Lower Access	Totals
Total Data Points	1,769	429	144	58	30	30	30	2,490
Rejects	4	2	0	0	0	0	0	6

4.2.1.4 QA/QC Evaluation

Hydrometrics J-flagged many results. None of the values failed internal laboratory quality assurance/quality control criteria, but instead the results were qualified due to issues with relative percent differences between natural and duplicate samples. Specifically, in any event in which the RPD between a natural sample and a duplicate sample result exceeded 20 percent, not only was the result of that analyte J-flagged for that particular sample, but as a conservative measure, the results for that particular analyte were J-flagged for all samples collected during the sampling event.

However, in evaluating data quality, failure of the RPD criteria does not warrant rejection of a result, either for the natural sample for which the RPD was exceeded or for any of other results in the full data set. Therefore, none of the J-flagged results in the data set were rejected on that or any other quality assurance/quality control criterion.

4.2.2 HCT Data

Chemical contributions to groundwater of each hydrostratigraphic unit are based on the baseline geochemistry testing conducted since 2011. Specifically, these data are from seven kinetic humidity cell tests (HCTs) and one diffusion test: the Ynl A, Ynl B, and USZ HCTs from 2012, and the Ynl B, LZ FW, USZ, and 4% cement HCTs from 2015, as well as the diffusion test of tailings with 4% cement. We used an average of HCT data for weeks 1-4. Due to the initially high solute release rate in weeks 1 and 2 of most HCT data, data from weeks 1-4 represents a reasonable, relatively conservative approach to modeling inputs because early solute release rates are often the high relative to subsequent weeks. To

address model sensitivity to this approach, an average of all weeks (available at the time the modeling was conducted) was also used as a sensitivity analysis for the UG model.

For the paste backfill during operations, we use data from the 4% cement HCT, averaged over weeks 1-4. For the closure model, we use the average diffusion test data for 14 samples were collected over 11 days, to account for the saturated conditions and longer-term exposure. The averages used as model inputs are presented in Appendix A of this report. All original geochemical test results, used in calculating averages, have been presented in the Final Baseline Geochemistry Evaluation of Waste Rock and Tailings (Appendix D, MOP).

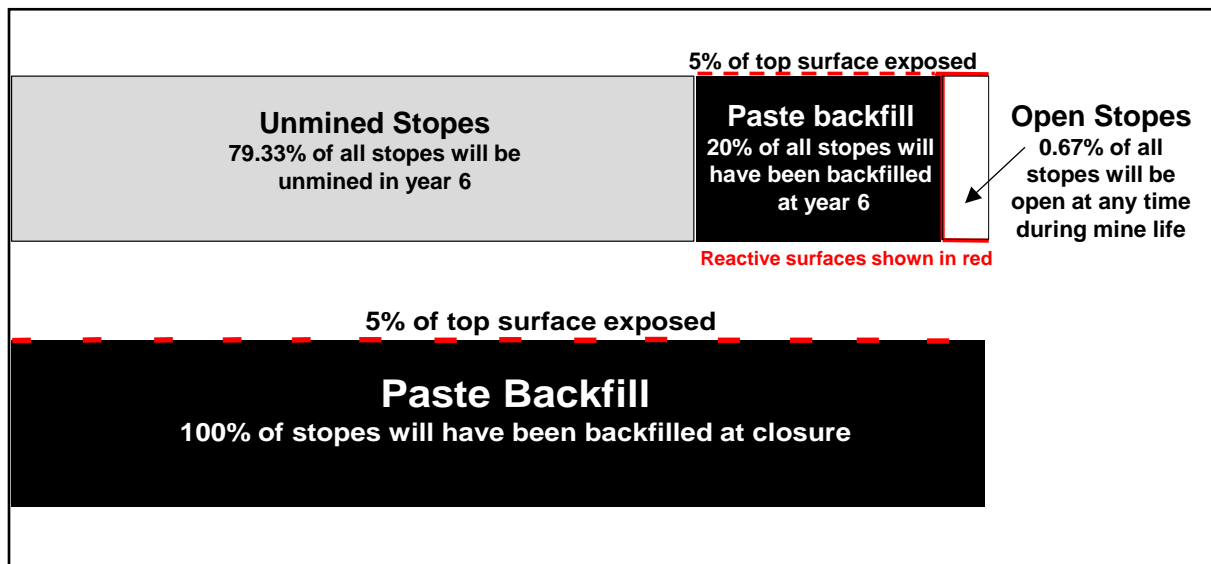
4.3 Mass Load Model Calculations

4.3.1 Surface Area Calculations

For each lithostratigraphic unit, Enviromin estimates open tunnel lengths based on the projected mine schedule for stope development in the upper and lower workings (Tintina MOP, 2015). Consistent with Tintina's design, the tunnels are assumed to be 5 m across and 5 m high and provide the basis to calculate the open surface area, including the back (roof) and sill (floor) walls. Surface areas for the year 6 underground model assume the conditions projected for the start of year 6 and are, therefore, based on surfaces exposed during years 1-5 of mine life. At that stage, Tintina has projected that approximately 20% of the stopes will have been mined and backfilled. Furthermore, Tintina proposes to have 0.67% of the stopes open at any given time in the mine life. Surface areas used for the closure scenario in the underground model assume that the mining is complete and all mined stopes have been backfilled, as proposed by Tintina. In contrast to the 2% material that will be used to fill the CTF, which will be made with excess water to ensure adequate flow during placement, the 4% cemented paste tailings used in the underground workings will be made with a limited volume of water to ensure compressive strength. It will also cure in a warm underground stope where it will be exposed to dry ventilation air, thus promoting hydration of the binder material and ensuring that very little water (less than 1% by weight) will be discharged in the underground workings (AMEC, 2016b, Appendix K-7 of Tintina's MOP). For these reasons, dewatering water is not included in the UG model.

To calculate the reactive mass of the paste backfill, which has much lower transmissivity, Enviromin has not assumed an equivalent porous media model as was done for the fractured walls. Rather we estimate the surface area of the backfill and scale it to the surface area of the samples used in diffusion tests. At year 6, ~20% of the stopes will have been backfilled; at closure, 100%. For the reactive surface of the backfilled paste, we assume that a 5-inch gap exists above 5% of the paste backfill surface; this conservatively represents the reality that backfilling process will leave some pockets where complete filling is not accomplished. Our estimate of 5%, which is based on 3rd party observation of paste backfilling operations at an existing underground mine (where similar methods are currently in use) is likely conservative, as the proactive management contemplated by Tintina improves the completeness of backfill and subsequent filling of adjacent stopes will provide lateral secondary backfilling (AMEC, 2016a, Appendix K-6 of Tintina's MOP). The size of the gap (i.e., 5") is not as relevant as the fact that it exists, and therefore exposes the reactive surfaces shown in red in **Figure 4-2**.

Figure 4-2. Conceptual Model of Surface Area Within Backfilled Stopes at Year 6 (above) and at Closure (below).



In addition to the stopes and backfills, we include the surface areas of all ramps and access tunnels, based on the primary lithologies of the workings. The final surface areas are summarized in **Table 4-3**.

Table 4-3. Surface Area Values for Year 6 and Closure

<u>Hydrometrics Hydrostratigraphic Categories</u>	<u>Contributions from Table 1 in Mine Development.pptx from Tintina</u>	<u>Calculated surface areas @ Year 6</u>	<u>Calculated surface areas @ Closure</u>
Surface Decline YNL A	Ynl under water table (a total of 740 meters with 495 meters below the water table)	9,900	9,900
Surface Decline UCZ	USZ (ramp) (60 meters)	1,200	1,200
UZ Access/Stopes (USZ/UCZ) + Ceiling of backfilled UZ stopes	Sum Open Access/stopes of USZ (3640 m) and linear feet of open stopes (770 m = 11 open stopes at 70 m) + 5% of the ceilings in backfilled stopes	91,545	72,800
UZ access Ynl B	Ynl B (UZ access (2500 meters)	50,000	50,000
Lower Decline Ynl B	Ynl B ramp (3170 meters)	63,400	63,400
Lower Zone Access, grouped with stopes in Hydrometrics classification	LZ FW (LZ access, 4720 meters)	94,400	<i>*94,400</i>
LCZ Stopes (LCZ)+ ceiling of backfilled LZ stopes	Linear feet of open stopes (350 meters = 7 open stopes @ 50 m) + 5% of ceilings in backfilled stopes	8,713	-
Lower Zone Access (Ynl B)	LZ FW (ramp, 1240 meters)	27,280	<i>*27,280</i>
Paste Tailings backfill-UZ	5% of ceiling of backfilled block. Ceiling dimension = total linear meters mined in USZ in years 3-5 multiplied by width of paste block.	3,346	14,653
Paste Tailings backfill-LZ	5% of ceiling of backfilled block. Ceiling dimension = total linear meters mined in USZ in years 3-5 multiplied by width of paste block.	1,714	<i>*13,176</i>
<i>* Lower zone surface areas have no effect at closure because the flow rate is assumed to be zero</i>			

4.3.2 Calculation of Reactive Mass

Using estimated surface areas, as described in Section 4.3.1, the reactive mass (R_m) of each fractured wall surface was estimated according to

$$R_m = S * F_D * T_{RZ} * \rho,$$

where S is the surface area (m^2 , shown in **Table 4-3**), F_D is the fracture density, ρ is the rock density, (kg/m^3), and T_{RZ} is the thickness of the reactive zone. The density of each rock type was estimated using measurements conducted by Tintina; $3,600 kg/m^3$ for Upper and Lower Copper Zones, and $2,710 kg/m^3$ for Ynl units, respectively.

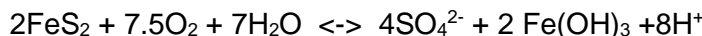
As an equivalent porous media model (EPM), F_D accounts for the difference in the surface area of a fractured volume and the surface area of unconsolidated HCT material. In other words, the finely-ground, unconsolidated material in HCT samples would have an F_D of 100%. At the opposite extreme, rock that is entirely impermeable would have an F_D of 0%. In the base case model, we assume an F_D of 10% in the upper zone, extending 1 meter from the wall surface, meaning that the fractures induced by the blasts have a reactive surface area that is 10% of the surface area of HCT material. A 10% F_D is conservative because it is on the high end of previously reported studies of pit walls fracture densities, which would be under less lithostatic pressure than subsurface workings and would be expected to have higher fracture density (Siskind and Fumanti, 1974; Kelsall et al., 1984). Beyond the 1-m fractured zone, we assume an F_D of 1% in one scenario, where we test a sensitivity to a 15-m oxidized, reactive zone. In the lower units we assume a F_D of 2% in the fractured zone, which is based on a higher lithostatic load and is supported by 2-3 lower orders of magnitude observed permeability in those units. We evaluate model sensitivity by changing F_D to twice the base case (i.e., 20% for upper unit and 4% for lower unit) and to half the base case (i.e., 5% and 1%).

The base case model assumes that T_{RZ} has a maximum of 1 meter, i.e. the limit of the fractured zone. Early reports (Kelsall 1984, and Siskind and Fumanti, 1974) indicate that blast fracturing in granite and basalt walls is generally limited to a depth of 1 meter, beyond which rock porosity was unchanged by blasting. Kelsall et al. (1984) also show that typical values range from 0.3 m to 1.0 m, so our estimate is conservative. We evaluate model sensitivity to this assumption by using a 2-meter maximum fractured zone in a sensitivity scenario. In another sensitivity scenario, we assume a 1-m fractured zone and a reactive zone up to 15 m.

While the maximum T_{RZ} in the base case is determined by fracture penetration from blasting, the actual T_{RZ} , and thus the R_m , is a function of oxidation of the sulfide minerals. Once the initial fracturing occurs, the reactive zone grows as oxygen diffuses from inside the tunnel and oxidizes sulfide minerals. Kempton et al. (2009) point out that physical processes (i.e., oxygen diffusion) are more important than chemical processes for determining intrinsic rate coefficients for sulfide oxidation, as suggested by the “shrinking core” model (Davis et al., 1986). The oxygen profile in the rock, and thus the sulfide oxidation rate, is related to sulfide content because the conversion of sulfide to sulfate consumes oxygen (Davis, 1983).

The base case model assumes an oxidation rate of $6 kg SO_4^{2-}/m^2/year$, based on observations and models describing rates of oxidation in pit walls (Kempton et al., 2009). Field observations reported by Kempton and Atkins (2009) suggest a maximum of $6 kg SO_4^{2-}/m^2/year$, while models have indicated an initial maximum rates of sulfide oxidation of $21 kg SO_4^{2-}/m^2/year$, with a subsequent decline to a value of $10 kg SO_4^{2-}/m^2/year$. A value of $40 kg SO_4^{2-}/m^2/year$ was reported for fresh surfaces on a pit bench. For a sensitivity

analysis, we use 40 kg SO₄/m²/year. To convert from these rates to a mass of sulfide oxidized, we assume the stoichiometry of the following reaction:



The actual calculation of R_m proceeds as follows:

$$R_m(\text{kg}) = \left(X \frac{\text{kg SO}_4}{\text{yr} * \text{m}^2} \right) \left(\frac{\text{kmol SO}_4}{96 \text{ kg SO}_4} \right) \left(\frac{\text{kmol S}}{\text{kmol SO}_4} \right) \left(\frac{32 \text{ kg S}}{\text{kmol S}} \right) \left(\frac{\text{kg rock}}{Y \text{ kg S}} \right) \left(\frac{2 \text{ kmol S}}{\text{kmol FeS}_2} \right) \left(\frac{2 \text{ kmol FeS}_2}{4 \text{ kmol SO}_4} \right) * S(\text{m}^2) * A(\text{days}) * \left(\frac{1 \text{ yr}}{365 \text{ days}} \right)$$

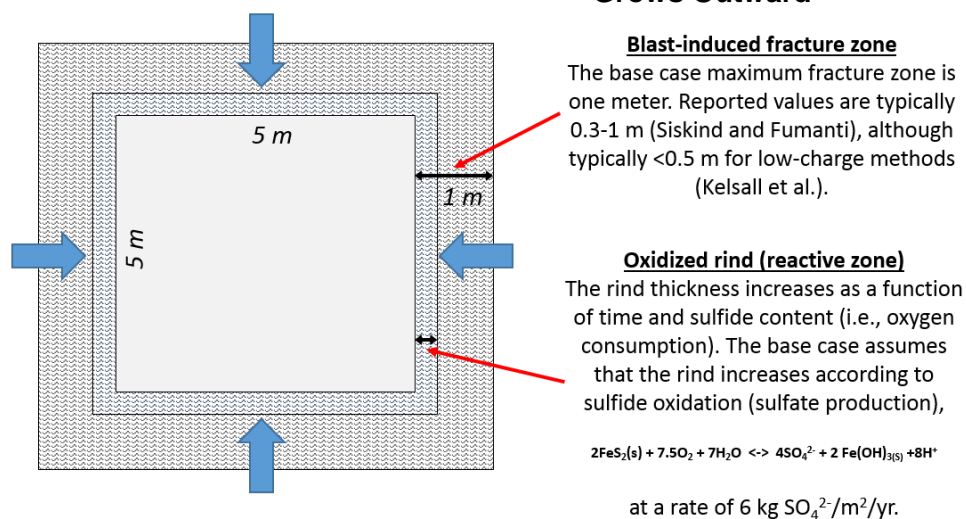
1. Use the sulfide oxidation rate ($X = 6 \text{ kg SO}_4/\text{m}^2/\text{year}$ in the base case) to calculate the mass SO₄²⁻ after A days of exposure.
2. Convert SO₄²⁻ produced to FeS₂ oxidized, based on the stoichiometry above
3. Convert mass of FeS₂ oxidized to mass of rock oxidized, (based on Y , the mass fraction of sulfur in the rock):

Hydrogeologic Units	YNL-A	USZ	USZ/UCZ	Backfill	YNLB-UA	YNLB-LD	LCZ	LZ FW	Backfill	YNLB-LA
HCTs	HCT - 2012 Ynl	HCT - 2012 USZ	HCT - 2015 USZ	2015 4% binder cyl. Diff. test	HCT - 2012 Ynl B	HCT - 2015 Ynl B	HCT - 2015 LZ FW	HCT - 2015 LZ FW	2015 4% binder cyl. Diff. test	HCT - 2015 LZ FW
Sulfide Source (n)	2012, 2015, and other Ynl A subsets ABA (44)	2012, 2015, and other USZ subsets ABA (39)	2012, 2015, and other USZ subsets ABA (39)	-	2012 and 2015 Ynl B subsets ABA (34)	2012 and 2015 Ynl B subsets ABA (34)	LCZ Whole Rock (198)*	LZ FW subset ABA (15)	-	LZ FW subset ABA (15)
Average % sulfide	1.6%	20.0%	20.0%	-	1.1%	1.1%	11.3%	1.9%	-	1.9%

4. Convert the mass of rock oxidized (R_m) to a T_{RZ} , based on the density of the rock, according to $R_m = S * F_D * T_{RZ} * \rho$. If the calculated T_{RZ} is less than 1 meter, then we use the calculated value for R_m . If the calculated T_{RZ} exceeds 1 meter, then we fix T_{RZ} at 1 meter and recalculate an R_m based on the rock density.

Figure 4-3 shows a cross-section of the maximum reactive zone, based on fracture penetration of one meter. The reactive zone (i.e., oxidized rind) grows over time, from the inside, as sulfide oxidizes. For the access tunnels, we assume that oxidation has occurred for 6 years, thus increasing the reactive thickness accordingly. We assume that flow infiltrates through the reactive zones on all four sides of the tunnels.

Figure 4-3. Schematic Cross-Section of Mine Workings with an Oxidized Zone That Grows Outward



4.3.3 Scaling of HCT Data to Reactive Mass

The model estimates the release of components in each unit based on data from humidity cell tests (HCTs). HCTs have a known volume of water, reactive mass of rock, and time of exposure. For each rock type that releases a component at a rate (\dot{r}), we scale HCT results based on the assumption that the concentration, C_i , of the released component (e.g., metals, protons, etc.) is proportional to the ratio of reactive mass (or surface area) to the volume of water per time (i.e., flux, Q). That is,

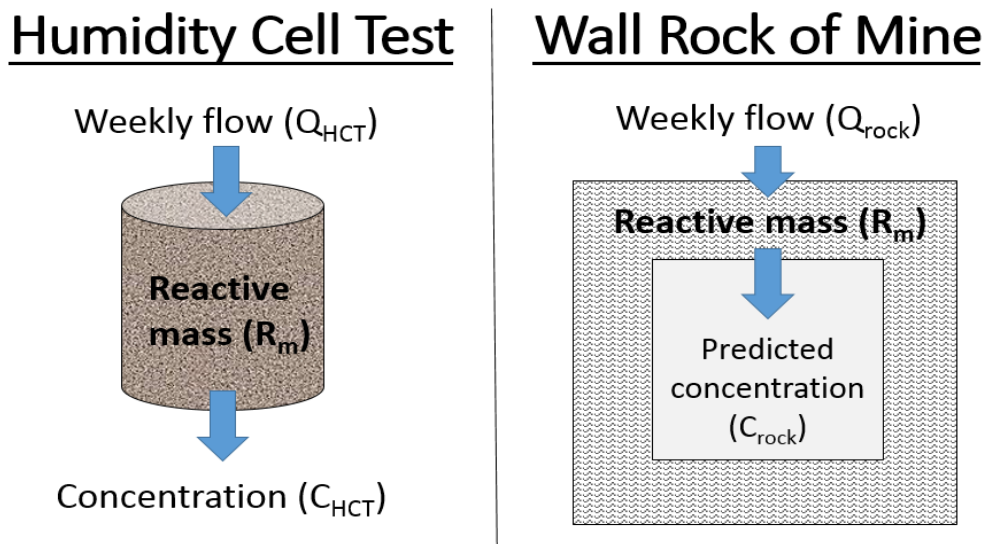
$$C_i = \frac{\text{Reactive mass } (R_m)}{\text{Volume of water per time } (Q)} \dot{r}.$$

Because (\dot{r}) is an intensive property of the material, we can use the proportionality ($C_i \propto R_m/Q$) to estimate the concentration of each constituent (i) released from the rock in the field ($C_{rock,i}$), according to

$$C_{rock,i} = \frac{(R_m/Q)_{rock}}{(R_m/Q)_{HCT}} C_{HCT,i}.$$

Figure 4-4 provides a visual description of how inflow (Q) into each known mass (R_m), then reacts to produce a concentration (C).

Figure 4-4. Schematic Showing Scaling of HCT Data to Predict Chemistry in the Wall Rock



In the model, the ratio of $(R_m/Q)_{rock}$ to $(R_m/Q)_{HCT}$ is referred to as the “scaling factor” because it provides a value that directly scales the field “reactor” to the lab “reactor”. After estimating the contribution of the rock from the scaling factor, we add the baseline groundwater contributions (data Appendix E), according to

$$C_{predicted,i} \left(\frac{mg}{L} \right) = C_{rock,i} \left(\frac{mg}{L} \right) + C_{groundwater,i} \left(\frac{mg}{L} \right).$$

Finally, we combine the contributions from all seven units to predict the mass load in the final solution in the sump. This mixed solution is then modeled using PHREEQC to evaluate the potential for precipitation and sorption.

4.4 Geochemical Modeling of Underground Water

For each solution that collects in the sump, the model allows precipitation of the following phases: alunite, celestite, gypsum, K-jarosite, barite, quartz, $Ba_3(AsO_4)_2$, gibbsite, ferrihydrite, fluorite, $MnHPO_4$, SbO_2 , and Cr_2O_3 . These phases were chosen based on supersaturation in calculated solutions, as well as general likelihood of occurrence in mine-affected water. If the solution is not supersaturated in one of the identified phases, then there is no effect on the solution. Dissolution of precipitated minerals or bedrock is not allowed in the model; these reactions are represented empirically by the accelerated weathering environment of the HCT.

If ferrihydrite is supersaturated, then sorption of metals is allowed on the surface using the default parameters for ferrihydrite surface area and sorption site density and isotherm data provided with the PHREEQC *minteq.dat* database (Parkhurst and Appelo 2013, Appendix C). Under reduced conditions, as would exist following saturation of the bedrock and cemented paste fill in the UG at closure, sorption to iron sulfide is calculated using published sorption isotherm data and mineralogy (Appendix F). This mechanism is included because pyrite is known to adsorb a variety of metals common to mining environments (Doyle et al., 2004; Borah and Senapati, 2006; Oxverdi and Erdem, 2006) and has been proposed for use in reactive barrier technology to remove metals from contaminated groundwater (Brown et al. 1979).

4.5 Water Quality Prediction for Year 6 Operations

For year 6 of operations, **Table 4.4** shows the predicted chemistry of the base case and all sensitivity analyses. We also provide the baseline groundwater chemistry and groundwater standards according to MT DEQ. We estimated a NO_3^- concentration of 33 ppm (as N) based on values from an effectively managed underground Montana mine currently in operation (Hydrometrics, 2017). This is because NO_3^- release will depend on future blasting practices and is difficult to predict in advance. The use of these data as a proxy for Tintina's planned blasting practices is reasonable. The mass loads calculated for each input source are shown in Appendix G.

The base case model predicts neutral to mildly acidic water during UG operations. The mass load calculations suggest that the greatest load of metals, acidity, and sulfate comes from the UCZ unit. As the groundwater flow rate from the UCZ is lower, this contribution is substantially diluted by cleaner water from the Ynl A and Ynl B units. Furthermore, the load contributed by the UCZ unit would decrease if the model allowed supersaturated phases to precipitate prior to mixing in the sump. While this is the more likely "real world" scenario, thermodynamic modeling of individual inputs prior to mixing would be time consuming for multiple sensitivity scenarios. By accounting for mineral precipitation and metal sorption after mixing, we have been conservative in our approach to predicting mass load, as all solute input to the model reports to the sump.

The predicted water quality for the year 6 underground base case suggests a slight decline in alkalinity to 183 mg/L, with an associated decrease in pH from 7.09 to 6.67. These changes are in response to sulfide oxidation during mining operations, as indicated by a

50% increase in sulfate to a predicted concentration of 304 mg/L. The abundant carbonate mineralization in the exposed lithotypes clearly provides neutralization potential in buffering acidity resulting from sulfide oxidation, and the extent of predicted oxidation is low at neutral pH. Alunite, $Ba_3(AsO_4)_2$, Cr_2O_3 , ferrihydrite, and quartz are predicted to be supersaturated in the base case, providing substrate for sorption of As, Ba, Be, Cd, Cu, Ni, Pb, and Zn. In the oxidizing environment of the active workings, no sorption to sulfide minerals was allowed.

The resulting predicted chemistry shows little change for many metals. The concentrations of Al, Fe, Ba, and As are reduced as a result of mineral precipitation. The concentrations of NO_3^- , Cu, F, Mn, Ni, Sb, Se, Tl, U and Zn in the sump water are predicted to increase (above background concentrations) prior to collection for treatment to meet non-degradation standards. Of these, only NO_3^- and U are predicted to exceed Montana DEQ groundwater quality standards in the operational base case and multiple sensitivity scenarios (**Table 4.4**). Arsenic exceeds water quality standards in the reactive mass and combined high reactive mass sensitivity scenarios. Arsenic also exceeds the standard in groundwater under background conditions, however, and only rises above the background concentration in the reactive mass and combined high reactive mass sensitivity scenarios. Likewise, the background concentration of Sr in groundwater is elevated above the MT DEQ standard of 4 mg/L; predicted concentrations under elevated oxidation rate and high reactive mass sensitivity scenarios are also higher than background. Thallium is predicted to exceed the standard in the conservative elevated sulfide oxidation rate scenario, while Sb is predicted to exceed the groundwater standard only in the combined high reactive mass scenario. In general, the assumptions about fracture density and reactive-zone thickness have the greatest effect on predicted metal release, and the inclusion of all week HCT data has the greatest effect on the pH. The predicted value of 33 mg/L nitrate (as N) assumes that no denitrification occurs during operations, when the workings will be fully ventilated. As noted, this value will depend considerably on operational blasting practices. Because all water will be collected during operational dewatering for treatment to meet non-degradation criteria prior to discharge, these predicted changes will not affect downgradient water quality.

The various sensitivity analyses show relatively minor variation in predicted pH (4.87-6.68), alkalinity (180-207), and sulfate (262-672 mg/L) across a range of changes: fracture density; HCT input; increasing the sulfate production rate to a maximum value of 40 kg/m²/yr; doubling of the oxidation zone to 2 meters; increasing the reactive zone potential to 15 meters; and doubling of the backfill surface area. Metal concentrations vary somewhat between sensitivity analyses (**Table 4-4**), and appear to be more sensitive to surface area assumptions (fracture density and reactive zone thickness) than to sulfide oxidation rates, which more directly influences pH and sulfate concentrations. Even in the high reactive mass sensitivity scenario (right side of Table 4-4), which incorporates conservative sensitivity values for multiple parameters, including the maximum oxidation rate, a 2 m rim thickness, and twice the backfill surface area and fracture density, pH is predicted to be 6.39, with 207 mg/L alkalinity and 672 mg/L sulfate. Metals are elevated in this scenario, with U, Tl, Sr, Sb, and As exceeding groundwater standards, although it is highly unlikely that all of these parameters would concurrently increase to theoretical maximum values in the underground workings at year 6. Regardless, these results show that any attendant uncertainty associated with the base case UG water quality predictions is modest. Despite these predicted changes in water quality, they are not material because water will be collected during operational dewatering of the workings for reverse-osmosis treatment to meet non-degradation criteria.

4.6 Water Quality at Closure

As the mine floods, stored oxidation products (which will have accumulated on some exposed surfaces during operations) will be flushed out of access workings that were not backfilled. Tintina proposes to flood the workings with treated RO permeate and pump water for treatment until steady state conditions develop in the saturated and backfilled workings. Enviromin has estimated that 3 to 6 rinses would be sufficient to remove soluble oxidation products from the workings, based on humidity cell test results for the *YnIB* and *USZ*, which are the rock types that would remain exposed at closure. The rate of RO injection will then be diminished to allow reduced groundwater to flood the workings. The basis for this analysis is described in Appendix N of this document. Reduced groundwater flowing through remaining voids will react with the exposed paste and bedrock surfaces, as described in **Section 4.3.2**. This model predicts chemistry under saturated, post-filling conditions.

Several parameters change in the closure model. We assume that all stopes are closed and backfilled, and that groundwater recovers to its original elevation. The decline and a portion of the access development will remain open, but it will be flooded creating suboxic conditions so that sulfide oxidation will not occur. At the relatively neutral pH of the system, iron oxide will precipitate, so oxidation by ferric iron is not a concern. Further, because the hydrostratigraphic units below the Volcano Valley Fault are predicted to contribute very little if any water in closure, and will be isolated from the upper workings by a hydraulic plug, they are not considered to function as aquifers post-closure (Hydrometrics, 2016b). They are therefore not included in the closure model. Changes in flow and flow ratios shift background groundwater quality slightly, compared to operating conditions. The estimated flow rates are shown in **Table 2-3**. **Table 4-5** shows the predicted water chemistry at steady state closure for the base case, as well as an analysis of model sensitivity to doubling backfill surface area. The mass load calculated for each input term is shown in Appendix H. Background groundwater chemistry, MT DEQ standards for groundwater quality and estimated non-degradation criteria for groundwater are included in Table 4-5 (Hydrometrics, 2016, in Appendix N1 of Tintina's MOP). We estimated an NO_3^- concentration of 3.30 ppm (as N) based on the assumption that 90% of the nitrate would be removed via denitrification under sub-oxic conditions within the flooded workings at closure. Denitrification (the conversion of NO_3^- to NO_2^- and N_2 gas) by native heterotrophic bacteria, is a common and highly efficient process under low oxygen conditions when carbon is available. Due to the low diffusivity of oxygen in water and low predicted flow of water in the mine post-closure, as well as the elevated carbon content of the lower Newland shales, denitrification is very likely to occur at a high level of efficiency, removing virtually all nitrate. As noted previously, the actual concentration of nitrate will be determined by blasting practices.

Table 4-4. Model Predictions for Underground Water Quality at Year 6 of Operations

		Mixed Groundwater with No Mine Influence	Underground model predictions at yr 6, after PhreeqC									Groundwater Standards (MT DEQ-7)
			BASECASE (HCT wk1-4, 1 m max rind, Fracture density 10% in UZ and 2% in LZ, Oxid. Rate = 6 kg/m2/yr)	Fracture density one half basecase	Fracture density twice basecase	All HCT data of wall rock	Oxid. Rate = 40 kg/m2/y	2 m fracture zone thickness	15 m reactive zone	Paste backfill surface area doubled	Combined High Reactive Mass Parameters (Oxid Rate 40, 2-meter rind, fracture density x2, backfill Sx2)	
pH	s.u.	7.09	6.67	6.68	6.65	4.87	6.55	6.65	6.64	6.51	6.39	na*
Al	mg/L	0.014	0.012	0.011	0.017	0.229	0.013	0.017	0.018	0.017	0.082	na
Alkalinity	mg/L CaCO ₃	218	183	180	188	182	183	188	188	183	207	na*
As	mg/L	0.051	0.004	0.002	0.010	0.068	0.004	0.010	0.010	0.005	0.101	0.01
Ba	mg/L	0.049	0.00122	0.00167	0.00075	0.00896	0.00167	0.00075	0.00076	0.00160	0.00034	1
Be	mg/L	0.0008	0.0006	0.0005	0.0008	0.0011	0.0007	0.0008	0.0008	0.0007	0.0020	0.0040
Ca	mg/L	76	89	83	100	89	103	100	103	89	141	na
Cd	mg/L	0.000045	0.000045	0.000045	0.000045	0.000045	0.000045	0.000045	0.000045	0.000045	0.000045	0.005000
Cl	mg/L	1.29	1.38	1.35	1.44	1.43	1.64	1.44	1.45	1.40	1.86	na*
Cr	mg/L	0.007	0.00066	0.00064	0.00070	0.01044	0.00089	0.00070	0.00072	0.00097	0.00147	0.1
Cu	mg/L	0.0019	0.0007	0.0006	0.0009	0.3693	0.0011	0.0009	0.0009	0.0009	0.0068	1.3
F	mg/L	0.64	1.14	0.90	1.60	0.83	1.16	1.60	1.67	1.14	2.63	4
Fe	mg/L	1.81	0.0024	0.0023	0.0025	0.0057	0.0031	0.0025	0.0025	0.0034	0.0024	na**
Hg	mg/L	0.000006	0.000006	0.000006	0.000006	0.000006	0.000006	0.000006	0.000006	0.000006	0.000006	0.002000
K	mg/L	3.4	11	8	17	10	12	17	18	11	37	na
Mg	mg/L	47	60	54	72	54	75	72	75	60	112	na
Mn	mg/L	0.146	0.165	0.162	0.172	0.186	0.313	0.172	0.173	0.166	0.334	na**
NO ₃	ppm as N	0.02	33.0	33.0	33.0	33.0	33.0	33.0	33.0	33.0	33.0	1
Na	mg/L	11	14.7	13.1	17.8	14.7	15.0	17.8	18.4	14.7	27.9	na
Ni	mg/L	0.004	0.007	0.005	0.009	0.049	0.010	0.009	0.009	0.007	0.017	0.1
P	mg/L	0.011	0.003	0.002	0.005	0.012	0.003	0.005	0.005	0.003	0.021	na
Pb	mg/L	0.001	0.00002	0.00002	0.00004	0.00112	0.00002	0.00004	0.00004	0.00002	0.00255	0.015
SO ₄	mg/L	205	304	262	388	284	398	388	405	305	672	na**
Sb	mg/L	0.0015	0.0032	0.0025	0.0046	0.0023	0.0033	0.0046	0.0047	0.0032	0.0089	0.006
Se	mg/L	0.0005	0.0039	0.0024	0.0069	0.0017	0.0042	0.0069	0.0073	0.0039	0.0151	0.05
Si	mg/L	8.78	1.55	1.55	1.55	1.54	1.55	1.55	1.55	1.55	1.54	na
Sr	mg/L	10.5	10.5	10.4	10.8	10.4	11.4	10.8	10.8	10.5	12.1	4
Tl	mg/L	0.001	0.002	0.002	0.002	0.002	0.005	0.002	0.002	0.002	0.006	0.002
U	mg/L	0.005	0.037	0.021	0.069	0.028	0.038	0.069	0.069	0.037	0.133	0.03
Zn	mg/L	0.029	0.030	0.029	0.032	0.040	0.031	0.032	0.033	0.031	0.041	2

Supersaturated phases in basecase: Alunite, Ba₃(AsO₄)₂, Cr₂O₃, ferrihydrite, quartz
See discussion of sensitivity scenarios in Section 4.1.

empirical prediction of endpoint, not based on modeling

*narrative standards may exist

**secondary standard

Results include the mass load from the seven lithological units, precipitation of supersaturated phases and sorption on ferrihydrite, based on PHREEQC models.

Table 4-5. Model Predictions for Underground Water Quality after closure

		Underground model predictions at closure, after PhreeqC			Groundwater Standards (MT DEQ-7)	Estimated Groundwater Non-degradation Criteria
		BASECASE	Paste backfill surface area doubled	Detection limits = 0		
pH	s.u.	6.81	6.77	6.81	na*	6.0-7.8
Al	mg/L	0.015	0.016	0.015	na	0.058
Alkalinity	mg/L CaCO ₃	144	147	144	na*	na
As	mg/L	0.0000	0.0000	0.0000	0.01	0.064
Ba	mg/L	0.0169	0.0159	0.0169	1	0.1928
Be	mg/L	<i>0.0002</i>	<i>0.0003</i>	<i>0.0001</i>	0.004	0.00095
Ca	mg/L	64	71	64	na	na
Cd	mg/L	0.000042	0.000042	0.000042	0.005000	0.0008
Cl	mg/L	1.7	2.0	1.7	na*	na
Cr	mg/L	0.00048	0.00052	0.00048	0.1	0.025
Cu	mg/L	<i>0.0002</i>	<i>0.0003</i>	<i>0.0001</i>	1.3	0.1970
F	mg/L	<i>0.36</i>	<i>0.40</i>	<i>0.33</i>	4	1.2
Fe	mg/L	0.00	0.00	0.00	na**	na
Hg	mg/L	0.000006	0.000006	0.000006	0.002	0.000010
K	mg/L	2.9	3.8	2.9	na	na
Mg	mg/L	22.1	20.9	22.1	na	na
Mn	mg/L	0.053	0.054	0.051	na**	na
NO ₃	ppm as N	3.30	3.30	3.30	1	7.5
Na	mg/L	4.8	5.3	4.8	na	na
Ni	mg/L	<i>0.0049</i>	<i>0.0057</i>	<i>0.0042</i>	0.1	0.025
P	mg/L	0.001	0.001	0.001	na	na
Pb	mg/L	0.00001	0.00001	0.00001	0.015	0.0028
SO ₄	mg/L	115	124	115	na**	250**
Sb	mg/L	0.0032	0.0037	0.0032	0.006	0.002
Se	mg/L	<i>0.0009</i>	<i>0.0012</i>	<i>0.0005</i>	0.05	0.0085
Si	mg/L	1.55	1.55	1.55	na	na
Sr	mg/L	2.1	2.2	2.1	4	6.48
Tl	mg/L	0.0037	0.0038	0.0037	0.002	0.0039
U	mg/L	0.00504	0.00511	0.00497	0.03	0.008
Zn	mg/L	<i>0.018</i>	<i>0.021</i>	<i>0.015</i>	2	0.317

Italicized predictions affected by detection limit propagation in the model *narrative standards may exist
prediction of endpoint, not based on modeling **secondary standard
 Supersaturated phases in basecase: Ba₃(AsO₄)₂, barite, Cr₂O₃, ferrihydrite, gibbsite, quartz

Results include precipitation of supersaturated phases and sorption to ferrihydrite and sulfide.

Diminished oxidation due to flooding, completion of backfilling, and reduced inflow of water from below the VVF produces the base case chemistry shown in **Table 4-5**. While the predicted pH and alkalinity are lower than background groundwater quality, and a bit lower than the quality predicted underground during operations, predicted pH is 6.81 with 144 mg/L alkalinity and a sulfate concentration of 115 mg/L. No parameters fail to meet MT groundwater standards or non-degradation criteria in post-closure groundwater. Our sensitivity analysis shows that propagation of detection limits for censored (less than detect) values results in overestimation of increased concentrations for Be, Cu, F, Ni and Zn. This is shown in Table 4-5 where the italicized values illustrate the predicted value when the detection limits are removed and replaced with zero.

The minerals Ba₃(AsO₄)₂, barite, Cr₂O₃, ferrihydrite, gibbsite, and quartz, are predicted to be oversaturated, and their precipitation influences the water quality prediction as shown in **Table 4-5**. Sorption of several metals, notably As, Cu, Ni, Sr, Tl, U and Zn, to precipitated ferrihydrite reduces their concentrations, as does sorption of Cd and Hg to pyrite (described in Appendix F).

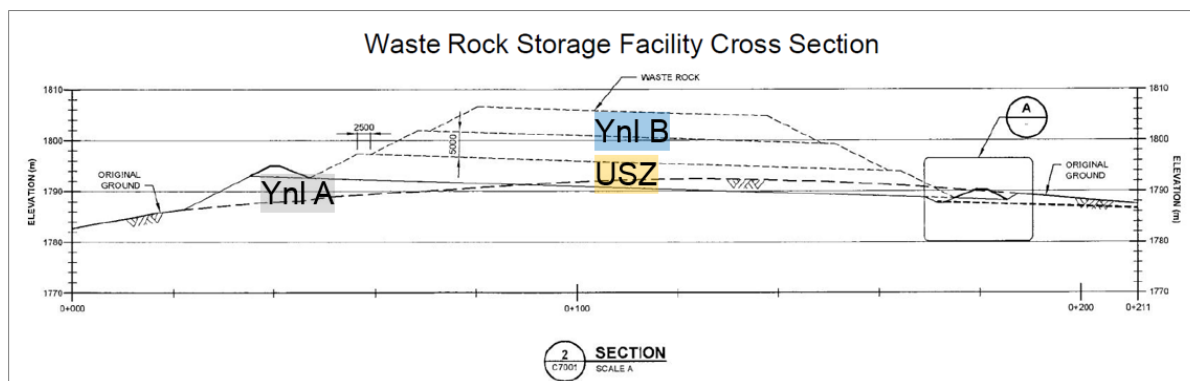
5 Waste Rock Storage Facility Water Quality Model

5.1 Conceptual Model

Approximately 411,537 tonnes (453,642 tons) of waste rock will have been generated from the Ynl A, USZ, and Ynl B at the end of year 2 of mining operations. This rock will be stockpiled on a temporary, lined waste rock storage (WRS) facility before it can be placed in or co-disposed with tailings in the cemented tailings facility (CTF). The WRS will be constructed in three 16-ft lifts, with 8-foot benches, up to a maximum height of 50 ft (15 m) above a 100 mil thick HDPE-lined pad (**Figure 5-1**). Additional waste rock to be produced from the LZ FW and LCZ after CTF construction begins will report directly to that facility and will not be placed on the stockpile. The waste rock has potential for acid generation and metal leaching (see Section 2.4.2 of the Tintina Operating Permit Application).

The model assumes that three types of waste rock will be stored on the WRS facility: Ynl A will be deposited first, followed by USZ and then Ynl B, based on the order they will be encountered during mine development (**Figure 5-1**). The LZ FW will not be produced for placement on the WRS pad. Therefore the model incorporates the relative tonnages of the remaining rock types that will be present on the WRS pad, i.e., 6.25% Ynl A, 43.75% USZ, and 50% Ynl B. However, all of this mass is not assumed to be reactive: rather, we estimate the reactive mass based on the maximum material that could be saturated by six months of water flow at the estimated flow rate (0.9 gpm). Precipitation is assumed to flow preferentially through the partially saturated waste rock after an initial year of wetting and collects in a drain system that then reports to the water treatment facility. The purpose of this model is to predict the chemistry of water that collects in the drain prior to treatment.

Figure 5-1. Conceptual Model of Waste Rock Storage Facility (from Knight Piesold)



The assumptions and inputs used in the WRS base case are compared with changes made by halving and doubling the reactive mass in the sensitivity analyses described in Appendix D. Functionally, these changes also represent the effect of halving or doubling duration of infiltration, porosity, or waste rock surface area. Supporting evidence for these assumptions and inputs is provided below.

5.2 Data Sources

5.2.1 Waste Rock HCT Data

The environmental geochemistry testing methods and assumptions were described in section 2.5. For the WRS facility, we use HCT data from 2012 Ynl to describe the Ynl A portion, 2015 USZ to describe the USZ portion, and 2015 Ynl B to describe the Ynl B

portion. For consistency with other models, data from week 1 to 4 were averaged for use in the model. Due to the short operating life of the WRS, use of the early weeks of testing is particularly appropriate. Appendix A shows these data.

5.2.2 Water Balance

Hydraulic behavior at the proposed WRS facility was modeled by Hydrometrics, Inc., using the Hydrologic Evaluation of Landfill Performance (HELP) model, developed by the Army Corps of Engineers (Hydrometrics 2016a; Shroeder et al., 1994). The HELP model uses climate data to predict one-dimensional moisture flow through a soil profile, accounting for evapotranspiration, snow removal, solar radiation, and average precipitation. The HELP model predicts an average flow rate of 4.31 L/min (0.9 gpm) through the WRS facility, once steady state saturated flow is achieved after year 1.

5.3 Mass Load Model Calculations

5.3.1 Calculation of Reactive Mass and Surface Area

The flow rate (4.31 L/min) is very low in relation to the size of the WRS facility, so it is not reasonable to assume that all of the waste rock surface will be saturated and exposed to infiltration at the end of year 2. To account for this, we conservatively estimate a reactive mass by calculating the amount of rock that can be saturated by 4.31 L/min of flow for one year. We chose one year as a calculation time frame based on the approximate time that it takes to establish a steady-state seepage, according to the HELP model.

To calculate the reactive mass, we start with the yearly water flow, 1,785,551 L/yr based on 4.31 L/min. We assume that the unconsolidated rock pile has 40% porosity to calculate the volume of rock that could be saturated. Lastly, using the density of the rock, we calculate the reactive mass for each rock type (*i*). The overall equation is

$$R_{m,i}(\text{tonnes}) = \frac{L_{H2O}}{yr} * \frac{1000 \text{ cm}^3_{H2O}}{L_{H2O}} * \frac{6 \text{ cm}^3_{rock}}{4 \text{ cm}^3_{H2O}} * \frac{g_{rock}}{\text{cm}^3_{rock}} * \frac{\text{tonne}_{rock}}{10^6 g_{rock}} * \frac{\text{tonne}_i}{\text{tonne}_{rock}}$$

The resulting calculation suggests that ~2% of the total WRS material is exposed to infiltrating meteoric water and is thus reactive. Using R_m , we then calculate a reactive surface area R_{SA} of each rock type by using a published gradation of run of mine waste rock from the underground workings of the Ashanti mine (**Figure 1-2**, from Hyle, 2016, Appendix D2 of Tintina's MOP) to predict the surface area of future waste rock for Black Butte Copper. This rock size gradation is representative of particle size distributions in rock mined using typical blasting practices. While some changes will exist between the gradation for Ashanti and the Black Butte Copper mine, this uncertainty that has been addressed through sensitivity analysis, by doubling and halving the surface area.

Figure 5-2. Waste Rock Gradation from Ashanti Mine (Hyle, 2016)



<u>Diameter (inch)</u>	<u>Mass %</u>
7.87	27.4
3.9	28.6
2.1	23.8
1.1	8.3
0.5	6
0.3	3.6
0.07	2.4

Assuming that the particles are spherical, the specific surface area is calculated to be 0.0559 m²/kg for the USZ and 0.0743 m²/kg for the Ynl B and Ynl A. The difference is based on the different rock densities (all calculations shown in the model). The spherical assumption underestimates true surface areas but is consistent with the spherical assumption in the surface area estimate for the humidity cell test material. Assuming that the sphericity of the particles is similar in the two cases, this assumption balances out when we scale the surface area between the two HCT samples and the blasted waste rock.

For the waste rock samples in the humidity cell tests, the reactive surface area was estimated from sieved analyses. From these calculations, assuming spherical particles, the specific surface areas are 2.01 m²/kg for USZ, 2.94 m²/kg for Ynl A and 3.01 m²/kg for Ynl B.

5.3.2 Scaling of HCT Data to Reactive Surface Area

For the waste rock water quality prediction, we use an approach to scaling that is similar to the UG model (Section 4.3.3) to predict mass load. Rather than scaling to a reactive mass within a fractured, equivalent porous media (EPM) model, we scale the WRS material to reactive surface area. We do this because the WRS material is unconsolidated and particle sizes (i.e., surface areas) control reactivity; fracture-density and rind-thickness estimates are thus not applicable.

The model estimates the release of components in each unit based on data from humidity cell tests (HCTs). HCTs have a known volume of water, reactive mass of rock, and time of exposure. For each rock type that releases a component at a rate (\dot{r}), we scale HCT results based on the assumption that the concentration, C_i , of the released component (e.g.,

metals, protons, etc.) is proportional to the ratio of reactive surface area to the volume of water per time (i.e., flux, Q). That is,

$$C_i = \frac{\text{Reactive surface area } (R_{SA})}{\text{Volume of water per time } (Q)} \dot{r}.$$

Because (\dot{r}) is an intensive property of the material, we can use the proportionality ($C_i \propto R_{SA}/Q$) to estimate the concentration of each constituent (i) released from the rock in the field ($C_{WRS,i}$), according to

$$C_{rock,i} = \frac{(R_{SA}/Q)_{WRS}}{(R_{SA}/Q)_{HCT}} C_{HCT,i}.$$

In the model, the ratio of $(R_{SA}/Q)_{WRS}$ to $(R_{SA}/Q)_{HCT}$ is referred to as the “scaling factor” because it provides a value that directly scales the field “reactor” to the lab “reactor.” The final solution after mass-load estimation is input into PHREEQC to allow for precipitation and sorption to ferrihydrite.

5.4 Predicted Water Quality at Year 2 of Mining

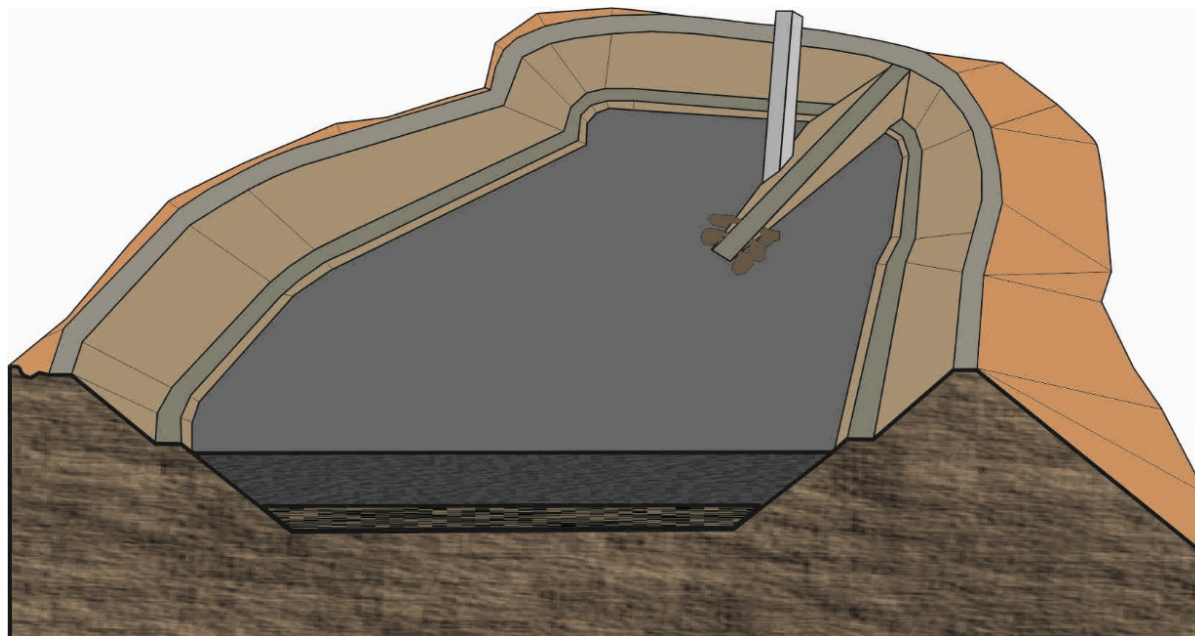
Table 5-1 shows the predicted chemistry of water draining from the WRS facility at year 2, in addition to the baseline groundwater chemistry and the MT DEQ groundwater standards for comparison. The sensitivity analyses (i.e., 0.5x and 2x) can be interpreted in a few ways: if the model assumes a 0.5x value for surface area, the effect is identical to assuming 0.5x infiltration time or 0.5x reactive mass. The same logic applies to the 2x scenario. Because we base the estimate of reactive mass on water infiltration over months, then a change in the precipitation would have no effect – i.e., the higher surface area is negated by the proportional water for dilution. The mass loads calculated for each input source are shown in Appendix I.

The model predicts a pH of 5.80 for the base case, where saturated flow occurs in 1% of the waste rock. Predicted sulfate concentration is high, at 2,212 ppm in the base case. This is likely conservative, due to dissolution of solutes from the HCT (with higher surface area and a higher water:rock ratio) into a very small predicted volume of water. We estimated a NO_3^- concentration of 344 ppm (as N) based on average values from the East Boulder Stillwater mine (Hydrometrics, 2017), although the actual concentration will vary with blasting practices. The predicted pH is 6.10 in the sensitivity scenario with the reactive mass halved and 5.48 in the sensitivity scenario with the reactive mass doubled. The model is very sensitive to rock/water ratio (e.g., changes in infiltration relative to surface area). Minerals predicted to precipitate in the base case include alunite, barite, celestite, and jarosite, based on PHREEQC predictions. No sorption was predicted due to the absence of ferrihydrite. Several metals increase in proportion to changes in infiltration/surface area in sensitivity analyses, together with SO_4^{2-} , but of these, only NO_3^- , Sr and Tl exceed the MT DEQ groundwater standard in the base case.

The waste rock on the temporary WRS pad will be stored on a liner with a small estimated volume of water reporting from the WRS pad liner drainage system to the lined contact water pond (CWP) where it will be collected for treatment until rock is placed into the CTF. Waste rock leachate will be treated to meet non-degradation criteria.

to the co-deposited waste rock. Water will additionally be introduced through dewatering of the wet 2% cement paste tailings. Unlike the 4% cement pasted tailings, which will be mixed to provide strength in roof support underground, the 2% cement paste tailings will have water added to ensure flow during deposition. Every day the mine will generate 2,900 tonnes of paste; on average, 55% will be deposited in the CTF and the remainder will go underground. From the deposited paste, as much as 5% of the mass will seep out as water, producing 29,029 m³/yr (AMEC, 2016b Appendix K-7 of Tintina's MOP).

Figure 6-1. Conceptual Model of CTF Showing Waste Rock Ramp and Local Placement of Waste Rock Mined from UG, Year 6 of Tailings Production



Using the estimated surface areas of the paste and the waste rock, we estimate mass-load inputs by scaling to the appropriate humidity cell test of pasted tailings, ultimately predicting water quality in the sump. The model further evaluates the predicted sump water quality with a PHREEQC geochemical model, allowing precipitation of supersaturated phases and sorption to ferrihydrite surfaces if ferrihydrite is supersaturated.

Water quality at year 6 of tailings production, and in early closure (when all tailings have been deposited) has been estimated as part of this study. In closure, all water from the sump will be pumped to the water treatment facility until the volume declines to acceptable closure levels (determined by DEQ) following placement of a composite geomembrane and fill / soil cover.

The quality of water in the CTF was predicted at year 6 of tailings production and in early closure, prior to placement of the geosynthetic cap and construction of the vegetated cover. The assumptions and inputs used in these base cases are compared with changes made in sensitivity analyses in Appendix D. The sensitivity of the model was tested by doubling the waste rock and cement surfaces. The cement surface was also halved. Supporting evidence for these assumptions and inputs is provided below.

6.2 Data Sources

The model assumes two sources of water input: precipitation (i.e., rain/snow water) and water seeping from the wet paste. Precipitation water is assumed to be distilled water, and the wet paste seepage is estimated from water quality measured in process water from metallurgical tests (Appendix J, from Austin, 2015). The metallurgical data did not report alkalinity; therefore we estimated total alkalinity values of in the mass-load model of 400 ppm (as CaCO₃), which slightly exceeded the calculated alkalinity input from other dissolved species that were measured, and thus allowed the PHREEQC model to run and close.

6.2.1 Cemented Paste HCT Data

Because the runoff water will contact the cemented-paste surface for a short time (i.e., the material will not be saturated like the cemented pasted backfill in the underground), we used humidity cell test data for the 2% paste to estimate a mass load on a weekly basis for the year 6 model and 4% paste for the closure model.

6.3 Mass Load Calculations

To calculate the mass load, we apply an approach similar to that used for the WRS facility, where we estimate the surface area and water flow, then scale according to a proportionality between flow and surface area. In other words, the concentration, C_i , of the released component (e.g., metals, protons, etc.) is proportional to the ratio of reactive surface area to the volume of water per time (i.e., flux, Q). That is,

$$C_i = \frac{\text{Reactive surface area } (R_{SA})}{\text{Volume of water per time } (Q)} \dot{r}.$$

6.3.1 Estimation of Paste Material Surface Area

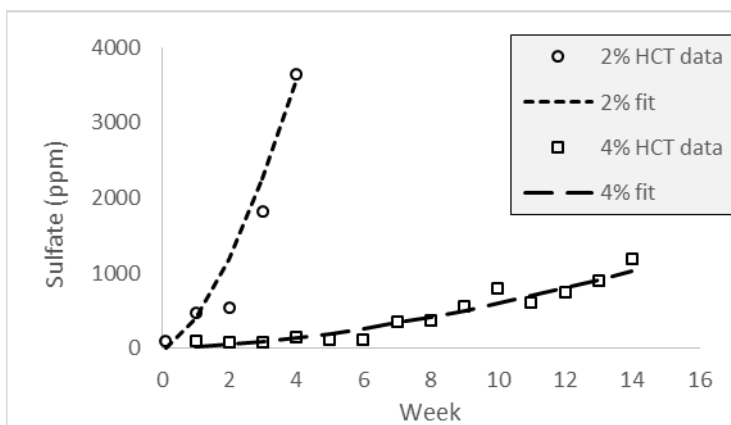
The reactive surface area of pasted tailings will increase over time. We estimate relative surface areas of the CTF surface and kinetic tests based on different extents of weathering. The 2% cemented paste cylinder showed visible evidence of disaggregation in the HCT; this was true to a lesser extent for the 4% cement. HCTs are designed and intended to expedite weathering, so it most likely that the CTF surface will weather at a slower rate; however, we do not have field data for a CTF to use and therefore cannot speculate as to how much slower the field rate will be. Further, the extent of disaggregation is strongly influenced by the amount of cement paste amendment, with incremental increases in cylinder disaggregation over changing time frames (e.g., weeks 1 and 4 in the HCT), but we only have surface area measurements at the start and end of testing (weeks 0 and 28).

We therefore account for the fact that the HCT data come from material that has been weathered for 1-4 weeks at the test cell scale, whereas the CTF will weather on a timeline of 1-8 weeks at full scale, which we represent with 1 week of equivalent test cell weathering.

The CTF mass-load model assumes that solute release is proportional to surface area and thus weathering. The HCT data support this assumption, in that the release of a conserved solute such as sulfate increased exponentially during early weeks of weathering, when progressive disaggregation was observed. We therefore use the HCT sulfate data to estimate the relationship between time and weathering on the relevant scale (i.e., compare the HCT surface area with the predicted CTF surface area). This requires that we assume that the intrinsic rates of reaction are the same in the HCT as they would be in the field; this is a strongly conservative assumption that is required in the absence of field scale data.

If we look at the 4% and 2% paste HCT data for the initial time frame when disaggregation occurs, both visibly and according to sulfate data, and we assume that sulfate production is proportional to surface area (as assumed in the UG mass-load model), both data sets are well described by a physical model of surface area that increases at an exponential rate with time, to the power of 1.6. Physically, this is explained by small particle disaggregating and exposing progressively more surface to disaggregate. The time frame of exponential disaggregation was approximately 4 weeks in the 2% HCT and 14 weeks in the 4% HCT (i.e., the 4% HCT crumbled exponentially at a slower rate). While the intrinsic rates are different between 2% and 4% material, both scale similarly with time. The data are shown below, and the fitted curves are sulfate = $390 \cdot t^{1.6}$ for 2% binder and $15 \cdot t^{1.6}$ for 4% binder, where t is time (weeks).

Figure 6-2. Polynomial Fit for Sulfate Data, Used to Estimate Surface Area



Using this correlation with sulfate release (and thus, surface area) over time, we compared 1 week of weathering to 2, 3, and 4 weeks of weathering, in terms of relative increase in surface area. According to $t^{1.6}$ increase, material at two weeks has weathered 3.03 times as much as material at one week. Similarly, material has weathered 5.8 times as much at 3 weeks and 9.19 times at 4 week. We estimate that the amount of weathering that occurred in the HCT data collected at weeks 1, 2, 3, and 4 was 4.75 times as much as the data collected at week 1. Therefore, we estimate that the CTF surface, which will weather for approximately 1 week, will have a surface area that is 4.75 times less than the surface area of the HCT samples that were used to provide the data to scale.

We believe this estimate to be conservative for a few reasons: 1) We assume the same rate of weathering, when HCT tests are designed to increase weather rates and are recognized to yield as much as an order or magnitude higher rates of oxidation when compared to field scale weathering processes, 2), the HCT weathering of cylinders occurred in a non-confined space, promoting disaggregation, which will not be the case in the CTF facility (tailings are laterally confined), and 3) fine, unconsolidated particles, with high surface areas were kept in the HCT, while they would likely be transported off of the CTF surface.

6.3.2 Estimations of Waste Rock Reactive Surface

At any given time during the filling of the CTF, approximately 4,000 tonnes of co-disposed waste rock will be exposed. This material will be comprised of 40% USZ, 21% YnI B, and 39% LZ FW. We assume that all of this mass is reactive and the surface area per mass is given by the particle sizes in the blast fragmentation of waste rock at the Ashanti mine (shown in **Figure 5-2**).

Additionally, the access ramp will be constructed of 203,537 tonnes of waste rock, composed of Ynl A (14.5%), USZ (1.5%), Ynl B (50%), and LZ FW (30%). The Knight Piesold design of the CTF basin drain system includes the initial placement of a sub-grade bedding protective layer above the CTF HDPE liner system with construction material that will be sourced from excavated bedrock from the CTF excavation footprint (see Section A of Design Drawing C2003 in Appendix K of the MOP Application). However, the water balance model for this study has substituted, as an alternative, pre-production waste rock for the CTF bedrock excavation material in this protective layer which represents a worst-case geochemical scenario alternative knowing that Tintina has committed in the MOP Application to use a cleaner rock, granodiorite excavated from the CTF excavation footprint (see Appendix D-1) to be the source of the sub-grade bedding material overlying the CTF HDPE liner system (see Table 3-14b in the MOP Application). In this alternate scenario, sub 3/8 inch screened fragments of Ynl B (4%) will first be deposited as an initial lift (cushion layer) to prevent punctures to the liner. Because this mass is large and it is unlikely or impossible that all surfaces would react with water, we used the same approach taken for the Waste Rock Storage Facility by calculating a reactive mass for the fraction of rock that could be saturated by water flow in one week, assuming a 30% porosity. The lower porosity compared to the WRS (40% porosity) is assumed because of compaction from use of the ramp. For a sensitivity analysis, we also assume that all mass in the waste rock drain is reactive.

For waste rock samples in the humidity cell tests, the reactive surface area was estimated from sieve analyses. From these calculations, assuming spherical particles, the specific surface areas are 2.01 m²/kg for USZ, 2.94 m²/kg for Ynl A and 3.01 m²/kg for Ynl B.

6.3.3 Water Balance

Given the footprint of the CTF, the model assumes 84,000 m³/year of precipitation and runoff, based on data collected by Knight Piesold (2015). This value accounts for snow accumulation, plowing, etc. All of this water is assumed to contact and react with the top surface of the CTF and the co-deposited waste rock at year 6.

At year 6, while paste continues to be deposited, the model assumes that 29,029 m³/year of water comes from the wet paste dewatering. This estimate is based on 5% dewatering (by mass) of the 1,595 tonnes of paste (55% of 2,900 tonnes) deposited per day on an annualized basis (AMEC, 2016b, Appendix K-7 of Tintina's MOP). Combined with the runoff water, this means that 113,029 m³/year of water reports to the sump. At closure, the dewatering contribution is removed, and only 84,000 m³/year of precipitation reports to the sump.

The model assumes that 10% of the runoff and the dewatered paste water also flows through the waste rock drain (access ramp) and receives additional load from the waste rock. This is based on the drain occupying 10% of the CTF surface area in year 6.

6.4 Predicted Water Quality at Year 6

Modeling results suggest that the water reporting to the CTF sump at year 6 will be acidic, with a pH of 4.13 in the base case (**Table 6-1**). Sulfate concentration is moderately high (765 mg/L) and several metals (e.g., As, Cu, Ni, Pb, Sb, and Tl) will exceed groundwater quality standards, requiring treatment. The minerals alunite, barite, jarosite and quartz are predicted to precipitate; the precipitation of these sulfate minerals explains the relatively lower sulfate concentrations under the more acidic conditions. No sorption is predicted. The mass loads calculated for each input sources are shown in Appendix K.

The sensitivity analyses suggest that the pH and some metal concentrations (e.g., Al, Cu, Fe, Se, Sr, and Tl) are linked to the estimation of paste surface area. Values for SO₄⁻², As, F, Sb, U, and Zn are more strongly linked to the estimation of the waste rock contribution. The sensitivity analysis which uses solute concentrations from the 4% cement paste HCT (in place of the 2% cement paste HCT) suggests that use of 4% cement paste could be an effective contingency for interim closure management.

Table 6-1. Predicted Water Quality in the CTF Sump at Year 6, Including Sensitivity Analyses

		Model predictions for CTF at yr 6 of mining					Groundwater Standards (MT DEQ-7)
		Base Case	Waste Rock Surface Area Doubled	Paste Cement Surface Area Doubled	Paste Cement Surface Area Halved	4% paste cement surface	
pH	s.u.	4.13	4.11	3.80	4.38	5.28	na*
Al	mg/L	17.73	16.18	38.26	4.80	0.08	na
Alkalinity	mg/L CaCO ₃	97	92	92	86	111	na*
As	mg/L	0.031	0.033	0.048	0.016	0.017	0.01
Ba	mg/L	0.004	0.003	0.003	0.005	0.015	1
Be	mg/L	0.0051	0.0051	0.0102	0.0026	0.0008	0.004
Ca	mg/L	132	137	246	75	42	na
Cd	mg/L	0.00141	0.00142	0.00281	0.00071	0.00005	0.0050
Cl	mg/L	34.3	34.3	38.0	32.4	31.7	na*
Cr	mg/L	0.012	0.013	0.023	0.007	0.006	0.1
Cu	mg/L	61.3	0.0	121.8	31.0	0.7	1.3
F	mg/L	0.68	0.73	1.24	0.40	0.24	4
Fe	mg/L	0.573	0.463	1.955	0.497	0.022	na**
Hg	mg/L	0.000127	0.000141	0.000240	0.000071	0.000066	0.002000
K	mg/L	0.00003	0.00005	0.00000	0.00004	3.46125	na
Mg	mg/L	95	100	148	68	2	na
Mn	mg/L	2.68	2.73	5.30	1.36	0.06	na**
NO ₃	ppm as N	34.4	34.4	34.4	34.4	34.4	1
Na	mg/L	13	13.6	15.9	12.1	12.6	na
Ni	mg/L	8.5	8.5	17.1	4.3	0.0	0.1
P	mg/L	0.26	0.26	0.50	0.05	0.02	na
Pb	mg/L	0.027	0.028	0.030	0.025	0.025	0.015
SO ₄	mg/L	765	797	1481	406	97	na**
Sb	mg/L	0.015	0.015	0.016	0.014	0.014	0.006
Se	mg/L	0.003	0.003	0.005	0.002	0.001	0.050
Si	mg/L	0.001	1.142	1.129	0.74	0.12	na
Sr	mg/L	2.62	2.92	4.67	1.59	0.86	4
Tl	mg/L	0.016	0.017	0.030	0.009	0.003	0.002
U	mg/L	0.019	0.015	0.021	0.008	0.003	0.03
Zn	mg/L	0.826	0.826	1.650	0.413	0.010	2

estimate - most nitrate removed by flotation
supersaturated phases in basecase: alunite, barite, jarosite, quartz

*narrative standards may exist
**secondary standard

Results include precipitation of supersaturated phases

6.5 Predicted Water Quality at Closure

The CTF closure model accounts for the increased surface area of the cemented paste and removes the contribution from dewatered paste. The final paste lift will be constructed with 4% cement paste. However, Tintina also proposes to cover the CTF with a welded HDPE cover, followed by fill, subsoil and topsoil (at a slope designed to preclude standing water), regraded and re-vegetated. This plan will eliminate long-term exposure to oxygen and water. The closure predictions shown here represent water quality at the end of tailing production, prior to placement of the cover, when the entire surface remains exposed to oxygen and water. The mass loads for each input source are shown in Appendix K.

Although the surface area of the CTF is higher at closure (210,000 m²) compared to year 6 (132,000 m²), the lower predicted acidity and metals result in better water quality due to the planned use of a cemented paste tailings lift containing 4% cement immediately prior to placement of the cover.

At closure, the water reporting to the CTF sump is predicted to be moderately acidic, with a pH of 4.95 in the base case (**Table 6-2**). Sulfate concentration is predicted to be much lower (90 mg/L) and the base case meets groundwater standards except for TI, and As under the scenario where reactive surface area of paste on the CTF is doubled. Sensitivity results indicate that metal concentrations are more sensitive to increases in reactive paste surface area than waste rock surface area. Barite and jarosite are predicted to precipitate. No sorption was calculated due to the lack of ferrihydrite precipitation. The mass loads calculated for each input sources are shown in Appendix L.

The cement pasted tailings will be placed on a double liner until a composite geomembrane/soil cover is constructed to eliminate infiltration at closure, and water will be collected from the sump for treatment until no standing water remains and the cover has eliminated any seepage. Water with the quality predicted at closure will be of limited duration, due to the elimination of run-on and precipitation by the cover at closure, and there will be no standing inventory of water on the liner. Because the surface area of the impoundment is an important factor, water quality should be expected to drop gradually as the facility approaches complete buildout with maximum reactive surface area, followed by improvement with the construction of the final 4% tailings lift and placement of the cover. The drain should be also managed to avoid plugging with secondary minerals. However, the drain is unlikely to be fully saturated with the predicted (215 L/min) flow of seepage, leaving multiple paths for water flow.

Table 6-2. Predicted Water Quality in the CTF Sump at Closure, Including Sensitivity Analyses

		Model predictions for CTF at closure				Groundwater Standards (MT DEQ-7)
		Base Case	Waste Rock Surface Area Doubled	Paste Cement Surface Area Doubled	Paste Cement Surface Area Halved	
pH	s.u.	4.95	4.95	4.65	5.25	na*
Al	mg/L	0.020	0.020	0.039	0.010	na
Alkalinity	mg/L CaCO ₃	53	53	106	53	na*
As	mg/L	0.0082	0.0086	0.0160	0.0043	0.01
Ba	mg/L	0.018	0.017	0.011	0.028	1
Be	mg/L	0.0016	0.0016	0.0031	0.0008	0.004
Ca	mg/L	54	54	108	27	na
Cd	mg/L	0.000066	0.000067	0.000130	0.000033	0.005000
Cl	mg/L	2.6	2.6	5.1	1.3	na*
Cr	mg/L	0.010	0.010	0.020	0.005	0.1
Cu	mg/L	0.0056	0.0056	0.0111	0.0028	1.3
F	mg/L	0.27	0.29	0.53	0.14	4
Fe	mg/L	0.012	0.012	0.007	0.021	na**
Hg	mg/L	0.000111	0.000111	0.000223	0.000056	0.002000
K	mg/L	4.2	4.4	8.3	2.2	na
Mg	mg/L	0.9	1.3	0.7	7.4	na
Mn	mg/L	0.018	0.018	0.034	0.009	na**
NO ₃	ppm as N	3.4	3.4	3.4	3.4	1
Na	mg/L	4.0	4.1	7.9	2.1	na
Ni	mg/L	0.019	0.019	0.037	0.009	0.1
P	mg/L	0.021	0.021	0.042	0.010	na
Pb	mg/L	0.00047	0.00049	0.00092	0.00024	0.015
SO ₄	mg/L	90	93	177	46	na**
Sb	mg/L	0.0011	0.0011	0.0021	0.0006	0.006
Se	mg/L	0.0020	0.0021	0.0040	0.0011	0.050
Si	mg/L	0.11	0.12	0.22	0.06	na
Sr	mg/L	0.65	0.66	1.29	0.33	4
Tl	mg/L	0.0022	0.0022	0.0044	0.0011	0.002
U	mg/L	0.0011	0.0018	0.0015	0.0009	0.03
Zn	mg/L	0.019	0.019	0.039	0.010	2
estimate - most nitrate removed by flotation				*narrative standards may exist		
supersaturated phases in basecase: barite, jarosite				**secondary standard		

Results include precipitation of supersaturated phases

7 Process Water Pond Water Quality Model

All water from the CTF and some of the RO brine from the water treatment plant will report to the PWP where it will mix with water from the mill (i.e., thickener overflow), direct precipitation and runoff. In the PWP model, we mix these solutions and equilibrate the solution using PHREEQC. **Figure 1-2** shows the facilities map. The water balance is provided by Knight Piesold (2017) for year 6.

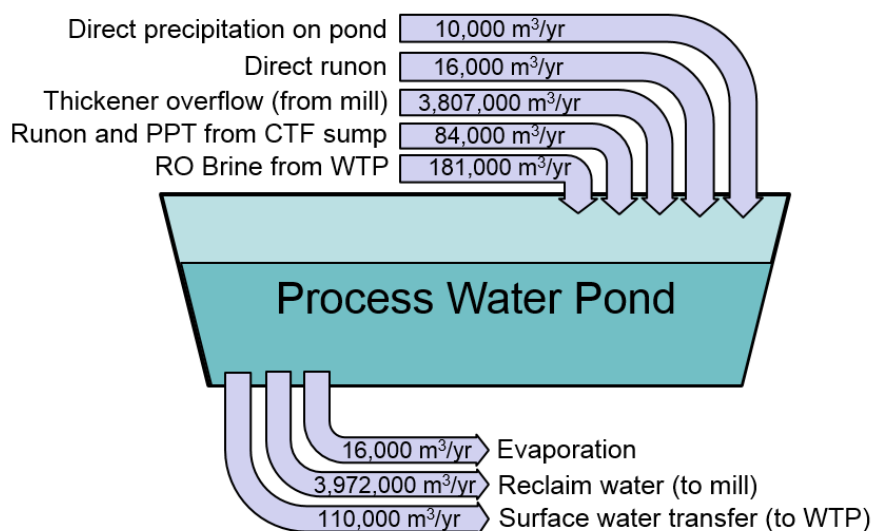
The quality of water in the PWP was predicted during operations at year 6. Model sensitivity was not tested as this is a straightforward mixing model which relies on assumptions tested

for the CTF model and the processes in the mill and the water treatment plant. Supporting evidence for this approach is provided below.

7.1 Process Water Pond Water Balance

Figure 7-1 shows the overall water balance in the PWP, including the sources and annual flow rates.

Figure 7-1. Water Balance for Process Water Pond



We use results from Section 6.4 to predict the water chemistry from the CTF facility. For the thickener overflow (from mill), we use chemistry provided by AMEC (2017), in conjunction with metallurgical data provided by Jeff Austin (2015). For the RO Brine, we use chemistry provided by AMEC (2017). In addition to these solutions, we add runoff and direct precipitation (assumed to be dionized water) and remove water for evaporation. These three fluxes of water add up to a net influx of 10,000 m³/yr of water, which dilutes the system by only a small amount. The final mixed solution is equilibrated in PHREEQC to predict the PWP chemistry that will report to the WTP.

7.2 Predicted Water Quality in PWP

Table 7-1 shows the results of the mixing and equilibration in the process water pond. The predicted pH is 5.81, with an alkalinity of 205 ppm and sulfate of 903 ppm. The mass-load model is shown in Appendix M. PHREEQC predicts precipitation of alunite, $Ba_3(AsO_4)_2$, barite, and jarosite. The model predicts that As, Cu, NO_3^- , Ni, Pb, Sb, Sr, and Tl will exceed groundwater standards prior to treatment to meet non-degradation criteria. Tintina plans to treat all of the water inventory in the PWP prior to removal and reclamation of the pond at closure.

Table 7-1. Predicted Water Quality in PWP at Year 6

		Model prediction of PWP	Groundwater Standards (MT DEQ-7)
pH	s.u.	5.81	na*
Al	mg/L	0.016	na
Alkalinity	mg/L CaCO ₃	205	na*
As	mg/L	0.033	0.01
Ba	mg/L	0.004	1
Be	mg/L	0.0002	0.0040
Ca	mg/L	509	na
Cd	mg/L	0.00009	0.00500
Cl	mg/L	141	na*
Cr	mg/L	0.004	0.1
Cu	mg/L	4.0	1.3
F	mg/L	0.547	4
Fe	mg/L	0.004	na**
Hg	mg/L	0.000011	0.002000
K	mg/L	28	na
Mg	mg/L	1	na
Mn	mg/L	0.1	na**
NO₃	ppm as N	87	1
Na	mg/L	44	na
Ni	mg/L	0.197	0.1
P	mg/L	0.10	na
Pb	mg/L	0.092	0.015
SO₄	mg/L	903	na**
Sb	mg/L	0.023	0.006
Se	mg/L	0.001	0.05
Si	mg/L	0.255	na
Sr	mg/L	4.22	4
Tl	mg/L	0.009	0.002
U	mg/L	0.009	0.03
Zn	mg/L	0.258	2
prediction based on assumed 33 ppm from underground and WTP balance			
*narrative standards may exist		**secondary standard	
Supersaturated phases: Alunite, Ba ₃ (AsO ₄) ₂ , Barite, Jarosite			

Results include precipitation of supersaturated phases and sorption.

8 Conclusions and Recommendations

Enviromin has predicted water quality for the proposed i.) underground workings (i.e., access, declines, and stopes), UG; ii.) temporary waste rock storage facility, WRS; iii.) cemented tailings facility, CTF; and iv.) the downgradient water treatment plant, WTP. For all models, Enviromin provides base case scenarios for likely and foreseeable conditions, which include inherent elements of conservatism. For the important parameters in the models, sensitivity analyses show variations from the base case parameters, which may over- or under-estimate true values. In general, the predicted changes are not extreme, even in the case of the compound conservative analysis, suggesting that the models provide a solid analysis of future water quality for the facilities.

In the UG, we estimate water quality at year 6 of mining operations and at post-closure conditions, when groundwater has rebounded fully. For the WRS facility, we estimate water quality only at the end of year 2, when it will begin to be dismantled and the material moved to the CTF for permanent storage. For the CTF, we estimate water quality at year 6 of production and at the start of closure, prior to placement of the cover which will eliminate all subsequent seepage to the CTF sump. Except for the groundwater in the underground workings at closure (following cessation of dewatering), water from each of the modeled facilities will report directly to the water treatment facility for treatment prior to discharge. This water is predicted to meet non-degradation criteria prior to discharge to shallow groundwater via the infiltration galleries.

- **UG:** For the UG model, we predict water quality in year 6 of operations to be neutral, with a pH of 6.67, abundant alkalinity (183 mg/L) and a moderate increase in sulfate concentration (over background) to 304 mg/L. The highest contributions of acidity, metals, and sulfate come from the LCZ, but the rate of groundwater flow from the LCZ is very low so the net effect is minor. Enviromin predicts precipitation of alunite, $\text{Ba}_3(\text{AsO}_4)_2$, Cr_2O_3 , ferrihydrite, and quartz, based on PHREEQC predictions of supersaturation in the mixed influent water in the sump, with sorption of metals As, Ba, Be, Cu, Pb, Ni, and Zn to ferrihydrite. Concentrations of NO_3^- , Cu, F, Mn, Ni, Sb, Se, Tl, U and Zn are predicted to increase in the resulting solution above background concentrations. Of these parameters, NO_3^- and U are predicted to exceed Montana DEQ groundwater quality standards in the operational base case and multiple sensitivity scenarios. Arsenic and Sr have a low potential to exceed their elevated background concentrations in groundwater. If a higher rate of sulfide oxidation or a greater reactive mass of rock were to be encountered, Tl and Sb could also exceed standards. Because all water will be collected during operational dewatering for treatment to meet non-degradation criteria prior to discharge, these predicted exceedances are not material and they are not expected to affect water quality.

The model includes several sensitivity analyses of the predicted underground water quality, addressing uncertainty in model inputs for i.) HCT data (i.e., all data vs. weeks 1-4), ii.) fracture density, iii.) fracture zone thickness, iv.) reactive zone thickness, iv.) estimated surface area, and v.) sulfide oxidation rate. Alkalinity is abundant in all sensitivity scenarios, including the compound conservative analysis which combines several conservative assumptions; predicted pH ranges from 4.87 to 6.68 and sulfate ranges from 262 to 672 mg/L in this combined scenario. In general, the assumptions about fracture density and reactive-zone thickness have the greatest effect on predicted metal release, and the sulfide oxidation rate has the most dominant, though minor effect, on the pH. The scenario which includes HCT

data for all weeks yields a lower pH, due to acidity produce later in the USZ HCT test.

At closure, following completion of mining, backfilling, and groundwater rebound, the water is predicted to have slightly higher pH (6.81) and lower alkalinity (144 mg/L) and sulfate (115 mg/L), due to changes in groundwater flow and an increase in paste cement surface area when compared to the operational predicted water quality. Concentrations of metals are also predicted to be lower. This model is most sensitive to the estimate of reactive surface area for the cemented backfill. Enviromin predicts potential precipitation of $Ba_3(AsO_4)_2$, barite, Cr_2O_3 , ferrihydrite, gibbsite, and quartz, based on PHREEQC predictions of supersaturation in the mixed water.

As mine water will be collected during dewatering operations for on-site treatment, but not when mine dewatering ceases, the predicted chemistry at closure is important. The predicted changes at closure represent minor changes in water quality, relative to the background water quality (pH of 6.97, with alkalinity of 193 mg/L and sulfate 111 mg/L). Concentrations of NO_3^- , SO_4^{2-} , P, Se, Sr, and Zn are predicted to increase modestly above background levels, but none exceed Montana DEQ groundwater quality standards or groundwater non-degradation criteria. The limited variation between the base case and sensitivity scenarios reflects the robust design and plan for management of the UG, which limits open stope area and provides for water treatment during operations and early closure; concurrent backfilling with a low transmissivity material; flooding with RO treated water at closure, and placement of hydraulic plugs.

- **WRS:** Water quality predicted for the WRS base case at the end of year 2 of mining is moderately acidic (pH 5.80) and high in sulfate (2,212 ppm), with some elevated metals. This prediction is conservative, as a result of the very small amount of water into which the mass of solutes released from the aggressively weathered HCT is scaled. Regardless, the volume of WRS seepage is small (473,000 gallons/year; 1,790 m³/year at a rate of 0.9 gpm) and water will be collected on a lined pad and discharged to the PWP prior to treatment. Our model predicts potential precipitation of alunite, barite, celestite and jarosite. Sensitivity analyses show that the model is sensitive to the rock water ratio and surface area assumptions. Because the WRS will be removed in years 2 to 3, no closure evaluation was needed.
- **CTF:** For the CTF, the predicted quality of water that will collect in the sump at year 6 of tailings placement is acidic (pH 4.13) with 765 mg/L sulfate and elevated metal concentrations. More acidity and metals are contributed by the surface of cemented tailings than the co-deposited waste rock or access ramp/rock drain, while most sulfate comes from the paste dewatering and waste rock. The minerals predicted to form during operations include alunite, barite, jarosite, and quartz. At closure, following placement of a 4% lift immediately prior to cover placement, a more neutral solution (pH 4.95) is predicted. The planned reclamation procedures (e.g., composite welded HDPE /soil cover, revegetation, etc.) are not accounted for in the model, as they will eliminate seepage. At closure, the minerals predicted by PHREEQC to form include barite and jarosite.

Results for the CTF show that the finely ground, sulfide-rich tailing will generate higher acidity and metals, but lower sulfate due to precipitation of sulfate-rich minerals, e.g. alunite, barite and jarosite. Water quality predictions for the CTF are sensitive to the calculated surface area, implying that the surface area should be managed to limit weathering through frequent placement of fresh lifts of paste

tailings. In the event of an interim closure, Tintina may elect to increase the cement content to 4%, to improve the stability of the upper paste cement during a lag in placement of fresh tailings.

- **PWP:** All water from the CTF sump and some RO brine from the water treatment plant will report to the Process Water Pond (PWP). These inflows mix with thickener overflow from the mill and direct precipitation. Results of the model predict that the overall chemistry of the PWP is dominated by the thickener overflow, which provides 93% of the flow. The predicted solution has a pH of 5.81, moderate sulfate (903 mg/L), and elevated concentrations of As, Cu, NO_3^- , Ni, Pb, Sb, Sr, and Tl. PHREEQC predicts that alunite, $\text{Ba}_3(\text{AsO}_4)_2$, barite, and jarosite could form. Excess water from the PWP will be sent to the WTP for treatment and discharged operationally to offset consumptive use; all water on the PWP will be treated prior to closure of the facility.

9 References

- AMEC, 2016a. *Examples of Existing Paste Backfill*. Memo prepared for Tintina Montana, 4 pp. 31 August 2016.
- AMEC, 2016b. *Paste Tailings for Johnny Lee Mine, Tintina Resources*. Memo prepared for Tintina Montana, 2 pp. 2 September 2016.
- AMEC, 2017. *Water Treatment Modeling*. Memo prepared for Tintina Resources, May 2, 2017.
- Austin, J, 2015. AMEC metallurgical testing for BBC project.
- Baas-Becking, L., Kaplan, I.R., Moore, D., 1960. Limits of the natural environment in terms of pH and oxidation-reduction potentials. *Geology*. Vol. 68, No. 3, pp. 243-284.
- Behra, P., P. Bonnissel-Gissingner, M. Alnot, R. Revel and J. J. Ehrhardt, 2001. "XPS and XAS study of the sorption of Hg(II) onto pyrite." *Langmuir* 17(13): pp. 3970-3979.
- Bethke, C.M., 2008. *Geochemical and Biogeochemical Reaction Modeling*. Cambridge, 2nd ed.
- Borah, D. and K. Senapati, 2006. Adsorption of Cd(II) from aqueous solution onto pyrite. *Fuel*, 85: 1929-1934.
- Bower, J., Savage, K.S., Weinman, B., and Harper, W., 2008. Immobilization of mercury by pyrite (FeS₂). *Environmental Pollution* 156(2):504-14.
- Brown, J. R., G. M. Bancroft, W. S. Fyfe and R. A. N. McLean, 1979. "Mercury Removal from Water by Iron Sulfide Minerals - Electron-Spectroscopy for Chemical-Analysis (Esca) Study." *Environmental Science & Technology* 13(9): pp. 1142-1144.
- Davis, G.B., 1983. *Mathematical modelling of rate-limiting mechanisms of pyretic oxidation in overburden dumps*. Doctor of Philosophy thesis, Department of Mathematics, University of Wollongong, N.S.W., Australia.
- Davis, G.B., Doherty, G, and Ritchie, A.I.M. 1986. A model of oxidation in pyritic mine waters: Part 2: Comparison of numerical and approximate solutions. *Appl. Math. Model.* 10:323-339.
- Doyle, CS; Kendelewicz, T; Bostick, BC, and Brown, G, 2004. Soft X-ray spectroscopic studies of the reaction of fractured pyrite surfaces with Cr(VI)-containing aqueous solutions. *Geochimica et Cosmochimica Acta*. Vol 68, issue 21, pp. 4287-4299.
- Enviromin, 2017. *Final Baseline Environmental Geochemistry Evaluation of Waste Rock and Tailings*. April 2017. Report prepared for Tintina Resources, Inc.
- Hydrometrics, Inc., 2012. *Tintina Resources Black Butte Copper Project Water Resources Monitoring 2011 Annual Report*. Report prepared for Tintina Resources, January 2012.

Hydrometrics, 2013. *Hydrological and Geochemical Assessment of Proposed Underground LAD Area, Black Butte Copper Project*. November 2013.

Hydrometrics, 2015. *Groundwater Modeling Assessment for the Black Butte Copper Project Meagher County MT*. Report prepared for Tintina Resources, Inc. November 2015.

Hydrometrics, 2016a. *Memorandum for Black Butte Copper Temporary Waste Rock Storage Facility Percolation Model*. Prepared for Geomin Resources Inc. and Enviromin, Inc. February 18, 2016.

Hydrometrics, 2016b. *Memorandum for Simulated Mine Inflow and Groundwater Flux at Closure*. Prepared for Geomin Resources Inc. and Enviromin, Inc. May 2, 2016.

Hydrometrics, 2017. Stillwater Mining Company - East Boulder Mine 2016 Compliance Report, January 2017.

Hyle, C., 2016. *Typical Underground Fragmentation*. Memo from Orca Mining Services prepared for Tintina Montana, 2 pp. 2 June 2016.

Kelsall, P.C., J.B. Case and CR Chabannes, 1984. Evaluation of Excavation-induced changes in Rock Permeability. *International Journal of Rock Mechanics and Mining Sciences & Geomechanics Abstracts*, Vol 21, N. 3, pp. 123-135.

Kempton, H. and D. Atkins, 2009. Direct Measurement of Sulfide Mineral Oxidation Rates and Acid Rock Drainage in Wall Rock of Open Pit Mines. *Proceeds of the 8th International Conference on Acid Rock Drainage*, June 23-29, 2009, Sweden.

Knight Piesold, 2015. Black Butte Copper Project Meteorology Data Analysis Update. Memo from Brendan Worrall to Bob Jacko, May 27, 2015.

Knight Piesold, 2016. *Black Butte Copper Project Water Balance – Surface Water transfer to Water Treatment Plant*, Memorandum prepared for Tintina Resources, Inc. April 28, 2016. 10 pages. (File No. VA 101-00460/03-A.01).

Oxverdi, A., Erdem, M. 2006. Cu²⁺, Cd²⁺ and Pb²⁺ adsorption from aqueous solutions by pyrite and synthetic iron sulphide. *Journal of Hazardous Materials*, 137, 1: 626-632.

Parkhurst, D.L., and Appelo, C.A.J., 2013, Description of input and examples for PHREEQC version 3—A computer program for speciation, batch-reaction, one-dimensional transport, and inverse geochemical calculations: U.S. Geological Survey Techniques and Methods, book 6, chap. A43, 497 p., available only at <http://pubs.usgs.gov/tm/06/a43/>.

Siskind, D., & Fumanti, R. (1974). *Blast-produced fractures in Lithonia granite*. U.S. Bureau of Mines, Report of investigations 7901.

Tintina Resources, Inc., 2015. Mine Operating Permit Application - Black Butte Copper Project, Meagher County, MT. Submitted to the Department of Environmental Quality, December 15, 2015. 312 p.

Tintina Resources, Inc., 2016, Mine Operating Permit Application - Black Butte Copper project, Meagher County, MT. Submitted to the Montana Department of Environmental Quality, August 2016.

APPENDIX C: PHREEQC Input for Underground Operations at Year 6

```
#ASSUMPTIONS
#starting pe + pH set to 13, to simulate a moderately opens system
#The following precipitates are allowed to form and reach equilibrium:
#Alunite, Celestite, Gypsum, K-Jarosite, Barite, Ba3(AsO4)2, Gibbsite, Ferrihydrite, Fluorite, MnHPO4, SbO2,
Cr2O3
#These phases were chosen based on supersaturation and general likelihood in mine-affected water. Goethite and
hematite were not allowed to precipitate because they are not likely to form at low temperatures in mine-
affected water (Bethke, Geochemical and Biogeochemical Reaction Modeling, 2008)

TITLE Groundwater base case Yr6

#solution predicted from mass loading model
SOLUTION 1
  temp      9.52
  pH        6.69
  pe        6.31
  redox     pe
  units     mg/kgw
  density   1
  Al        0.0335547
  Alkalinity 225.5543058
  As        0.0693722
  Ba        0.0536516
  Be        0.0010995
  Ca        88.9408254
  Cd        8.33e-005
  Cl        1.3952021
  Cr        0.0096426
  Cu        0.0028212
  F         1.1359132
  Fe        1.8627779
  Hg        1.63e-005
  K         10.8784163
  Mg        60.3967574 charge
  Mn        0.1652352
  N(5)     0.5322581 mMol/kgw
  Na        14.6610865
  Ni        0.006497
  P         0.0110735
  Pb        0.0010093
  S(6)     3.1657251 mMol/kgw
  Sb        0.0031708
  Se        0.0038824
  Si        6.7319409
  Sr        10.4846032
  Tl        0.0019632
  U         0.037117
  Zn        0.031939
  -water   1 # kg
EQUILIBRIUM_PHASES 1
  Alunite  0 0 precipitate_only
  Ba3(AsO4)2 0 0 precipitate_only
  Barite   0 0 precipitate_only
  Celestite 0 0 precipitate_only
  Cr2O3    0 0 precipitate_only
  Ferrihydrite 0 0
  Fluorite 0 0 precipitate_only
  Gibbsite(C) 0 0 precipitate_only
  Gypsum   0 0 precipitate_only
  Jarosite-K 0 0 precipitate_only
  MnHPO4(C) 0 0 precipitate_only
  Quartz   0 0 precipitate_only
  SbO2     0 0 precipitate_only
SURFACE 1
  Hfo_sOH Ferrihydrite equilibrium_phase 0.005 64200
  Hfo_wOH Ferrihydrite equilibrium_phase 0.2
  -donnan 1e-008

END
```

APPENDIX D: Base Case and Sensitivity Scenarios for UG, WRS, CTF, and PWP Models

		Parameters					NOTES
Underground at Year 6		Fracture Density	Weeks of HCT data used	Sulfide Oxidation Rate (kg SO ₄ /m ² /yr)	Maximum Fracture Zone Thickness	Paste Backfill Surface Area (m ²)	
Base case		10% in UZ, 2% in LZ	Weeks 1-4	6	1 meter	3346 for UZ, 1714 for LZ	Likely and foreseeable scenario for UG working sump water at year 6
Sensitivity	Fracture Density Halved	5% in UZ, 1% in LZ	Bc	Bc	Bc	Bc	Model sensitivity to high fracture density estimate
	Fracture Density Doubled	20% in UZ, 4% in LZ	Bc	Bc	Bc	Bc	Model sensitivity to low fracture density estimate
	All HCT Data	Bc	All Weeks	Bc	Bc	Bc	Model sensitivity to HCT data selection
	Oxidation Rate 40 kg SO ₄ /m ² /yr	Bc	Bc	40	Bc	Bc	Model sensitivity to sulfide oxidation rate
	Two Meter Max Reactive Zone	Bc	Bc	Bc	2 meter	Bc	Model sensitivity to fracture zone thickness
	Paste Backfill Surface Area Doubled	Bc	Bc	Bc	Bc	6692 for UZ, 3428 for LZ	Model sensitivity to paste backfill surface area
	Combined Highest Reactive Mass Parameters	20% in UZ, 4% in LZ	Bc	40	Bc	6692 for UZ, 3428 for LZ	Model sensitivity to estimates of multiple parameters affecting reactive mass. This scenario compounds affect of multiple conservative estimates.
Underground at Closure		Paste Backfill Surface Area (m ²)	Assumed values for non-detects				
Base case		14,653 for UZ and 13176 for LZ	Detection limit				Likely and foreseeable scenario for UG post-closure
Sensitivity Analyses	Paste Backfill Surface Area Doubled	29306 for UZ, 26353 for LZ	Bc				Model sensitivity to paste backfill surface area
	Detection Limits = 0	BC	Zero				Influence of detection limit propagation in model calculations (replace d.l. values with 0).

		Parameters				NOTES
CTF at Year 6		Waste Rock Surface Area (m2)	Paste Cement Surface Area (m2)	Kinetic Test Used for Paste (m2)		
Base case		267,590 on surface, 111,012 in ramp/drain	13200	2% Paste HCT		Likely and foreseeable prediction of WRS seepage in year 2. Conservative application of HCT results for wk 1-4, based on higher surface area and water flux of HCT, to very low volume of predicted seepage.
Sensitivity Analyses	Waste Rock Surface Area Doubled	535180 for surface 222,025 for ramp/drain	Bc	Bc		Uncertainty about future BBC particle size gradation.
	Paste Cement Surface Area Doubled	Bc	264000	Bc		Influence of low paste cement surface area
	Paste Cement Surface Area Halved	Bc	66000	Bc		Influence of high paste cement surface area
	4% Paste Cement Surface	Bc	Bc	4% Paste HCT		Evaluates use of 4% cement paste in place of 2%
CTF at Closure		Waste Rock Surface Area (m2)	Paste Cement Surface Area (m2)			
Base case		82,501 in ramp/drain	210000			Likely and foreseeable scenario for CTF at closure
Sensitivity Analyses	Waste Rock Surface Area Doubled	165,003	Bc			Influence of underestimating waste rock surface area
	Paste Cement Surface Area Doubled	Bc	420000			Influence of low waste rock surface area
	Paste Cement Surface Area Halved	Bc	105000			Influence of high waste rock surface area
WRS at Year 2		Reactive Mass (tonnes)				
Base case		8301				Likely and foreseeable scenario for WRS in year 2
Sensitivity Analyses	Reactive Mass Halved	4150				Influence of high estimate of reactive mass (also, proportional to surface area and flow).

APPENDIX E: Groundwater Chemistry Model Inputs, from Hydrometrics Inc. (2015)

Parameter	Units*	Groundwater contribution							AVERAGE OF ALL GW
		surface decline		upper access/stopes		lower decline	lower access/stopes		
		YNL-A	USZ	USZ/UCZ	YNLB-UA	YNLB-LD	LCZ & LZFW	YnlB-LA	
		<i>Avg (MW-1B, -2A, -2B, -4B, -9, PW-1 and -8)</i>	<i>PW-9 Avg</i>	<i>Avg (MW-3, PW-2, PW-4)</i>	<i>PW-10</i>	<i>PW-10</i>	<i>From PW-9 in UCZ (worst case), because data for PW-7 are poor</i>	<i>PW-10</i>	
Flow rate	L/min	386	34	1037	49	450	37.85	64	2059
	L/week	3891997	343411	10454972	496039	4540663	381568	648666	20757317
Fraction of total flow	-	0.188	0.017	0.504	0.024	0.219	0.018	0.031	1
Surface area	m2								
Rock density	kg/m3								
Mass fraction sulfide (as S)	-								
Exposure time (days)	days								
Reactive mass (kg)	kg								
Oxidized rind thickness (m)	m								
Scaling factor w.r.t. HCT	-								
pH	s.u.								7.03
Activity of hydrogen	-	9.43E-08	2.75E-07	8.66E-08	4.07E-08	4.07E-08	2.75E-07	4.07E-08	8.21E-08
Temperature	°C	7.1	10.3	9.3	8.5	8.5	10.3	8.5	8.7
Total Alkalinity	mg/L as CaCO ₃	189	204	223	230	230	204	230	218
Aluminum	mg/L	0.015	0.009	0.016	0.009	0.009	0.009	0.009	0.014
Antimony	mg/L	0.003	0.001	0.002	0.001	0.001	0.001	0.001	0.001
Arsenic	mg/L	0.018	0.086	0.063	0.048	0.048	0.086	0.048	0.051
Barium	mg/L	0.059	0.014	0.014	0.111	0.111	0.014	0.111	0.049
Beryllium	mg/L	0.001	0.001	0.001	0.001	0.001	0.001	0.001	0.001
Cadmium	mg/L	0.00004	0.00003	0.00005	0.00004	0.00004	0.00003	0.00004	0.00005
Calcium	mg/L	58	83	84	74	74	83	74	76
Chloride	mg/L	1.41	1.40	1.40	1.00	1.00	1.40	1.00	1.29
Chromium	mg/L	0.007	0.005	0.005	0.010	0.010	0.005	0.010	0.007
Copper	mg/L	0.002	0.002	0.002	0.002	0.002	0.002	0.002	0.002
Fluoride	mg/L	0.290	0.600	0.693	0.800	0.800	0.600	0.800	0.644
Iron	mg/L	5.77	2.18	1.12	0.340	0.340	2.18	0.340	1.81
Lead	mg/L	0.002	0.000	0.000	0.000	0.000	0.000	0.000	0.001
Magnesium	mg/L	28	48	53	47	47	48	47	47
Manganese	mg/L	0.043	0.041	0.034	0.437	0.437	0.041	0.437	0.146
Mercury	mg/L	0.000007	0.000005	0.000007	0.000005	0.000005	0.000005	0.000005	0.00001
Nickel	mg/L	0.005	0.001	0.005	0.001	0.001	0.001	0.001	0.004
Nitrate + Nitrite	mg/L as N	0.069	0.016	0.010	0.010	0.010	0.016	0.010	0.021
Phosphorus	mg/L	0.015		0.010					0.011
Potassium	mg/L	2.007	3.000	3.143	5.000	5.000	3.000	5.000	3.43
Selenium	mg/L	0.001	0.000	0.001	0.000	0.000	0.000	0.000	0.000
Silicon	mg/L	10.060		8.300					8.78
Sodium	mg/L	3.059	11.800	14.267	11.000	11.000	11.800	11.000	11.18
Strontium	mg/L	0.566	8.654	13.480	11.900	11.900	8.654	11.900	10.5
Sulfate	mg/L	88	250	253	190	190	250	190	205
Thallium	mg/L	0.004	0.001	0.0004	0.0002	0.0002	0.001	0.0002	0.001
Uranium	mg/L	0.005	0.002	0.004	0.008	0.008	0.002	0.008	0.005
Zinc	mg/L	0.019	0.056	0.046	0.002	0.002	0.056	0.002	0.029

APPENDIX F: Prediction of Metal Attenuation by Sulfide in Bedrock Post-Closure

At closure, the water table will rebound to the pre-mining level. Any solutes stored in the mined out workings will dissolve into groundwater and be collected for treatment during the initial flooding of the mine at closure. Under steady state, post-closure groundwater flow and chemistry conditions, the submerged wall rock will be exposed to reduced groundwater typical of the natural background environment. Sulfide oxidation and associated metal release from exposed rock in the mine back will drop to low levels. We assume groundwater flowing through remaining voids between the paste backfill and the back will continue to acquire solutes from the exposed paste surface and react with the fractured bedrock surface. At closure, pyrite within the relatively high-surface-area zone around the workings will be stable under reducing conditions.

Pyrite is known to adsorb a variety of metals common to mining environments, including Pb, Hg, Cu, Cd, Cr, and As (Doyle et al., 2004; Borah and Senapati, 2006; Oxverdi and Erdem, 2006). In fact, pyrite has been proposed for use in reactive barrier technology to remove metals from contaminated groundwater (Brown et al. 1979). Of these metals, only Cd and Hg were predicted in post-closure groundwater. We therefore calculated the capacity for their sorption to pyrite in the USZ using this analytical model. Using the USZ pyrite concentration (46 wt %) reported by CAMP, and surface area-adjusted isotherm data for comparable pH and metal concentrations (Borah and Senapati (2006) for Cd, and Bower et al. (2008) for Hg), we estimate that Hg will be completely removed via sorption to pyrite, with an attenuation capacity of over 20 thousand years. Likewise, we estimate that capacity exists for Cd will be completely attenuated within the bedrock fracture zone for millions of years.

The concentration of metals used in these calculations are scaled, from surface area and water flux rates typical of the laboratory diffusion tests to conditions relevant to the post-closure mine setting. The concentrations measured in diffusion tests are scaled up due to the increased paste backfill surface area and reduce flow of groundwater post-closure.

These calculations conservatively rely on constant, long term release of metals by paste backfill (which are likely to decline over time) and rates published for experiments that were conducted at higher concentrations of Cd and Hg. Data are not available for experiments conducted at lower concentrations, because Cd and Hg removal efficiency is 100% and therefore, lower metal concentrations are not quantifiable in solution.

<u>Assumptions:</u>		
* 1 m fracture zone above back	See section 4.3.2	
* mass of rock in 1 m zone above the back is calculated from the density of the upper sulfide zone		
* fracture density of 10% in the upper zone implies that the specific surface area is 10% of the humidity cell test material		
<u>Calculations:</u>		
Top surface area of backfilled paste in USZ	293060 m ²	
Volume of fracture zone above back (1-m thick)	293060 m ³	
Mass of fracture zone above back	1.06E+09 kg	*based on 3600 kg/m ³ in USZ)
Surface area of HCT (used for Fd scaling)	2.0107 m ² /kg	*based on calculation from sieved material
Surface area of fracture zone	2.12E+08 m ²	*based on 10% of the specific surface area of the HCT
Surface area of FeS ₂ in fracture zone	9.76E+07 m ²	*assumes that 46% of the surface area is pyrite, i.e. that the relative surface area is proportional to mass of pyrite reported by CAMP (Enviromin, 2016b)
Intrinsic attenuation capacity per mass	0.0002 g Hg/g FeS ₂	*based on data collected by Bower et al. (2008) at lowest concentration of Hg, where 100% removal was attained in 2 days
Intrinsic attenuation capacity per surface area	0.0004762 g Hg/m ² FeS ₂	*based on BET data from Bower et al., 2008, 0.42 m ² /g in samples. ¹
Total attenuation capacity of fracture zone	46468 g Hg	
Flow rate through USZ at post-closure	190784 L/week through the USZ/UCZ	
<u>Duration of attenuation capacity = Hg</u>		
Assuming 224 ppt Hg released from scaled paste surface, prior to dilution	2.09E+04 years of attenuation capacity	
Intrinsic attenuation capacity per mass	0.1676 g Cd/g FeS ₂	*based on data collected by Borah and Senapati, 2006 at lowest Cd concentration, where 100% removal was attained in 2 days
Intrinsic attenuation capacity per surface area	0.69833 g Cd/m ² FeS ₂	*based on BET data from Borah and Senapati, 2006, 0.24 m ² /g in samples. ¹
Total attenuation capacity of fracture zone	68145006 g Cd	
Flow rate through USZ at post-closure	190784 L/week through the USZ/UCZ	
<u>Duration of attenuation capacity - Cd</u>		
Assuming 238 ppt Cd released from scaled paste surface	2.88E+07 years of attenuation capacity	
¹ Note that BET, which probably overestimates surface area compared to the geometric assumption used above, is conservative.		

APPENDIX G: Mass-Load Inputs from the Base Case Underground Model at Year 6

Parameter	Units*	Groundwater contribution							Oxidized surface contribution										Combined input (GW + rock/stope)						
		surface decline		upper access/stopes		lower decline	lower access/stopes		surface decline		upper access/stopes		lower decline	lower access/stopes				surface decline		upper access/stopes		lower decline	lower access/stopes		
		YNL-A	USZ	USZ/UCZ	YNLB-UA	YNLB-LD	LCZ & LZFW	YnlB-LA	YNL-A	USZ	USZ/UCZ	Backfill	YNLB-UA	YNLB-LD	LCZ	LZFW	Backfill	YNLB-LA	YNL-A	USZ	USZ/UCZ	YNLB-UA	YNLB-LD	LCZ	YnlB-LA
		Avg (MW-1B, -2A, -2B, -4B, -9, PW-1 and -8)	PW-9 Avg	Avg (MW-3, PW-2, PW-4)	PW-10	PW-10	From PW-9 in UCZ (worst case), because data for PW-7 are poor	PW-10	HCT - 2012 Ynl	HCT - 2012 USZ	HCT - 2015 USZ	2015 4% binder cyl. Diff. test	HCT - 2012 Ynl B	HCT - 2015 Ynl B	HCT - 2015 LZFW	HCT - 2015 LZFW	2015 4% binder cyl. Diff. test	HCT - 2015 LZFW	YNL-A	USZ	USZ/UCZ	YNLB-UA	YNLB-LD	LCZ	YnlB-LA
Flow rate	L/min	386	34	1037	49	450	37.85	64	Assumptions										386	34	1037	49	450	37.85	64
	L/week	3891997	343411	10454972	496039	4540663	381568	648666	*Upper zone fracture density 0.1 applies to surface decline and upper access/stopes *Lower zone fracture density 0.02 applies to lower decline and lower access/stopes *Oxidation rate (kg SO4/y/m2) 6										3891997	343411	10454972	496039	4540663	381568	648666
Fraction of total flow	-	0.188	0.017	0.504	0.024	0.219	0.018	0.031											0.188	0.017	0.504	0.024	0.219	0.018	0.031
Surface area	m2								9900	1200	91545	3346	50000	63400	8713	94400	1714	27280							
Rock density	kg/m3								2710	3600	3600	-	2710	2710	3600	3600	-	3600							
Mass fraction sulfide (as S)	-								0.016	0.200	0.200	-	0.011	0.011	0.113	0.019	-	0.019							
Exposure time (days)	days								2160	2160	90	-	90	2160	90	-	90								
Reactive mass (kg)	kg								2682900	71209	226347	-	2247752	3436280	38298	6796800	-	710006							
Oxidized rind thickness (m)	m								1.000	0.165	0.007	-	0.166	1.000	0.061	1.000	-	0.361							
Scaling factor w.r.t. HCT	-								0.31	0.09	0.01	0.02	2.06	0.32	0.04	7.71	0.32	0.47							
pH	s.u.	7.03	6.56	7.06	7.39	7.39	6.56	7.39	7.81	7.87	7.64	6.89	7.68	8.17	8.77	6.52	5.74	7.73	6.96	6.54	6.62	7.21	7.32	5.62	7.23
Activity of hydrogen	-	9.43E-08	2.75E-07	8.66E-08	4.07E-08	4.07E-08	2.75E-07	4.07E-08	1.6E-08	1.4E-08	2.3E-08	1.3E-07	2.1E-08	6.8E-09	1.7E-09	3.0E-07	1.8E-06	1.9E-08	1.10E-07	2.89E-07	2.39E-07	6.15E-08	4.75E-08	2.41E-06	5.95E-08
Temperature	°C	7.1	10.3	9.3	8.5	8.5	10.3	8.5	7.1	10.3	9.3	9.3	8.5	8.5	9.3	9.3	8.5	8.5	7.1	10.3	9.3	8.5	8.5	9.3	8.5
Total Alkalinity	mg/L as CaCO3	189	204	223	230	230	204	230	4.51	1.14	0.16	0.03	56	9	1	177	0.481	11	193	205	223	286	239	383	241
Aluminum	mg/L	0.015	0.009	0.016	0.009	0.009	0.009	0.009	0.004	0.001	0.001	0.007	0.080	0.023	0.003	0.447	0.003	0.027	0.019	0.010	0.024	0.089	0.032	0.462	0.036
Antimony	mg/L	0.003	0.001	0.002	0.001	0.001	0.001	0.001	0.000	0.000	0.000	0.000	0.011	0.001	0.000	0.064	0.000	0.004	0.004	0.001	0.002	0.011	0.001	0.065	0.004
Arsenic	mg/L	0.018	0.086	0.063	0.048	0.048	0.048	0.048	0.000	0.000	0.000	0.000	0.005	0.001	0.006	1.030	0.001	0.063	0.018	0.087	0.063	0.053	0.049	1.124	0.111
Barium	mg/L	0.059	0.014	0.014	0.111	0.111	0.014	0.111	0.007	0.001	0.000	0.001	0.012	0.009	0.001	0.206	0.009	0.013	0.066	0.015	0.015	0.123	0.120	0.230	0.124
Beryllium	mg/L	0.001	0.001	0.001	0.001	0.001	0.001	0.001	0.000	0.000	0.000	0.000	0.002	0.000	0.000	0.006	0.000	0.000	0.001	0.001	0.001	0.002	0.001	0.007	0.001
Cadmium	mg/L	0.00004	0.00003	0.00005	0.00004	0.00004	0.00003	0.00004	0.000	0.000	0.000	0.000	0.000	0.000	0.000	0.001	0.000	0.000	0.000	0.000	0.000	0.000	0.000	0.001	0.000
Calcium	mg/L	58	83	84	74	74	83	74	25	11	5	0	36	9	1.4	249	9	15	83	94	89	110	83	342	89
Chloride	mg/L	1.41	1.40	1.40	1.00	1.00	1.40	1.00	0.101	0.70	0.073	0.023	0.002	0.000	0.014	3	0.427	0.16	1.513	2.101	1.496	1.002	1.000	4.385	1.156
Chromium	mg/L	0.007	0.005	0.005	0.010	0.010	0.005	0.010	0.003	0.001	0.000	0.000	0.021	0.003	0.000	0.077	0.002	0.005	0.010	0.006	0.005	0.031	0.013	0.084	0.015
Copper	mg/L	0.002	0.002	0.002	0.002	0.002	0.002	0.002	0.001	0.000	0.000	0.000	0.004	0.001	0.000	0.015	0.001	0.001	0.003	0.002	0.002	0.006	0.003	0.018	0.003
Fluoride	mg/L	0.29	0.60	0.69	0.80	0.80	0.60	0.80	0.18	0.02	0.00	0.002	1.85	0.60	0.09	16.4	0.043	1.01	0.47	0.62	0.70	2.65	1.40	17.18	1.81
Iron	mg/L	5.77	2.18	1.12	0.340	0.340	2.18	0.340	0.006	0.002	0.104	0.000	0.041	0.006	0.001	0.154	0.006	0.009	5.78	2.18	1.22	0.381	0.346	2.337	0.349
Lead	mg/L	0.002	0.000	0.000	0.000	0.000	0.000	0.000	0.000	0.000	0.000	0.000	0.001	0.001	0.000	0.013	0.000	0.001	0.002	0.000	0.000	0.001	0.001	0.014	0.001
Magnesium	mg/L	28	48	53	47	47	48	47	15	17	4	0.01	31	11	2	373	0.328	23	43	65	58	78	58	423	70
Manganese	mg/L	0.043	0.041	0.034	0.437	0.437	0.041	0.437	0.020	0.083	0.049	0.000	0.010	0.002	0.001	0.105	0.003	0.006	0.062	0.123	0.083	0.447	0.439	0.150	0.443
Mercury	mg/L	0.000007	0.000005	0.000007	0.000005	0.000005	0.000005	0.000005	0.000003	0.000001	0.000015	0.000001	0.000017	0.000002	0.000000	0.000039	0.000018	0.000002	0.000009	0.000006	0.000022	0.000022	0.000007	0.000062	0.000007
Nickel	mg/L	0.005	0.001	0.005	0.001	0.001	0.001	0.001	0.001	0.002	0.001	0.000	0.004	0.001	0.001	0.100	0.003	0.006	0.006	0.004	0.006	0.005	0.002	0.105	0.007
Nitrate + Nitrite	mg/L as N	0.069	0.016	0.010	0.010	0.010	0.016	0.010	0.000	0.000	0.000	0.002	0.000	0.000	0.000	0.032	0.000	0.000	0.069	0.016	0.012	0.010	0.010	0.048	0.010
Phosphorus	mg/L	0.015		0.010					0.002	0.000	0.000	0.001	0.010	0.002	0.001	0.098	0.003	0.006	0.017	0.000	0.011	0.010	0.002	0.102	0.006
Potassium	mg/L	2.0	3.0	3.1	5.0	5.0	3.0	5.0	3.6	2.0	0.2	0.055	51.4	8.1	1.1	203	0.7	12.5	5.6	5.0	3.4	56.4	13.1	207.7	17.5
Selenium	mg/L	0.001	0.000	0.001	0.000	0.000	0.000	0.000	0.002	0.001	0.000	0.000	0.014	0.003	0.001	0.116	0.000	0.007	0.002	0.001	0.001	0.014	0.003	0.117	0.007
Silicon	mg/L	10.1		8.3					0.3	0.1	0.0	0.007	3.1	0.6	0.1	21.3	0.060	1.3	10.4	0.1	8.3	3.1	0.6	21.5	1.3
Sodium	mg/L	3.1	11.8	14.3	11.0	11.0	11.8	11.0	3.8	0.3	0.0	0.033	28.1	4.4	0.4	77.1	0.646	4.7	6.8	12.1	14.3	39.1	15.4	90.0	15.7
Strontium	mg/L	0.6	8.7	13.5	11.9	11.9	8.7	11.9	0.3	0.1	0.3	0.007	0.3	0.5	0.0	4.6	0.10	0.3	0.8	8.7	13.8	12.2	12.4	13.4	12.2
Sulfate	mg/L	88	250	253	190	190	250	190	126	82	30	1	178	85	13	2279	14.4	140	214	332	283	368	275	2556	330
Thallium	mg/L	0.004	0.001	0.0004	0.0002	0.0002	0.001	0.0002	0.001	0.000	0.001	0.000	0.000	0.000	0.000	0.005	0.000	0.000	0.005	0.001	0.002	0.001	0.000	0.006	0.000
Uranium	mg/L	0.005	0.002	0.004	0.008	0.008	0.002	0.008	0.000	0.000	0.000	0.000	0.002	0.000	0.010	1.7	0.000	0.105	0.006	0.002	0.004	0.010	0.008	1.728	0.113
Zinc	mg/L	0.019	0.056	0.046	0.002	0.002	0.056	0.002	0.002	0.001	0.000	0.000	0.016	0.003	0.000	0.062	0.003	0.004	0.021	0.057	0.046	0.018	0.005	0.122	0.006

not measured
detection limits

For the paste backfill, results from HCTs are scaled to surface area rather than Rm, because this material is not a fractured porous media like the walls. Secondly, the ASTM method recommends normalization to the diffusion tests based on diffusion through the surface. Surface area calculations in supporting document *Workings_SA_Calc_LS_final_4walls*

The calculation of Rm is based on sulfide oxidation rate (i.e., sulfate production), which depends on rock density, sulfide content, and exposure time. Including unit conversions, the equation is described by:



Purple indicates that oxidized rind has maxed out at the extent of blast-induced fractures (i.e., 1 m), so we recalculate the reactive mass based on the max thickness

For pH, we convert to H activity, and scale, and then recalculate after scaling.

APPENDIX H: Mass-Load Inputs from the Base Case Underground Model at Closure

Parameter	Units*	Groundwater contribution							Oxidized surface contribution								Combined input (GW + rock/stope)							
		surface decline		upper access/stopes		lower decline	lower access/stopes		surface decline		upper access/stopes		lower decline	lower access/stopes			surface decline		upper access/stopes		lower decline	lower access/stopes		
		YNL-A	USZ	USZ/UCZ	YNLB-UA	YNLB-LD	LCZ & LZFW	YnlB-LA	YNL-A	USZ	USZ/UCZ	Backfill	YNLB-UA	YNLB-LD	LCZ	LZFW	Backfill	YNLB-LA	YNL-A	USZ	USZ/UCZ	YNLB-UA	YNLB-LD	LCZ
Flow rate	L/min	344	30	19	11	15	4	1	ASSUMPTIONS All oxidized wall-rock terms shut off and paste backfill becomes the only input Surface area of stopes increases because 100% of stopes have been mined At closure, all sides of the cement backfill are reactive								344	30	19	11	0	0	0	
	L/week	3472272	305255	190784	114470	152627	38157	11447									3472272	305255	190784	114470	0	0	0	
Fraction of total flow	-	0.810	0.071	0.045	0.027	0.036	0.009	0.003	0.810	0.071	0.045	0.027	0.000	0.000	0.000									
Surface area	m2								14653								13176							
Rock density	kg/m3								-								-							
Mass fraction sulfide (as S)	-								-								-							
Exposure time (days)	days								-								-							
Reactive mass (kg)	kg								-								-							
Oxidized rind thickness (m)	m								-								-							
Scaling factor w.r.t. HCT	-								7.73								34.77							
pH	s.u.	7.03	6.56	7.06	7.39	7.39	6.56	7.39	6.51	It is assumed that fractured surfaces go anoxic once the underground water table rebounds, and thus do not add to the groundwater concentrations							5.86	7.03	6.56	6.41	7.39	7.39	5.78	7.39
Activity of hydrogen	-	9.43E-08	2.75E-07	8.66E-08	4.07E-08	4.07E-08	2.75E-07	4.07E-08	3.1E-07								1.4E-06	9.43E-08	2.75E-07	3.93E-07	4.07E-08	4.07E-08	1.65E-06	4.07E-08
Temperature	°C	7.1	10.3	9.3	8.5	8.5	10.3	8.5	9.3	628	7.1	10.3	9.3	8.5	8.5	9.3	8.5							
Total Alkalinity	mg/L as CaCO ₃	189	204	223	230	230	204	230	81.75	368	189	204	304	230	230	572	230							
Aluminum	mg/L	0.015	0.009	0.016	0.009	0.009	0.009	0.009	2.403	10.8	0.015	0.009	2.420	0.009	0.009	10.8	0.009							
Antimony	mg/L	0.003	0.001	0.002	0.001	0.001	0.001	0.001	0.011	0.051	0.003	0.001	0.013	0.001	0.001	0.051	0.001							
Arsenic	mg/L	0.018	0.086	0.063	0.048	0.048	0.086	0.048	0.140	0.63	0.018	0.086	0.202	0.048	0.048	0.7	0.048							
Barium	mg/L	0.059	0.014	0.014	0.111	0.111	0.014	0.111	0.390	1.8	0.059	0.014	0.404	0.111	0.111	1.8	0.111							
Beryllium	mg/L	0.001	0.001	0.001	0.001	0.001	0.001	0.001	0.006	0.028	0.001	0.001	0.007	0.001	0.001	0.029	0.001							
Cadmium	mg/L	0.00004	0.00003	0.00005	0.00004	0.00004	0.00003	0.00004	0.000238	0.001	0.000	0.000	0.000	0.000	0.000	0.001	0.000							
Calcium	mg/L	58	83	84	74	74	83	74	140	628	58	83	224	74	74	711	74							
Chloride	mg/L	1.41	1.40	1.40	1.00	1.00	1.40	1.00	7.79	35	1.4	1.4	9.2	1.0	1.0	36	1.0							
Chromium	mg/L	0.007	0.005	0.005	0.010	0.010	0.005	0.010	0.039	0	0.007	0.005	0.044	0.010	0.010	0.179	0.010							
Copper	mg/L	0.002	0.002	0.002	0.002	0.002	0.002	0.002	0.018	0.082	0.002	0.002	0.020	0.002	0.002	0.084	0.002							
Fluoride	mg/L	0.290	0.600	0.693	0.800	0.800	0.600	0.800	0.773	3.5	0.290	0.600	1.467	0.800	0.800	4.077	0.800							
Iron	mg/L	5.77	2.18	1.12	0.340	0.340	2.18	0.340	0.155	0.70	5.8	2.2	1.3	0.3	0.3	2.9	0.3							
Lead	mg/L	0.002	0.000	0.000	0.000	0.000	0.000	0.000	0.002	0.007	0.002	0.000	0.002	0.000	0.000	0.007	0.000							
Magnesium	mg/L	28	48	53	47	47	48	47	3.867	17.4	28	48	57	47	47	66	47							
Manganese	mg/L	0.043	0.041	0.034	0.437	0.437	0.041	0.437	0.040	0.182	0.043	0.041	0.074	0.437	0.437	0.223	0.437							
Mercury	mg/L	0.00007	0.00005	0.00007	0.00005	0.00005	0.00005	0.00005	0.000224	0.001	0.00007	0.00005	0.000230	0.00005	0.00005	0.001010	0.00005							
Nickel	mg/L	0.005	0.001	0.005	0.001	0.001	0.001	0.001	0.016	0.07	0.005	0.001	0.021	0.001	0.001	0.073	0.001							
Nitrate + Nitrite	mg/L as N	0.069	0.016	0.010	0.010	0.010	0.016	0.010	0.773	3.477	0.069	0.016	0.783	0.010	0.010	3.493	0.010							
Phosphorus	mg/L	0.015		0.010					0.204	0.9	0.015	0.000	0.214	0.000	0.000	0.919	0.000							
Potassium	mg/L	2.007	3.000	3.143	5.000	5.000	3.000	5.000	18.73	84	2.007	3.000	21.9	5.000	5.000	87.2	5.000							
Selenium	mg/L	0.001	0.000	0.001	0.000	0.000	0.000	0.000	0.008	0.035	0.001	0.000	0.008	0.000	0.000	0.035	0.000							
Silicon	mg/L	10.060		8.300					2.447	11.0	10.060	0.000	10.747	0.000	0.000	11.0	0.000							
Sodium	mg/L	3.059	11.800	14.267	11.000	11.000	11.800	11.000	11.25	51	3.1	12	26	11	11	62	11							
Strontium	mg/L	0.566	8.654	13.480	11.900	11.900	8.654	11.900	2.215	10	0.6	8.7	15.7	11.9	11.9	18.6	11.9							
Sulfate	mg/L	88	250	253	190	190	250	190	212.7	956	88	250	465	190	190	1206	190							
Thallium	mg/L	0.004	0.001	0.0004	0.0002	0.0002	0.001	0.0002	0.003	0.015	0.004	0.001	0.004	0.000	0.000	0.015	0.000							
Uranium	mg/L	0.005	0.002	0.004	0.008	0.008	0.002	0.008	0.002	0.007	0.005	0.002	0.006	0.008	0.008	0.009	0.008							
Zinc	mg/L	0.019	0.056	0.046	0.002	0.002	0.056	0.002	0.069	0.31	0.019	0.056	0.115	0.002	0.002	0.367	0.002							

not measured in groundwater wells
detection limits

Removed these units

Note that the LCZ input described here is highly supersaturated in several phases. The reason is that the surface area to flow ratio is s

APPENDIX I: Mass-Load Inputs from the Base Case Model for the WRS at Year 2

Parameter	Units*	Contribution from exposed rock			Water to sump (pre-Phreeq)	
		USZ	YnlB	YnlA	FINAL MIX	
		HCT - 2015 USZ	HCT - 2015 YnlB	HCT - 2012 Ynl		
Flow rate	gpm	0.9	0.9	0.9	Percolation value comes from the HELP model (Hydrometrics, 2016), which considers evapotranspiration (e.g., wind), snow removal, solar radiation, and average precipitation.	
	L/week	34338	34338	34338		
	L/yr	1785551	1785551	1785551		
Surface area	m2	203093	308333	38542	Average density of WR mix 3.099375	
specific gravity	g/cm3	3.60	2.71	2.71		
surface area per mass	m2/kg	0.0559	0.0743	0.0743		
Total mass in WRS (tonne = 1000 k)	tonnes	180047	205769	25721		
Calculated Rm (from H2O saturation)	tonnes	3632	4151	519		
Scaling factor w.r.t. HCT	-	1.29	1.28	0.24	Assumes total WR on pile (411,537 tonnes) to be 4% YnlA, 28% USZ, 32% YnlB, and 35% LZFW.	
pH	s.u.	5.51	7.57	7.91	5.50	Assumes 40% porosity, calculates the mass of waste rock that can be saturated by the water flow in 1 yr, according to
Activity of hydrogen	-	3.09E-06	2.66E-08	1.24E-08	3.13E-06	$R_{m,i}(\text{tonnes}) = \frac{L_{H2O}}{\text{yr}} * \frac{1000 \text{ cm}^3_{H2O}}{L_{H2O}} * \frac{6 \text{ cm}^3_{rock}}{4 \text{ cm}^3_{H2O}} * \frac{g_{rock}}{\text{cm}^3_{rock}} * \frac{\text{tonne}_{rock}}{10^6 g_{rock}} * \frac{\text{tonne}_i}{\text{tonne}_{rock}}$
Temperature	°C	2.20	2.20	2.20	2.20	
Aluminum	mg/L	0.0766	0.0920	0.0030	0.1716	set to average annual temperature at Tintina weather station
Alkalinity	mg/L as CaCO ₃	21.313	35.449	3.562	60.324	
Arsenic	mg/L	0.0026	0.0047	0.0002	0.00751	
Barium	mg/L	0.0177	0.0358	0.0055	0.0589	
Beryllium	mg/L	0.0010	0.0010	0.0002	0.0022	
Calcium	mg/L	613.9869	34.4909	19.7245	668.202	
Cadmium	mg/L	0.0005	0.0001	0.0000	0.000615	
Chloride	mg/L	9.907	0.001	0.080	9.988	
Chromium	mg/L	0.01	0.01	0.00	0.0281	
Copper	mg/L	0.06	0.00	0.00	0.0641	
Fluoride	mg/L	0.34	2.36	0.14	2.853	
Iron	mg/L	14.15	0.03	0.00	14.179	
Mercury	mg/L	0.00	0.00	0.00	0.00202	
Potassium	mg/L	28	32	3	63.172	
Magnesium	mg/L	567	42	12	620.781	
Manganese	mg/L	6.70	0.01	0.02	6.725	
Nitrate + Nitrite	mg/L as N	0.00	0.00	0.00	5.548	mmol N(5) for phreeq input, based on data from the underground of a mine in MT
Sodium	mg/L	4	17	3	24.32	
Nickel	mg/L	0.14	0.00	0.00	0.143	
Phosphorus	mg/L	0.01	0.01	0.00	0.0163	
Lead	mg/L	0.00	0.00	0.00	0.0068	
Sulfate	mg/L	4026	336	99	46.44	mmol S(6) for phreeq input
Antimony	mg/L	0.0013	0.0028	0.0003	0.0044	
Selenium	mg/L	0.01	0.01	0.00	0.0172	
Silicon	mg/L	1.79	2	0.27	4.238	
Strontium	mg/L	39.7	1.88	0.21	41.824	
Thallium	mg/L	0.16	0.00	0.00	0.1655	
Uranium	mg/L	0.00	0.00	0.00	0.00249	
Zinc	mg/L	0.03	0.01	0.00	0.04272	

APPENDIX J: Data Used for Wet Paste Seepage and 2% Paste in the Cement Tailings Facility

		2% paste HCT	Dewatered cement paste	4% paste HCT
Parameter	Units	Enviromin, 2015	from metallurgy data	from Enviromin, 2015
pH	s.u.	4.09873	9.32	5.86000
activity of hydrogen	-	7.97E-05	4.79E-10	1.38E-06
Temperature	°C	23.80	21.0	23.85
Alkalinity	mg/L as CaCO ₃	2.40		1.50000
Aluminum	mg/L	23.29400	0.2810	0.01000
Antimony	mg/L	0.00147	0.0523	0.00053
Arsenic	mg/L	0.02067	0.0452	0.00400
Barium	mg/L	0.03867	0.3020	0.02867
Beryllium	mg/L	0.00620	0.0000	0.00080
Cadmium	mg/L	0.00171	0.0000	0.00003
Calcium	mg/L	140.00000	47.5000	27.75000
Chloride	mg/L	4.66667	120.0000	1.33333
Chromium	mg/L	0.01333	0.0042	0.00500
Copper	mg/L	73.38237	2.7600	0.00200
Fluoride	mg/L	0.68333	0.2800	0.13333
Iron	mg/L	18.87500	0.0100	0.02000
Lead	mg/L	0.00327	0.0964	0.00020
Magnesium	mg/L	75.40000	0.6230	1.02500
Manganese	mg/L	3.20923	0.0008	0.00500
Mercury	mg/L	0.00014		0.00003
Nickel	mg/L	10.35300	0.0160	0.00950
Nitrate	mg/L as N		0.6000	
Phosphorus	mg/L	0.29933	0.0470	0.01067
Potassium	mg/L	3.16667	3.1000	2.09000
Selenium	mg/L	0.00267	0.0005	0.00100
Silicon	mg/L	5.65000	0.6600	0.18667
Sodium	mg/L	3.16667	40.7000	2.01667
Strontium	mg/L	2.50000	0.9880	0.32667
Sulfate	mg/L	890.00000	83.0000	45.00000
Thallium	mg/L	0.01710	0.0036	0.00113
Uranium	mg/L	0.01060	0.0000	0.00020
Zinc	mg/L	1.01200	0.0030	0.00800
	detection limits			
	not measured			

APPENDIX K: Mass-Load Inputs from the Base Case CTF at Year 6 of Mining

Parameter	Units*	Surface exposure				Wet paste dewatering based on 55% of 2900 tons of paste per day going to the CTF, and 5% of that mass seeping out as water	Ramp/drain term					Water to sump FINAL MIX	
		From cemented surface	From exposed waste rock "lenses"				Ynl	USZ	YnlB (ramp)	YnlB (liner), 3/8" (0.009525 m)	LZFW		
		HCT - 2% binder	USZ	YnlB	LZFW								HCT - 2012 Ynl
Flow rate	m3/yr	84000	84000	84000	84000	29029	11303	11303	11303	11303	11303	113029	assumes that 10% of flow goes through the ramp/drain
	L/week	1615385	1615385	1615385	1615385	558250	217363	217363	217363	217363	217363	2173635	
Surface area	m2	132000	90000	61522	116068		14878	1159	51304	12890	30782		0.0456037 surface area of cylinder ((h = 15.24 cm, d = 7.62 cm)
specific gravity	g/cc		3.60	2.71	2.71		2.71	3.60	2.71	2.71	2.71		2.72335 average rock density in ramp/drain
surface area per mass	m2/kg		0.0559	0.0743	0.0743		0.0743	0.0559	0.0743	0.2333	0.0743		assumes that the surface area increases the same as in one week in the 2% humidity cell test
Total mass (tonne = 1000 kg)	tonnes		1609	828	1562		56550	5850	195000	15600	117000		
Calculated Rm	tonnes		1609	828	1562		200	21	691	55	414		Assumes 30% porosity, calculates the mass of waste rock in drain that can be saturated by the water flow in 1 week
Scaling factor w.r.t. HCT	-	1.1023	0.0122	0.0054	0.0155		0.0103	0.0012	0.0336	0.0084	0.0305		
pH	s.u.	4.06	7.54	9.95	9.21	9.32	9.277	8.555	9.155	9.755	8.919	4.185204	$R_{m,i}(\text{tonnes}) = \frac{L_{H2O}}{wk} * \frac{1000 \text{ cm}^3_{H2O}}{L_{H2O}} * \frac{7 \text{ cm}^3_{rock}}{3 \text{ cm}^3_{H2O}} * \frac{g_{rock}}{\text{cm}^3_{rock}} * \frac{\text{ton}_{rock}}{10^6 g_{rock}} * \frac{\text{ton}_i}{\text{ton}_{rock}}$
Activity of hydrogen	-	8.78E-05	2.91E-08	1.13E-10	6.11E-10	4.79E-10	5.28E-10	2.78E-09	7.00E-10	1.76E-10	1.20E-09	6.53E-05	
Temperature	°C	2.2	2.2	2.2	2.2	2.2	2.2	2.2	2.2	2.2	2.2	2.2	based on yearly temperature average collected at site
Aluminium	mg/L	25.676	0.00722	0.000390	0.0009	0.28100	0.0001	0.0001	0.0024	0.0006	0.0018	19.155745	
Alkalinity	mg/L as CaCO3	2.645405	0.200763	0.150353	0.355603	520.00000	0.2	0.0	0.9	0.2	0.7	136.245531	not measured - estimated by Jeffrey Austin (metallurgist at In1 MET), based on water data from other projects
Arsenic	mg/L	0.022780	0.000024	0.000020	0.002067	0.04520	0.0000	0.0000	0.0001	0.0000	0.0041	0.030531	
Barium	mg/L	0.042620	0.000166	0.000152	0.000412	0.30200	0.0002	0.0000	0.0009	0.0002	0.0008	0.110003	
Beryllium	mg/L	0.006834	0.000010	0.000004	0.000012	0.00001	0.0000	0.0000	0.0000	0.0000	0.0000	0.005107	
Calcium	mg/L	154.3153	5.783599	0.146289	0.499906	47.50000	0.8429	0.5533	0.9066	0.2278	0.9853	132.012186	1595
Cadmium	mg/L	0.001885	0.000004	0.000001	0.000003	0.00004	0.0000	0.0000	0.0000	0.0000	0.0000	0.001418	
Chloride	mg/L	5.143844	0.093324	0.000005	0.005102	120.00000	0.0034	0.0089	0.0000	0.0000	0.0101	34.717503	
Chromium	mg/L	0.014697	0.000122	0.000054	0.000155	0.00421	0.0001	0.0000	0.0003	0.0001	0.0003	0.012333	
Copper	mg/L	80.885875	0.000564	0.000014	0.000031	2.76000	0.0000	0.0001	0.0001	0.0000	0.0001	60.821450	
Fluoride	mg/L	0.753206	0.003245	0.010024	0.032984	0.28000	0.0062	0.0003	0.0621	0.0156	0.0650	0.680970	
Iron	mg/L	20.805010	0.133274	0.000108	0.000309	0.01000	0.0002	0.0128	0.0007	0.0002	0.0006	15.565068	
Mercury	mg/L	0.00015156	0.00001890	0.00000004	0.00000008	0.00000	0.0000	0.0000	0.0000	0.0000	0.0000	0.000127	
Potassium	mg/L	3.49047	0.26768	0.13545	0.40709	3.10000	0.1204	0.0256	0.8394	0.2109	0.8024	4.192195	
Magnesium	mg/L	83.10982	5.34151	0.17699	0.74728	6.2300	0.5126	0.5110	1.0969	0.2756	1.4729	66.968354	
Manganese	mg/L	3.53738	0.06311	0.00004	0.00021	0.00076	0.0007	0.0060	0.0003	0.0001	0.0004	2.676913	
Nitrate + Nitrite	mg/L as N	0.00000	0.00000	0.00000	0.00000	0.60000	0.0000	0.0000	0.0000	0.0000	0.0000	0.554839	mmol N(5)/L for Phreeq Input - estimated by mine-affected water from an underground mine
Sodium	mg/L	3.49047	0.03650	0.07407	0.15461	40.70000	0.1273	0.0035	0.4590	0.1153	0.3047	13.344965	
Nickel	mg/L	11.41162	0.00131	0.00001	0.00020	0.01600	0.0000	0.0001	0.0001	0.0000	0.0004	8.486103	
Phosphorus	mg/L	0.32994	0.00006	0.00003	0.00020	0.04700	0.0001	0.0000	0.0002	0.0001	0.0004	0.257565	
Lead	mg/L	0.00360	0.00003	0.00002	0.00003	0.09640	0.0000	0.0000	0.0001	0.0000	0.0001	0.027505	
Sulfate	mg/L	981.00446	37.92191	1.42496	4.57131	83.00000	4.2384	3.6281	8.8310	2.2187	9.0098	8.180338	mmol S(6)/L for Phreeq input 785.8032282
Antimony	mg/L	0.00162	0.00001	0.00001	0.00013	0.05230	0.0000	0.0000	0.0001	0.0000	0.0003	0.014782	
Selenium	mg/L	0.00294	0.00005	0.00005	0.00023	0.00050	0.0001	0.0000	0.0003	0.0001	0.0005	0.002642	
Silicon	mg/L	6.22772	0.01683	0.00926	0.04278	0.66000	0.0114	0.0016	0.0574	0.0144	0.0843	4.865877	
Strontium	mg/L	2.75563	0.37435	0.00796	0.00928	0.98800	0.0088	0.0358	0.0494	0.0124	0.0183	2.605138	
Thallium	mg/L	0.01885	0.00155	0.00000	0.00001	0.00356	0.0000	0.0001	0.0000	0.0000	0.0000	0.016102	
Uranium	mg/L	0.01168	0.00001	0.00001	0.00344	0.00000	0.0000	0.0000	0.0000	0.0000	0.0068	0.011937	
Zinc	mg/L	1.11548	0.00029	0.00004	0.00012	0.00300	0.0001	0.0000	0.0003	0.0001	0.0002	0.830171	

APPENDIX L: Mass-Load Inputs from the Base Case CTF at Closure

Parameter	Units	Surface exposure	Ramp/drain term					Water to sump
		From cemented surface	Ynl	USZ	YnlB (ramp)	YnlB (liner), 3/8" (0.009525 m)	LZFW	FINAL OUTPUT
		HCT - 4% binder	HCT - 2012 Ynl	HCT - 2012 USZ	HCT - 2012 YnlB	HCT - 2012 YnlB	HCT - 2015 LZFW	
Flow rate	m3/yr	84000	8400	8400	8400	8400	8400	84000
	L/week	1615385	161538	161538	161538	161538	161538	1615385
Surface area	m2	210000	11057	861	38127	9579	22876	
specific gravity	g/cc		2.71	3.60	2.71	2.71	2.71	
surface area per mass	m2/kg		0.0743	0.0559	0.0743	0.2333	0.0743	
Total mass (tonne = 1000 kg)	tonnes		56550	5850	195000	15600	117000	
Calculated Rm	tonnes		149	15	513	41	308	
Scaling factor w.r.t. HCT	-	1.9415	0.0103	0.0012	0.0336	0.0084	0.0305	
pH	s.u.	4.951870	9.28	8.56	9.15	9.75	8.92	4.95
Activity of hydrogen	-	1.12E-05	5.28E-10	2.78E-09	7.00E-10	1.76E-10	1.20E-09	1.12E-05
Temperature	°C	2.2	2.2	2.2	2.2	2.2	2.2	2.2
Aluminum	mg/L	0.019415	0.0001	0.0001	0.0024	0.0006	0.0018	0.0199135
Alkalinity	mg/L as CaCO ₃	2.912200	0.1522	0.0192	0.9318	0.2341	0.7009	3.1160209
Arsenic	mg/L	0.007766	0.0000	0.0000	0.0001	0.0000	0.0041	0.0081899
Barium	mg/L	0.055655	0.0002	0.0000	0.0009	0.0002	0.0008	0.0558793
Beryllium	mg/L	0.001553	0.0000	0.0000	0.0000	0.0000	0.0000	0.0015599
Calcium	mg/L	53.875708	0.8429	0.5533	0.9066	0.2278	0.9853	54.2272930
Cadmium	mg/L	0.000065	0.0000	0.0000	0.0000	0.0000	0.0000	0.0000658
Chloride	mg/L	2.588623	0.0034	0.0089	0.0000	0.0000	0.0101	2.5908658
Chromium	mg/L	0.009707	0.0001	0.0000	0.0003	0.0001	0.0003	0.0097913
Copper	mg/L	0.005501	0.0000	0.0001	0.0001	0.0000	0.0001	0.0055270
Fluoride	mg/L	0.258862	0.0062	0.0003	0.0621	0.0156	0.0650	0.2737860
Iron	mg/L	0.038829	0.0002	0.0128	0.0007	0.0002	0.0006	0.0402700
Mercury	mg/L	0.000111	0.0000	0.0000	0.0000	0.0000	0.0000	0.0001112
Potassium	mg/L	4.057666	0.1204	0.0256	0.8394	0.2109	0.8024	4.2575415
Magnesium	mg/L	1.990004	0.5126	0.5110	1.0969	0.2756	1.4729	2.3768981
Manganese	mg/L	0.016826	0.0007	0.0060	0.0003	0.0001	0.0004	0.0175701
Nitrate	mg/L as N	0.000000	0.0000	0.0000	0.0000	0.0000	0.0000	0.0554839
Sodium	mg/L	3.915292	0.1273	0.0035	0.4590	0.1153	0.3047	4.0162724
Nickel	mg/L	0.018444	0.0000	0.0001	0.0001	0.0000	0.0004	0.0185083
Phosphorus	mg/L	0.020709	0.0001	0.0000	0.0002	0.0001	0.0004	0.0207807
Lead	mg/L	0.000453	0.0000	0.0000	0.0001	0.0000	0.0001	0.0004707
Sulfate	mg/L	87.366012	4.2384	3.6281	8.8310	2.2187	9.0098	0.9385656
Antimony	mg/L	0.001035	0.0000	0.0000	0.0001	0.0000	0.0003	0.0010714
Selenium	mg/L	0.001941	0.0001	0.0000	0.0003	0.0001	0.0005	0.0020285
Silicon	mg/L	0.362407	0.0114	0.0016	0.0574	0.0144	0.0843	0.3793222
Strontium	mg/L	0.634213	0.0088	0.0358	0.0494	0.0124	0.0183	0.6466757
Thallium	mg/L	0.002200	0.0000	0.0001	0.0000	0.0000	0.0000	0.0022219
Uranium	mg/L	0.000388	0.0000	0.0000	0.0000	0.0000	0.0068	0.0010732
Zinc	mg/L	0.019415	0.0001	0.0000	0.0003	0.0001	0.0002	0.0194837

assumes that 10% of flow goes through the ramp/drain

2.72335 average rock density in ramp/drain
0.0456037 surface area of cylinder ((h = 15.24 cm, d = 7.62 cm)
Assumes 30% porosity, calculates the mass of waste rock in drain that can be saturated by the water flow in 1 week
assumes that the surface area increases the same as in one week in the 2% humidity cell test

mmol N(5)/L for PhreeqC, estimated as 10% of of mine-affected value (34.4) during operations

mmol S(6)/L for Phreeq input 90.15860748

APPENDIX M: Mass-Load Inputs from Water Process Plant

Parameter	Units*	Contributions into PWP			Mixed water, before PhreeqC	
		Thickener overflow (from mill) - from AMEC	RO Brine from WTP - from AMEC	Water from CTF	FINAL FLOW PER YEAR	
Flow rate	m3/yr	3807000	181000	84000	4082000	includes 10000 m3/yr direct precipitation
Fraction of water input		0.933	0.044	0.021		=SUM(C4:E4)+10000
pH	s.u.	10.40	6.93	4.13	5.82	
Activity of hydrogen	-	3.98E-11	1.17E-07	7.40E-05	1.53E-06	
Temperature	°C	2.20	2.20	2.20	2.20	
Aluminum	mg/L	0.85595	0.05989	17.73360	1.16587	
Alkalinity	mg/L as CaCO ₃	77	660	97	255	set to balance in PHREEQ
Arsenic	mg/L	0.045	0.050	0.031	0.044814	
Barium	mg/L	0.302	0.164	0.004	0.2890	
Beryllium	mg/L	0.000007	0.00307	0.00510	0.00025	
Calcium	mg/L	511	696	132	510.15	
Cadmium	mg/L	0.00005	0.00030	0.00141	0.000089	
Chloride	mg/L	136	334	34	142.353	
Chromium	mg/L	0.0040	0.0020	0.0123	0.00407	
Copper	mg/L	2.7600	2.01	61.25	3.924	
Fluoride	mg/L	0.300	5.70	0.68	0.5465	
Iron	mg/L	0.0100	19.4	0.573	0.8813	
Mercury	mg/L	0.00001	0.00003	0.00013	0.000011	
Potassium	mg/L	28.00	66.0	0.000	29.040	
Magnesium	mg/L	1.000	388	94.9	20.090	
Manganese	mg/L	0.0010	0.82	2.68	0.09236	
Nitrate + Nitrite	mg/L as N	83.700	197	34	1.411	converted to mmol N(5) for phreeq
Sodium	mg/L	42.0	92	13	43.525	
Nickel	mg/L	0.01600	0.13	8.53	0.19626	
Phosphorus	mg/L	0.100	0.044	0.26	0.1005	
Lead	mg/L	0.096	0.047	0.027	0.0922	
Sulfate	mg/L	865	1912	765	9.445	converted to mmol S(6) for phreeq
Antimony	mg/L	0.0236	0.0159	0.0148	0.02300	
Selenium	mg/L	0.00058	0.01942	0.0026	0.00146	
Silicon	mg/L	0.587	7.4	0.00094	0.8754	
Strontium	mg/L	1.49	62.2	2.62	4.200	
Thallium	mg/L	0.00832	0.00980	0.0161	0.00852	
Uranium	mg/L	0.000080	0.186	0.0188	0.00869	
Zinc	mg/L	0.24700	0.274	0.826	0.25950	

** red values are non-detects from metallurgy tests *estimated as 5x Underground

APPENDIX N: Prediction of Rinsing Required at Closure of Underground Mine Workings



15 April 2017

TO: Tintina Montana

FROM: Dr. Lisa Bithell Kirk, P.Geo, Principal Biogeochemist
Dr. Logan Schultz, Senior Geochemical Engineer
Ms. Katharine Seipel, Senior Environmental Scientist

RE: Prediction of Rinsing Required at Closure of Underground Mine Workings
Black Butte Copper Mine Project

Enviromin has predicted long-term water quality for the Black Butte Copper Mine workings post-closure, following rebound of the groundwater and attainment of steady state chemistry. Under these conditions, ten percent of the rock within the zone damaged by blasting will react with oxygen, and release solutes to groundwater at rates conservatively represented by humidity cell weathering.

Tintina Montana has committed to treating water from the underground until the steady state, background chemistry described in Enviromin's predictive model, is attained. Specifically, Tintina plans to continuously flood portions of the workings with reverse osmosis (RO) permeate while pumping to remove the affected water for treatment. Tintina proposes to initially rinse the lower access (*Ynl B*) and then place bulkheads to isolate the *USZ* for rinsing. Ultimately, the RO permeate injection and groundwater withdrawal rates will be reduced so that groundwater replaces the injected water.

Conditions during the early rinsing stages of closure will be different than Enviromin's predicted post-closure. As the mine workings are flooded with RO permeate, eliminating oxygen exposure and reducing sulfide oxidation, rinsing of accumulated oxidation products from surfaces that were not rinsed during operations is expected. Salts accumulated on bedrock surfaces, which is the result of direct reaction of wall rock with oxygen under humid operational conditions as well as the evaporation of water during operations, are expected to include oxide, hydroxide, and sulfate minerals. These minerals are likely to have variable solubility; sulfates (e.g., alunite, jarosite, gypsum) are likely to be more soluble than iron oxides or barite, for example. Salts will dissolve into the RO permeate that will be pumped through the

workings; the most soluble minerals will dissolve rapidly, while others will dissolve more slowly. Initially elevated concentrations are thus expected to decline with rinsing, ultimately achieving a steady state concentration. As the closure process continues, pumping rates will be adjusted so that groundwater infiltration will replace flooding with RO permeate. The reaction of groundwater with exposed paste backfill under suboxic conditions is the basis for long term post-closure conditions addressed in the water quality prediction model (Enviromin, 2017).

Here, Enviromin has used humidity cell test (HCT) data for the *USZ* and *Ynl B* to estimate the mass and rate of dissolution of oxidation products, as a basis for predicting the time required to accomplish the removal of the stored minerals during closure.

The HCT results for the 2015 *USZ* are shown in Figure 1. Using sulfate release as a proxy for mineral dissolution, we observe a steep rinsing curve through week 2 followed by relatively steady release of sulfate due to oxidation of sulfide minerals during testing. The mass of sulfate released per mass of leached rock subsequently increased late in the test, when this material demonstrated acid production. The steep initial slope of the sulfate release curve reflects the rinsing of stored oxidation products from the crushed rock sample, which has relatively high surface area and which was stored for weeks to months prior to humidity cell testing. During this time, sulfide oxidation occurred. We define the rinsing curve from the start of the HCT to the point when the sulfate begins to increase in concentration due to oxidation. Other rock types, such as the 2015 *Ynl B* (Figure 2), which Tintina proposes to rinse prior to placing a bulkhead to isolate the *USZ*, reached the end of the rinsing phase by the end of week 3. Likewise, the 2012 *USZ* (Figure 3) reached end of the rinsing phase by week 6. Lacking actual rates for the accumulation of oxidation products on unrinsed underground surfaces, Enviromin has relied upon the rinsing of oxidation products during the initial phases of HCT testing to predict the time required for flushing. This was the basis of our original prediction of 3 to 6 rinses, as reported in the 2016 revised MOP. We support this baseline assessment here.

Enviromin recognizes that the rate of weathering in the underground could potentially exceed that observed in the stored samples, due to enhanced exposure to oxygen and water., and that the accumulation of salts over time could be greater. We propose to bound the likely mass using the total cumulative solute released during each HCT test. This cumulative solute represents the mass released under optimized oxidation conditions, and in our opinion, conservatively represents an upper bound of oxidation product formation. In Table 1, we calculate a cumulative sulfate release of 6,713 mg/kg during rinsing (weeks 0 through 2 for this HCT), and a total cumulative release of 67,649 mg/kg throughout the 73 week test. Dividing the total mass of sulfate released by the mass removed during rinsing suggests that no more than 10 rinses would be needed to remove the accumulated sulfate at the rate of rinsing observed during the early 2015 *USZ* HCT. In contrast, we made the same calculation for the 2012 *USZ* test, which did not develop acid conditions before it was terminated at 24 weeks, and show that 3 rinses should be sufficient to remove all oxidation products accumulated during that test.

Enviromin repeated this calculation for the 2015 *Ynl B* HCT, using the data summarized in Table 1 and Figure 2. A total of 824 mg/kg sulfate was released during the rinsing phase (weeks 0 to 3) of that test. Dividing the total sulfate released during that HCT (4,916 mg/kg) by the sulfate released during rinsing

suggests that, for this material, 6 rinses would be sufficient to dissolve the total sulfate released throughout the 36 week test.

These calculations suggest that 6 rinses of the 2015 USZ or 2015 Ynl B exposed within workings should remove stored oxidation products. If we conservatively estimate that the total solute released during the entire 2015 USZ HCT would be rinsed, as many as 10 rinses could be required. This is a highly conservative estimate because the oxidation rate in the mine will be slower than that observed in the optimized HCT test and water: rock surface area ratio used to flush the workings is more than three orders of magnitude greater than was used in the HCTs.

Table 1. Cumulative Sulfate Release Calculations, 2015 USZ and Ynl B

	<i>Week</i>	<i>Cumulative Sulfate mg/kg</i>	<i>Estimated Maximum Rinses</i>
2015 USZ	0	4333.9	
	1	5574.8	
	2	6713.8	$67649.9 \div 6713.8 = 10.0$
	Total (73)	67649.9	
2012 USZ	0	724.4	
	1	1213.3	
	2	1664.2	
	3	2035.3	
	4	2382.7	$2808.0 \div 7735.8 = 2.8$
	5	2777.0	
	6	2808.0	
Total (36)	7735.8		
2015 Ynl B	0	536.8	
	1	713.4	
	2	776.0	$4916.4 \div 824.4 = 6.0$
	3	824.4	
Total (36)	4916.4		

Bold text represents the inflection point of the sulfate release curve (from rinsing of stored products to oxidative production).

Bold italicized represent the total sulfate released for entire HCT.

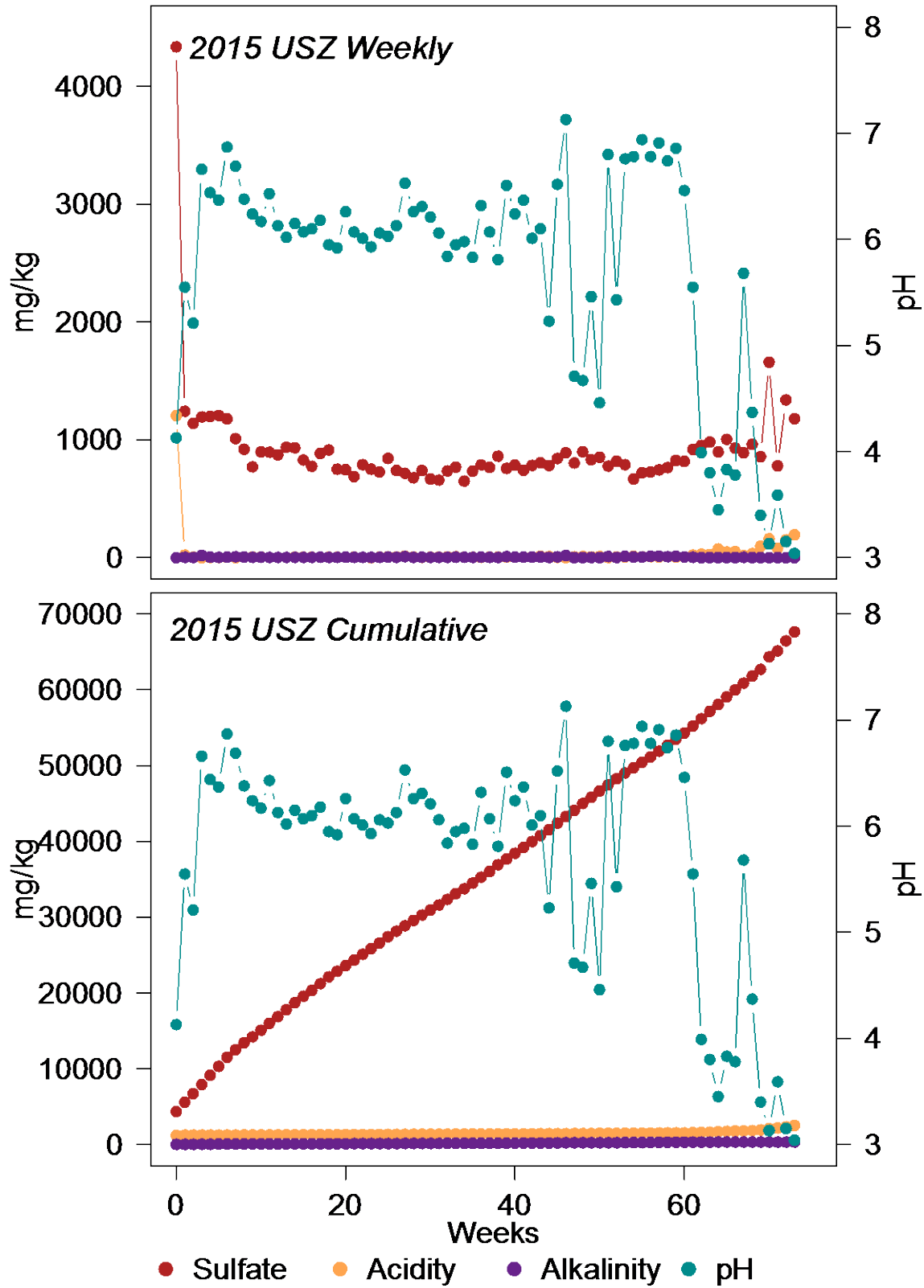


Figure 1. 2015 USZ HCT Summary

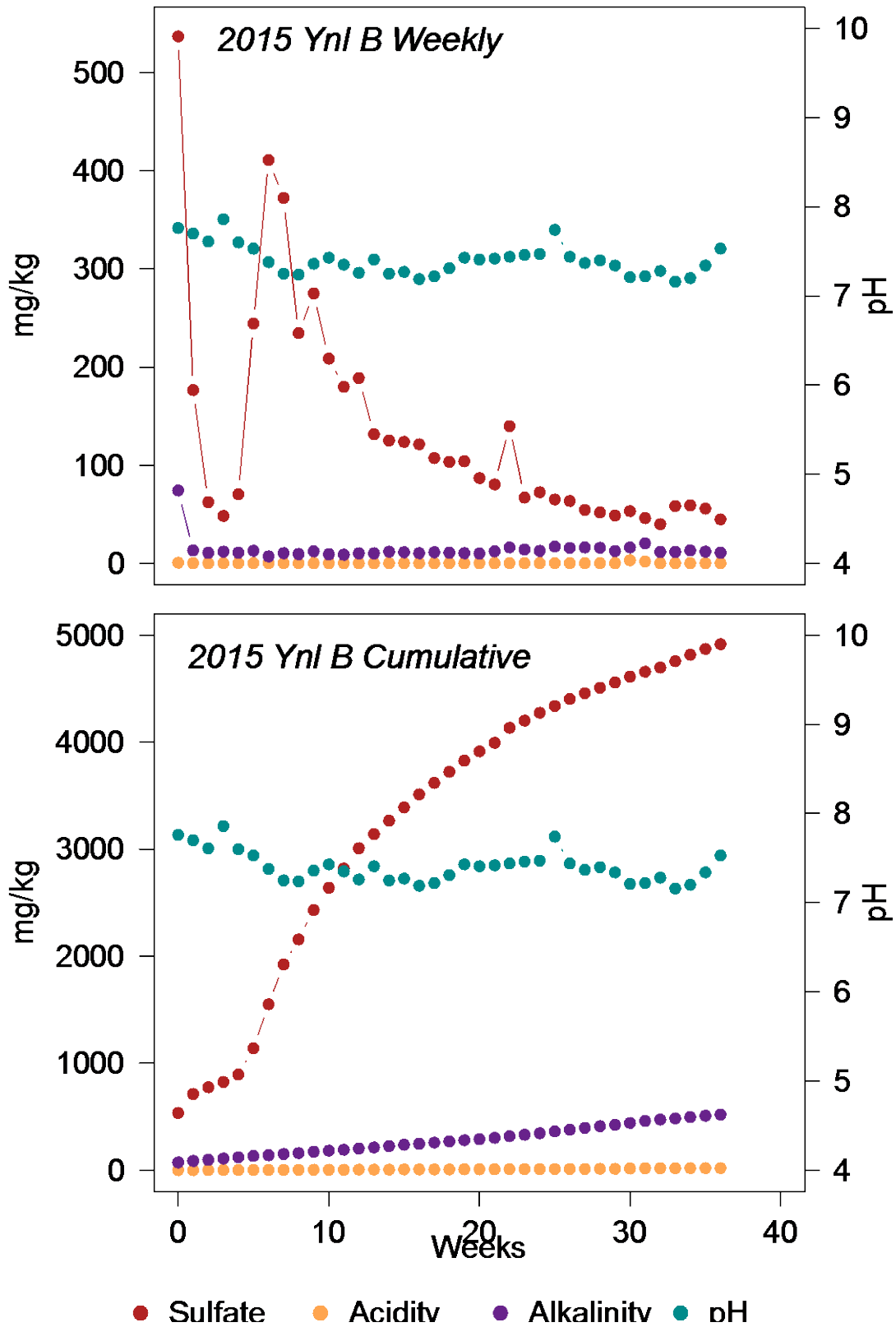


Figure 2. 2015 Ynl B HCT Summary

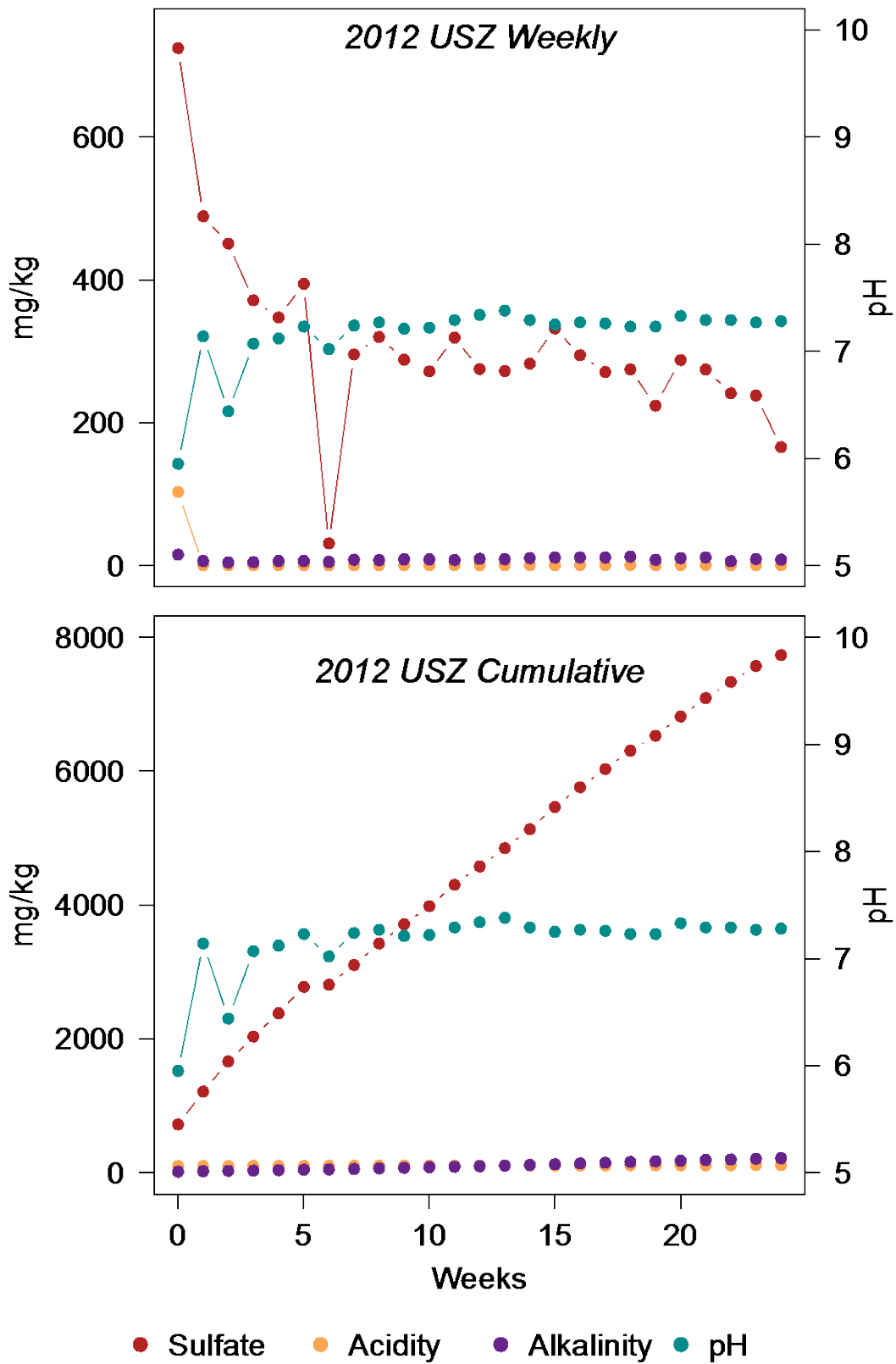


Figure 3. 2012 USZ HCT Summary